UNIVERSITY OF OKLAHOMA

GRADUATE COLLEGE

A BONE TISSUE ENGINEERING APPROACH BASED ON THE COMBINATION OF BIOMIMETIC SCAFFOLDS AND FLOW PERFUSION CULTURE

A DISSERTATION

SUBMITTED TO THE GRADUATE FACULTY

in partial fulfillment of the requirements for the

degree of

Doctor of Philosophy

By

JOSE F. ALVAREZ-BARRETO
Norman, Oklahoma
2007

Downloaded from SHAREOK. Persistent Handle URL: https://hdl.handle.net/11244/1303

UMI Number: 3291936



UMI Microform 3291936

Copyright 2008 by ProQuest Information and Learning Company.
All rights reserved. This microform edition is protected against unauthorized copying under Title 17, United States Code.

ProQuest Information and Learning Company
300 North Zeeb Road
P.O. Box 1346
Ann Arbor, MI 48106-1346

A BONE TISSUE ENGINEERING APPROACH BASED ON THE COMBINATION OF BIOMIMETIC SCAFFOLDS AND FLOW PERFUSION CULTURE

A DISSERTATION APPROVED FOR THE
SCHOOL OF CHEMICAL, BIOLOGICAL AND MATERIALS ENGINEERING

BY

_____
Dr. Vassilios I. Sikavitsas

_____
Dr. Edgar. O'Rear III

_____
Dr. Robert L. Shambaugh

_____
Dr. Matthias U. Nollert

_____
Dr. Rong Z. Gan

_____
Dr. Paul DeAngelis

© Copyright by JOSE F. ALVAREZ-BARRETO 2007
All Rights Reserved.

Acknowledgments

I would like to acknowledge everybody who helped me achieve this goal, not only to those that offered me all their love and support but also all the people who tried to discourage me because they made me try even harder. I would like to express my immense gratitude to Dr. Vassilios Sikavitsas for all his advice, trust and guidance so necessary for the fulfillment of my PhD. I would also like to thank all my committee members for their input. Special thanks to Drs. Matthias Nollert, Daniel Resasco, Peter McFetridge, and Lance Lobban for their valuable advices and help.

There are no words that I can find to tell my parents, Morela María Barreto Alcoba and Francisco Javier Alvarez Rodríguez, how infinitely thankful I am to them. More than parents, they were also the best friends I could wish for, and without them I would not be half the man I am today; we will meet again in our next life. I will be forever thankful to my sister and excellent friend, Celeste Yumila Alvarez Barreto, for her love and tenderness. To my aunt, Carmen Ivette Barreto Alcoba, and my grandmother, Carmen Miguelina Alcoba Morales, my other mothers, my endless gratitude. My special thanks to the Alvarez Alayón family for all their unconditional love, support and encouragement. I also want to thank my extended family; I really have been blessed for having such a beautiful support system, including Araira Marín and Patricia Armando. My admiration to my academic masters, Rosabel Dueñes, Luz Vestalia Pinto, Julie Carrier and Edgar Clausen; the helped me see that everyone is special and valuable and allowed me to see my potential.

I want to acknowledge everybody that helped me and shared wonderful moments with me in the lab: Rita Abousleiman, Mark Shreve, Jessica Yankovich,

Shawna Linehan, Laura Place, Bonnie Grider, Sam VanGordon, Valerie Rivera, Erica Brown, Yuliana Reyes, Hope Baumgarner, and Harold Castano. Many thanks to my friends in Sarkeys and everywhere else, you guys know who you are. Jena Vieira, Carina Joly, Diego Acosta and Martina Dreyer, you were my family in Norman and now are part of my extended family, those who were by my side always unconditionally. I want to acknowledge Donna King, Terri Colliver, Sherri Childress, Claudia Draper, Vernita Farrow, Lysa Park and Alan Miles for their kindness and help.

Finally, I thank the universal energy, love, for always conspiring in my favor, and to all the true spiritual masters for giving me the best example; I try my best to follow it. I embarked in this project because I have a genuine desire to help people.

Table of Contents

Acknowledgments iv

Figures and Tables xii

Dissertation Abstract xv

Chapter 1 1

Overview and Research Objectives 1

References 7

Chapter 2 11

Bone Tissue Engineering: An Introduction 11

2.1 Overview of Bone 12

2.1.1. Cellular component 12

2.1.2. Organic extracellular matrix (ECM) 13

2.1.3. Mineral phase 13

2.1.4. Bone structure 14

2.1.5. Mechanisms of bone formation 16

2.2 The need for bone tissue engineering 18

2.3. Cell Source for Bone Tissue Engineering 20

2.4. Scaffold Technologies in Bone Tissue Engineering 22

2.5. Bioreactors in Bone Tissue Engineering 26

2.5.1. Common Bioreactors Designs in Tissue Engineering 26

2.5.2. Cell Seeding in Bioreactors 29

2.5.3. Development of Bone-Like Extracellular Matrix in Bioreactor Systems .. 32

2.6. References 42

Chapter 3 57

Oscillating Flow perfusion improves seeding of different tissue engineering scaffolds....57
3.1 Introduction....58
3.2 Materials and Methods....61
3.2.1 Scaffolds....61
3.2.2. Cell Source....63
3.2.3. Seeding Techniques....63
3.2.4. Cell detachment....64
3.2.5 Cell number quantification....65
3.2.6. Assessment of cell spatial distribution throughout the scaffold surface....66
3.2.7. Statistical analysis....68
3.3. Results....69
3.3.1 Effect of the seeding technique and fiber diameter on initial scaffold cellularity and seeding efficiency in fibrous scaffolds....69
3.3.2. Cell detachment after seeding....77
3.3.3. Assessment of cell spatial distribution....79
3.4. Discussion....85
3.4.1. Influence of the seeding technique on seeding efficiency....86
3.4.2. Relation between cell attachment and scaffold architecture....89
3.4.3. Influence on the initial cell spatial distribution throughout the entire scaffold surface....90
3.5. Conclusions....92
3.6. References....93
Chapter 4....102

Preparation of a functionally flexible, three-dimensional, biomimetic poly (L-lactic acid) scaffold with improved cell adhesion 102
4.1. Introduction 103
4.2. Materials and Methods 106
4.2.1 Materials 106
4.2.2 Determination of the optimal entrapment technique 107
4.2.3 Modification of 3-D PLLA scaffolds 109
4.2.4 Varying the amount of entrapped polyK in PLLA foams 110
4.2.5. Stability of the modified surface 111
4.2.6. Effect of the acetone treatment on the porous architecture of 3-D foams 111
4.2.7. Incorporation of RGDC peptides to the polyK modified surface 112
4.2.8 Cell seeding on RGDC-modified surfaces 113
4.2.9 Statistical analysis 115
4.3. Results 116
4.3.1 Determination of the optimal polyK entrapment technique 116
4.3.2 Modification of 3-D porous foams 119
4.3.3 Varying the amount of the entrapped polyK 120
4.3.4. Effect of the acetone treatment on the porous architecture of 3-D foams. 121
4.3.5 Stability of the modified surface 122
4.3.6 Incorporation of RGDC peptides to the poly-modified surfaces 122
4.3.7. Cell seeding on RGDC-modified surfaces 125
4.4. Discussion 129
4.5. Conclusions 136
4.6. References 137

Chapter 5 146
Improved Mesenchymal Stem Cell Seeding on RGD-Modified Poly(L-lactic acid) Scaffolds using Flow Perfusion 146
5.1 Introduction 147
5.2 Materials and Methods 150
5.2.1. Scaffold Preparation 150
5.2.2. Surface Modification 150
5.2.3. Cell Culture 151
5.2.4. Scaffold Seeding 152
5.2.5. Detachment Studies 153
4.2.6. Evaluation of cell morphology on RGD-modified scaffolds 154
5.3.7. Determination of the number of cells attached to the scaffolds (Scaffold Cellularity) 154
5.2.8. Statistical analysis 155
5.3 Results 156
5.3.1. Effect of RGD modification on scaffold cellularity after oscillatory flow perfusion seeding 156
5.3.2. Effect of oscillatory flow perfusion on seeding efficiency of RGD-modified scaffolds 158
5.3.3. Cell detachment on dynamically seeded RGD-modified scaffolds 160
5.4. Discussion 163
5.4.1. Effect of RGD modification on scaffold cellularity after oscillatory flow perfusion and static seeding 163
5.4.2. Comparison of oscillatory flow perfusion and static seeding of RGD-modified scaffolds 165

5.4.3. Cell detachment on oscillatory flow perfusion seeded RGD-modified scaffolds 166
5.5. Conclusions 168
5.6. References 169
Chapter 6 178
RGD Peptides Affect the Osteoblastic Differentiation of Rat Mesenchymal Stem Cells under Flow Perfusion in a Dose Dependent Manner 178
6.1 Introduction 179
6.2. Materials and Methods 183
6.2.1. Scaffold Preparation 183
6.2.2. Surface Modification 183
6.2.3. Cell Culture 184
6.2.4. Scaffold Seeding 185
6.2.5. Long term cultures 186
6.2.6. Determination of the number of cells attached to the scaffolds (Scaffold Cellularity) 186
6.2.7. Alkaline phosphatase (ALP) activity 187
6.2.8. Calcium deposition 187
6.2.9. Statistical analysis 188
6.3. Results and Discussion 189
6.3.1. Scaffold Cellularity 189
6.3.2.. Alkaline Phosphatase Activity 192
6.3.3. Calcium Deposition 194
6.4. Discussion 196
6.5. Conclusions 200

6.6. References 201

Chapter 7 211

Project Conclusions and Future Directions 211

7.1. Project Conclusions 211

7.2. Future Directions 215

Figures and Tables

Figure 1.1. An integral bone tissue engineering approach ……... 4

Figure 2.1. Macroscopic bone structure ……..……15

Figure 2.2. The tissue engineering paradigm ……..……20

Figure 2.3. Differentiation potential of adult bone marrow mesenchymal stem cells. ……...……...21

Figure 2.4. Common bioreactors used in tissue engineering ……..28

Figure 2.5. Schematics of a flow perfusion bioreactor …….……...36

Figure 2.6. Steady state linear velocity profile of a Newtonian fluid between two plates ……... 40

Figure 3.1. Effect of seeding technique and fiber size on the number of cells attached per scaffold …….…….69

Figure 3.2. Effect of cell inoculation number on the seeding efficiency ……...71

Figure 3.3. Dependence of the number of cells attached per scaffold (cellularity) on the cell inoculation number and fiber size …….……..……73

Figure 3.4. Dependence of cell surface density on cell inoculation number and fiber size ……..…….75

Figure 3.5. Effect of scaffold morphology on cell surface density after seeding in a flow perfusion system ……..……...76

Figure 3.6. Effect of seeding technique on the cell seeding efficiency of prous scaffold scaffolds ……. 77

Figure 3.7. Detachment curve of cells seeded both statically and dynamically on oxygen plasma treated fibrous meshes with a fiber size of 20 μm …….…….……...78

Figure 3.8. Fluorescent micrographs of the top, middle and bottom portions of fibrous matrices ……..…….……80

Figure 3.9. Cell stretching on fibrous matrices ……..…….……80

Figure 3.10. Fluorescent micrographs of the top and bottom portions of polystyrene porous foams seeded statically, and dynamically …..……..…….……..… 81

Figure 3.11. Axial histological sections of PLLA foams seeded statically and dynamically, in the flow perfusion bioreactor …….……82

Figure 3.12. Percent uniformity of scaffold dynamic and static seeding ……83

Figure 4.1. Detection of poly(L-lysine) entrapped in poly(L-lactic acid) discs with different techniques ……...117

Figure 4.2. Physical entrapment of Poly(L-lysine) (PolyK) on the surface of poly (L-lactic acid) and further incorporation of SPDP, and the release of pyridine-2-thione due to the action of DTT …….. 118

Figure 4.3. Fluorescent micrographs of the surface of (a) polyK-modified (using the acetone/DMSO procedure) and (b) unmodified discs …….……..119

Figure 4.4. Demonstration of the presence of polyK on the surface of 3-D scaffolds modified with the acetone/DMSO procedure ……120

Figure 4.5. Quantification of the amount of entrapped polyK in the surface of PLLA foams at different concentrations of polypeptide in the stage of incubation after the soaking with acetone …….121

Figure 4.6. Micro-computed tomography scan of a PLLA foam after being treated with a mixture of acetone and water (7:3) for 1 hr ……121

Figure 4.7. Incorporation of RGDC to the Poly-modified PLLA surface …… 126

Figure 4.8. Cell adhesion test on RGDC-modified PLLA discs ……...126

Figure 4.9. Effect of the extent of polyK entrapment on cell surface area after linkage of RGDC peptides to polyK entrapped in PLLA discs …….127

Figure 4.10. Effect of the extent of modification on the adhesion of cells to three-dimensional, porous PLLA foams ……128

Figure 5.1. Scaffold cellularity at different levels of RGD modification after oscillatory flow perfusion seeding at 0.15 ml/min ……157

Figure 5.2. Dependence of scaffold cellularity on the cell suspension number at different levels of modification ……157

Figure 5.3. Dependence of seeding efficiency on the different techniques used to seed RGD-modified scaffolds at different modification levels ……159

Figure 5.3. Dependence of seeding efficiency on the different techniques used to seed RGD-modified scaffolds at different modification levels ……160

Figure 5.5. Detachment profile of cells seeded under oscillatory flow perfusion on RGD-modified scaffolds ……...161

Figure 6.1. Effect of the RGD modification level (expressed as the concentration of polyK in the incubation phase of the modification) on the growth of cells cultured under (a) static conditions, and under flow perfusion at flow rates of (b) 0.1 ml/min and (c) 1.0 ml/min. ……191

Figure 6.2. Effect of RGD modification level on Alkaline Phosphatase Activity……...…193

Figure 6.3. Effect of the RGD modification level (concentration of polyK in the initial incubation phase) on the deposition of calcium by cells cultured under (a) static conditions, and under flow perfusion at flow rates of (b) 0.1 ml/min and (c) 1.0 ml/min ……...195

Table 3.1. Cell coverage fractions of statically and dynamically seeded scaffolds 84

Dissertation Abstract

Bone tissue engineering has progressively emerged as a response to the current limited replacement therapies for damaged or lost bone tissue. Ideally, the implanted construct should aid in complete bone regeneration in a reasonably short time, without causing significant inconvenience to the patient. General tissue engineering approaches are based on three different bioactive factors: scaffolding, a cellular component, and a molecular component. These factors are closely conjoined to create successful constructs and fit into a bone tissue engineering paradigm that includes the extraction of a cellular biopsy from a healthy site of the patient. Cells are then expanded in vitro and seeded onto the scaffold. The cell-scaffold construct is cultured under mechanical and/or chemical stimuli for a certain amount of time so as to allow the in vitro secretion of a bone-like extracellular matrix (ECM). This construct, which now possesses an osteoinductive nature due to the secreted ECM, is implanted in the defective site for bone regeneration. The main objective of the present research project was to create an integral tissue engineering approach that combines both mechanical and chemical stimulation by. To fulfill this goal, four major steps were successfully carried out. First, a dynamic scaffold seeding technique based on oscillatory flow perfusion that improved initial cellular distribution throughout the scaffold surface, and cell-matrix interactions was developed. Secondly, a biomimetic poly(L-lactic acid scaffold) with improved cell adhesion using RGD peptides that could additionally allow the evaluation of the effect of different modification levels on cell adhesion, proliferation and differentiation was created. Thirdly, the oscillatory flow perfusion seeding of these RGD-modified scaffolds was characterized. And lastly, the effect of the level of RGD scaffold modification on the osteoblastic differentiation of mesenchymal stem cells when cultured under

conditions of flow perfusion was evaluated. What makes this approach unique is the combination of mechanical and chemical stimulation of mesenchymal stem cells to direct them towards an osteoblastic path. This combinatorial approach resulted more successful than those based on chemical or mechanical stimulation alone.

Chapter 1

Overview and Research Objectives

Over the past two decades, bone tissue engineering has progressively emerged as a response to the current limited replacement therapies for damaged or lost bone tissue. Ideally, the implanted construct should aid in complete bone regeneration in a reasonably short time, without causing significant inconvenience to the patient. The optimum alternative would be the use of autografts, in which a bone biopsy is extracted from a healthy site of the patient and implanted into the injured site. Nevertheless, donor site morbidity and lack of graft availability pose major limitations on the application of this therapy. Other choices are allografts extracted from a different individual of the same species, and xenografts, which come from an individual of a different species. These last two therapies have shown a certain degree of success, but they may result in strong immune responses and disease transmission. [1-3] Tissue engineering creatively combines biology and engineering principles to create constructs capable of replacing damaged or lost tissue and overcoming the aforementioned obstacles [4].

General tissue engineering approaches are based on three different bioactive factors: scaffolding, a cellular component, and a molecular component. These factors are closely conjoined to create successful constructs that can induce the efficient regeneration of the damaged tissue once implanted [4]. In the case of bone, the scaffolding is usually a porous matrix that can support cell adhesion, migration and proliferation [5,6]. Scaffolds are made out of natural or synthetic materials. Collagen, poly(ethylene glycol), ceramics, titanium and poly-α- hydroxyl esters are among

some of the most popular choices [7-11]. A wide variety of cell types; but progenitor cells, such as mesenchymal stem cells (MSC) have grown in popularity and will continue to do so due to their great osteogenic potential [12-15]. The molecular component consists of growth and differentiation factors, which are basically proteins or other molecules that are capable of eliciting specific cellular responses. In many instances growth factors are incorporated into scaffolding technologies to create a biomimetic scaffold. As the name suggests, biomimetic scaffolds are matrices designed to mimic a certain feature correspondent to the native extracellular matrix (ECM) and have the purpose of inducing a desired cellular response, such as the differentiation of MSCs towards the osteoblastic phenotype [16-21].

All these components fit into a bone tissue engineering paradigm, on which this project is based, that includes the extraction of a cellular biopsy from a healthy site of the patient. Cells are then expanded *in vitro* and seeded onto the scaffold. The cell-scaffold construct is cultured for a certain amount of time so as to allow the *in vitro* secretion of a bone-like extracellular matrix (ECM). This construct, which now possesses an osteoinductive nature due to the secreted ECM, is implanted in the defective site for bone regeneration [4]. Conditions of culture prior to implantation are crucial in the development of an efficient construct. Furthermore, researches have realized that mimicking the *in vivo* mechano-chemical conditions in which the tissue operates dramatically enhances the secretion and rearrangement of the ECM that more closely resembles the morphology of the native tissue [22-28]. Bioreactors effectively modulate the desired mechanical conditions. Additionally, they enhance the transportation of nutrients to the interior of the scaffolds and yield homogenous distribution of cells and ECM [23,29].

This study ultimately focuses on a novel approach that employs both chemical and mechanical stimulation to enhance MSC osteogenesis. This innovative concept can therefore yield more efficient constructs than those produced through individual stimulation. Mechanical stimulation was exerted by the application of shear forces on the cells in a flow perfusion bioreactor that has been shown to induce higher degrees of MSC osteoblastic differentiation than those achieved by static cultures [23,30-32]. Moreover, in order to amplify the effect of flow perfusion on the development of bone constructs, the system was not only used for long term cultures but also in scaffold seeding. Traditional static seeding techniques, in which the cell suspension is added in a drop-wise manner on top of the scaffolds, yield rather low number of cells on the scaffolds and poor cellular distributions throughout the scaffold surface. Flow perfusion is capable of overcoming external and internal diffusion limitations and thereby could potentially yield a more homogenous initial cellular distribution [23].

Chemical stimulation was based on enhancing the cell interactions with the scaffolding material, poly (L- lactic acid) (PLLA). Cell-matrix interactions play an important role in bone tissue engineering since they affect the proper cell growth, migration and differentiation towards the osteoblastic phenotype [33-35]. The interaction of cells with PLLA is very limited due to the inert nature of the polymer; thus, it is desired to incorporate bioactive molecules that support cell adhesion. This was done by the linkage of adhesion peptides, most specifically Arginine-Glycine-Aspartic Acid (RGD), to an amine-functionalized PLLA surface.

In the present project, it was hypothesized that the combination of this novel biomimetic scaffold with flow perfusion cultures would result in improved MSC osteoblastic differentiation, when compared to their sole effects. MSCs were seeded on the scaffold using the newly developed technique and cultured under mechano-chemical conditions beneficial to their osteoblastic differentiation. Therefore, the main objective of the present research project (shown in Figure 1.1) was to create an integral tissue engineering approach that combines both mechanical and chemical stimulation by utilizing the three different bioactive components (scaffold, cells and growth factors).

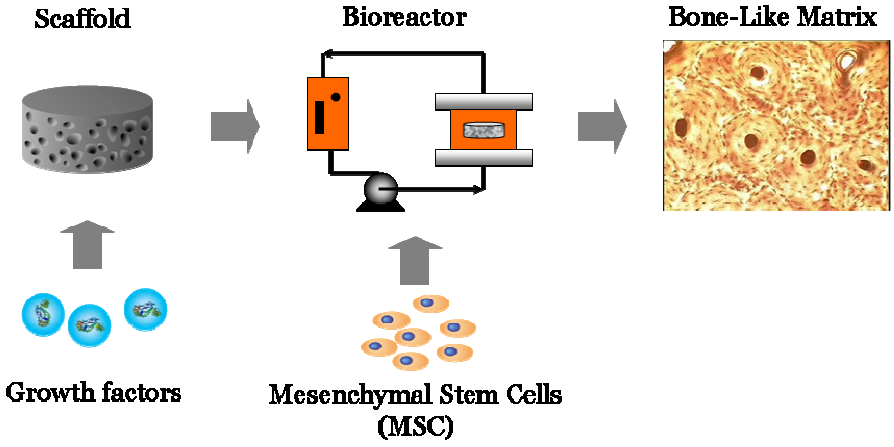


Figure 1.1. An integral bone tissue engineering approach that includes biomimetic scaffolds and bioreactor technologies to produce efficient constructs with a bone-like matrix secreted by mesenchymal stem cells. The biomimetic scaffold is produced by incorporating growth factors in the scaffold making process

The proposed approach can result in enhanced MSC osteoblastic differentiation when compared to those achieved by the stimulatory mechanisms individually. In order to fulfill the main objective, four specific aims were proposed:

1) To develop a dynamic scaffold seeding technique based on oscillatory flow perfusion and evaluate its effects on seeding efficiency, initial cellular distribution throughout the scaffold surface, and cell-matrix interactions.
2) To create a biomimetic poly(L-lactic acid scaffold) with improved cell adhesion using RGD peptides that can additionally allow the evaluation of the effect of different modification levels on cell adhesion, proliferation and differentiation.
3) To characterize the newly developed oscillatory flow perfusion seeding of mesenchymal stem cells on the modified scaffolds based on cell spatial distribution, seeding efficiency and strength of cell attachment at different modification levels and flow conditions.
4) To evaluate the effect of the level of RGD scaffold modification on the osteoblastic differentiation of mesenchymal stem cells when cultured under conditions of flow perfusion.

In order to better understand the reasons behind the main objective of this project, Chapter 2 provides a more detailed background on bone tissue engineering, the bioactive components involved in it, and an overview on biomimetic scaffolds and bioreactor technologies. Chapter 3 describes the development of a new oscillatory flow perfusion seeding technique that resulted in improved seeding efficiency and distribution of osteoblastic cells onto fibrous matrices and porous foams. The creation of a functionally flexible, biomimetic scaffold with improved cell adhesion is presented in Chapter 4, while the characterization of the seeding of MSCs on these scaffolds is highlighted in Chapter 5. In Chapter 6, the effect of different extents of

RGD incorporation into PLLA foams on the osteogenic differentiation of MSCs under conditions of flow perfusion at different flow rates is presented. Finally, Chapter 7 provides general conclusions addressing the general research objective and specific aims. This chapter also provides ideas for future projects that aim at answering new questions that arose during the development of the present project.

References

1. Bostrom, RD, Mikos, AG. Tissue Engineering of Bone. In: Atala A, Mooney DJ, eds. Synthetic biodegradable polymer scaffolds. Boston: Birkhäuser; 1997:215.
2. Brown, KL, Cruess, RL. Bone and cartilage transplantation in orthopaedic surgery. A review. J Bone Joint Surg Am. 1982;64:270-279.
3. Freeland, AE, Rehm, JP. Autogenous bone grafting for fractures of the hand. Tech Hand Up Extrem Surg. 2004;8:78-86.
4. Bonassar, LJ, Vacanti, CA. Tissue engineering: the first decade and beyond. J Cell Biochem Suppl. 1998;30-31:297.
5. Saltzman, MW. Cell Interactions with Polymers. In: Lanza R, Langer R, Vacanti J, eds. Principles of Tissue Engineering. 2 ed. San Diego: Academic Press; 2000:221.
6. Vacanti, JP, Langer, R, Upton, J, Marler, JJ. Transplantation of cells in matrices for tissue regeneration. Adv Drug Deliv Rev. 1998;33:165-182.
7. Benoit, DS, Anseth, KS. Heparin functionalized PEG gels that modulate protein adsorption for hMSC adhesion and differentiation. Acta Biomater. 2005;1:461-470.
8. Cristino, S, Grassi, F, Toneguzzi, S, et al. Analysis of mesenchymal stem cells grown on a three-dimensional HYAFF 11-based prototype ligament scaffold. J Biomed Mater Res A. 2005;73:275-283.
9. Farrell, E, Byrne, EM, Fischer, J, et al. A comparison of the osteogenic potential of adult rat mesenchymal stem cells cultured in 2-D and on 3-D collagen glycosaminoglycan scaffolds. Technol Health Care. 2007;15:19-31.

10. Lisignoli, G, Cristino, S, Piacentini, A, et al. Cellular and molecular events during chondrogenesis of human mesenchymal stromal cells grown in a three-dimensional hyaluronan based scaffold. Biomaterials. 2005;26:5677-5686.

11. Sagnella, S, Anderson, E, Sanabria, N, Marchant, RE, Kottke-Marchant, K. Human endothelial cell interaction with biomimetic surfactant polymers containing Peptide ligands from the heparin binding domain of fibronectin. Tissue Eng. 2005;11:226-236.

12. Bruder, SP, Kraus, KH, Goldberg, VM, Kadiyala, S. The effect of implants loaded with autologous mesenchymal stem cells on the healing of canine segmental bone defects. J Bone Joint Surg Am. 1998;80:985-996.

13. Bruder, SP, Kurth, AA, Shea, M, Hayes, WC, Jaiswal, N, Kadiyala, S. Bone regeneration by implantation of purified, culture-expanded human mesenchymal stem cells. J Orthop Res. 1998;16:155-162.

14. Kadiyala, S, Young, RG, Thiede, MA, Bruder, SP. Culture expanded canine mesenchymal stem cells possess osteochondrogenic potential *in vivo* and *in vitro*. Cell Transplant. 1997;6:125-134.

15. Vilquin, JT, Rosset, P. Mesenchymal stem cells in bone and cartilage repair: current status. Regen Med. 2006;1:589-604.

16. Elbert, DL, Hubbell, JA. Conjugate addition reactions combined with free-radical cross-linking for the design of materials for tissue engineering. Biomacromolecules. 2001;2:430.

17. Rowley, JA, Madlambayan, G, Mooney, DJ. Alginate hydrogels as synthetic extracellular matrix materials. Biomaterials. 1999;20:45.

18. Schense, JC, Hubbell, JA. Cross-linking exogenous bifunctional peptides into fibrin gels with factor XIIIa. Bioconjug Chem. 1999;10:75-81.

19. Shin, H, Jo, S, Mikos, AG. Biomimetic materials for tissue engineering. Biomaterials. 2003;24:4353.

20. van den Dolder, J, Bancroft, GN, Sikavitsas, VI, Spauwen, PH, Jansen, JA, Mikos, AG. Flow perfusion culture of marrow stromal osteoblasts in titanium fiber mesh. J Biomed Mater Res A. 2003;64:235-241.

21. Yang, XB, Roach, HI, Clarke, NM, et al. Human osteoprogenitor growth and differentiation on synthetic biodegradable structures after surface modification. Bone. 2001;29:523.

22. Alvarez-Barreto, JF, Linehan, SM, Shambaugh, RL, Sikavitsas, VI. Flow Perfusion Improves Seeding of Tissue Engineering Scaffolds with Different Architectures. Ann Biomed Eng. 2007.

23. Alvarez-Barreto, JF, Sikavitsas, VI. Tissue Engineering Bioreactors. In: Boronzino JD, ed. Tissue Engineering and Artificial Organs. Vol 3. 3 ed. Boca Raton: Taylor & Francis Group; 2006:44-41.

24. Botchwey, EA, Pollack, SR, Levine, EM, Laurencin, CT. Bone tissue engineering in a rotating bioreactor using a microcarrier matrix system. J Biomed Mater Res. 2001;55:242-253.

25. Cartmell, SH, Porter, BD, Garcia, AJ, Guldberg, RE. Effects of medium perfusion rate on cell-seeded three-dimensional bone constructs *in vitro*. Tissue Eng. 2003;9:1197.

26. Vunjak-Novakovic, G, Obradovic, B, Martin, I, Bursac, PM, Langer, R, Freed, LE. Dynamic cell seeding of polymer scaffolds for cartilage tissue engineering. Biotechnol Prog. 1998;14:193.

27. Vunjak-Novakovic, G, Obradovic, B, Martin, I, Freed, LE. Bioreactor studies of native and tissue engineered cartilage. Biorheology. 2002;39:259-268.

28. Wendt, D, Marsano, A, Jakob, M, Heberer, M, Martin, I. Oscillating perfusion of cell suspensions through three-dimensional scaffolds enhances cell seeding efficiency and uniformity. Biotechnol Bioeng. 2003;84:205.

29. Abousleiman, RI, Sikavitsas, VI. Bioreactors for tissues of the musculoskeletal system. Adv Exp Med Biol. 2006;585:243-259.

30. Bancroft, GN, Sikavitsas, VI, van den Dolder, J, et al. Fluid flow increases mineralized matrix deposition in 3D perfusion culture of marrow stromal osteoblasts in a dose-dependent manner. Proc Natl Acad Sci U S A. 2002;99:12600.

31. Gomes, ME, Bossano, CM, Johnston, CM, Reis, RL, Mikos, AG. *In vitro* localization of bone growth factors in constructs of biodegradable scaffolds seeded with marrow stromal cells and cultured in a flow perfusion bioreactor. Tissue Eng. 2006;12:177.

32. Sikavitsas, VI, Bancroft, GN, Holtorf, HL, Jansen, JA, Mikos, AG. Mineralized matrix deposition by marrow stromal osteoblasts in 3D perfusion culture increases with increasing fluid shear forces. Proc Natl Acad Sci U S A. 2003;100:14683-14688.

33. Alvarez-Barreto, JF, Shreve, MC, DeAngelis, PL, Sikavitsas, VI. Preparation of a functionally flexible, three-dimensional, biomimetic scaffold for different tissue engineering applications. Tissue Eng. 2007;13:1205-1217.

34. Boyan, BD, Hummert, TW, Dean, DD, Schwartz, Z. Role of material surfaces in regulating bone and cartilage cell response. Biomaterials. 1996;17:137-146.

35. Liu, X, Ma, PX. Polymeric scaffolds for bone tissue engineering. Ann Biomed Eng. 2004;32:477-486.

Chapter 2

Bone Tissue Engineering: An Introduction

Chapter Abstract

An increasing number of bone-related injuries has propelled the quest for finding efficient therapies, particularly in the cases where the body cannot regenerate the lost tissue by itself. Current techniques have limited success, driving researchers towards developing tissue engineering approaches. In bone tissue engineering, it is desirable to create an implant that can induce and conduct new tissue formation without compromising the mechanical and other functional properties of the tissue. The main bone tissue engineering components consist of a scaffolding material, osteoblastic and/or osteoprogenitor cells, and growth and differentiation factors. An interaction between these three elements is desired. A recent growing application is the use of bioreactors that can mimic the physiomechanical conditions in which the tissue operates. This chapter gives an insight into the main aspects of bone structure and function, the fundamentals of bone tissue engineering, as well as some of the common, existent technologies on tissue engineering scaffolds and bioreactor cultures.

2.1 Overview of Bone

Bone, the major component of the skeletal system, is a hard, calcified, connective tissue that protects vital organs, provides support for body motion, and serves as storage of calcium and other ions. Bone is viscoelastic, porous and semi rigid. The major components of this tissue are: cells, extracellular matrix, and an inorganic mineral phase, with weight percentages of about 8%, 25% and 67% respectively [1,2].

2.1.1. Cellular component

The most relevant cell types related to bone formation and modeling are the osteoblasts, osteocytes and osteoclasts. Osteoblasts and osteocytes are responsible for the bone-making process and reside along with the bone-lining cells, which are immediate osteoblast precursors [3,4]. Osteoblasts also derive from local pluripotent progenitor cells, such as mesenchymal stem cells (MSC). In their last stage of differentiation, osteoblasts synthesize alkaline phosphatase, and secrete calcium and other extracellular matrix proteins, such as osteopontin, osteocalcin, and bone sialoprotein [3]. Once they have secreted sufficient calcified ECM, osteoblasts are entrapped and become osteocytes. They communicate among themselves and other cells on the bone surface through gap-junction-coupled cell processes that take place in the extracellular matrix via channels called canaliculi [5-7]. However, bone is a dynamic tissue that is undergoing a constant process of remodeling; thus, as there is a process of bone formation, a process of bone digestion must also exist in order to maintain the integrity of the tissue. The resorption of bone matrix is carried out by

osteoclasts, which are multinucleated cells of hematopoietic origin formed by the fusion of mononucleated cells of the monocyte/macrophage family [5,8].

2.1.2. Organic extracellular matrix (ECM)

The extracellular matrix of bone is mainly composed of approximately 90% collagen type I, and a series of non-collagenous proteins and proteoglycans in smaller quantities [5]. It is important to point out that osteoblasts secrete, on a mole basis, one non-collagenous protein molecule per one collagen molecule, and that the difference in quantity is due mainly to molecular weights [8,9]. Collagen fibers in bone present many intra and intermolecular crosslinks, diminishing their solubility. Their structure and degree of crosslinking affect the strength and general function of bone. Some of the non-collagenous molecules found in bone ECM are osteopontin, osteonectin, glycosaminoglycans (chondroitin sulfate, dermatan sulfate, keratan sulfate, and hyaluronic acid), fibronectin, and some growth factors from the morphogenetic protein (BMP) family entrapped in the matrix during bone formation [5,8-10].

2.1.3. Mineral phase

The mineral phase of bone is based on calcium compounds. This is the main feature that differentiates the composition of bone from that of other musculoskeletal tissues and is a major player in bone strength. The mineral component of bone is comprised of a crystalline analog of hydroxyapatite [$Ca_{10}(PO_4)_6(OH)_2$]. This structure is often called dahllite. It is deficient in calcium and less crystalline when compared to

hydroxyapatite, in addition to containing carbonate [5]. The mineral crystals are arranged in a parallel fashion within the bone collagenous matrix and appear as plate-shaped crystals that are hundreds of angstroms in length and 20-30 angstroms thick [1,2,5,8].

2.1.4. Bone structure

Macroscopically, there are different types of bone in the skeleton and different ways to classify them. The macroscopic classification of bone can be based on its function; it can be weight bearing, protecting, articulating, etc. Another categorization is based on the shape, long, short or flat. The most used macroscopic cataloguing of bone is based on its mechanism of formation: endochondral bone formation or intramembraneous ossification.

However, in long bones there are two different types of tissue: cortical or compact bone, found mostly in the diaphyses, and cancellous or trabecular (also called spongy bone) found mainly in the metaphyses and epiphyses (see Figure 2.1). Cancellous bone is spongy in appearance, formed by thin trabeculae and arranged in a 3D lattice, and is located in the extremities of the bone. Cortical bone, on the other hand, is a compact, continuous mass usually located at the cortices of mature bone. Thus, the main difference between cancellous and trabecular bone is their porosity. The diaphysis of a long bone can withstand bending and torsional loads imposed on its shaft due to its tubular design, basically a thick cylinder with bone marrow in the cavity. The metaphysis and epiphysis however, are designed to withstand mostly compression forces [5,11-13].

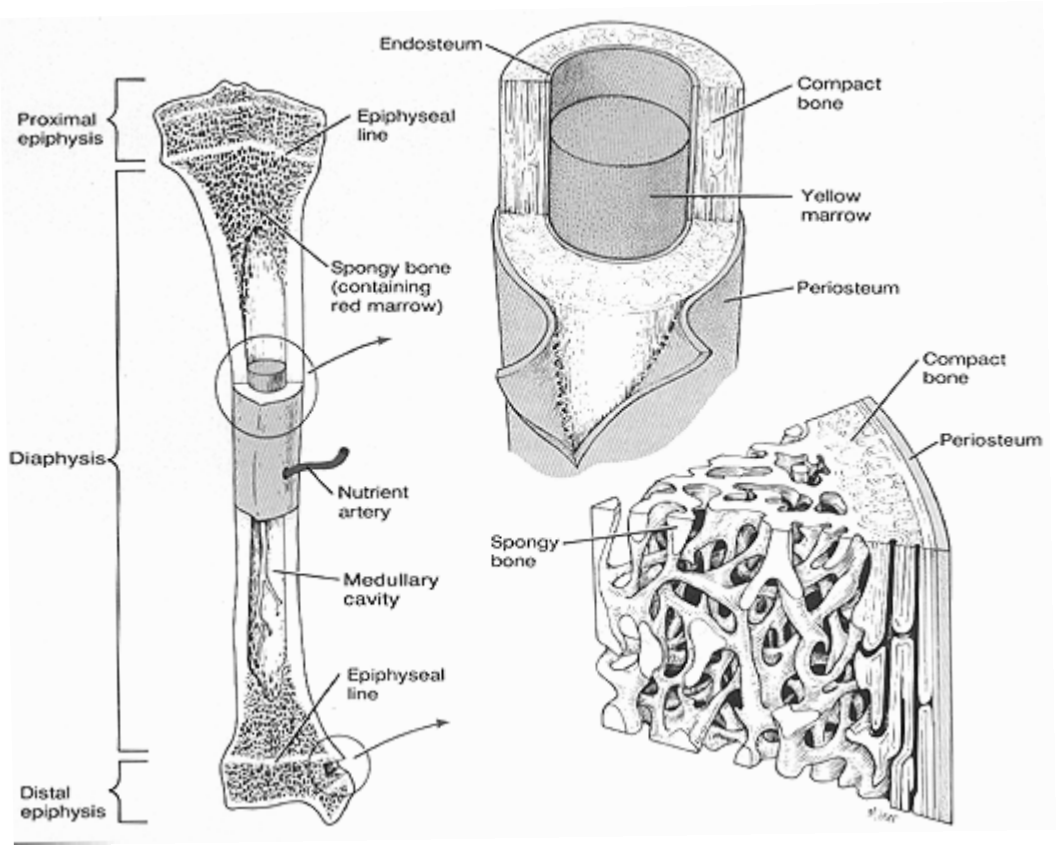


Figure 2.1. Macroscopic bone structure. The different areas of a long femur are shown, as well as the different types of bone in each area: cancellous or spongy, and cortical or compact [14].

On a microscopic level, there are two different types of bone: woven and lamellar. Woven bone is generally immature tissue that is generated for rapid bone formation such as in the repair of fractures and other injuries. Collagen fibers are arranged in a random fashion and give the tissue an isotropic behavior. Lamellar bone presents a more organized structure that consists of parallel sheets and bundles[1,5].

Cortical bone is made up in two thirds by osteons and the remaining is composed of interstitial bone derived from previous generations of osteons. Osteons are branching cylindrical columns with a diameter in the order of 150 μm and a

central vasculature canal called the Harvesian canal [11]. These canals connect with one another and with the marrow cavity via Volkmann's canals whose blood vessels are in fact larger than those of the Harvesian canal. In lamellar bone, osteons are oriented in a parallel fashion along the axis of the tubular bone section. They are surrounded by a cement line that is a region of reduced mineral and collagen content. Osteons of woven bone have a different shape, a more random orientation and are bound to the bone marrow on one side and an irregular cement line on the other side [11,15,16].

2.1.5. Mechanisms of bone formation

After injury, bone can be replaced through two distinct mechanisms of bone formation (osteogenesis): intramembranous ossification and endochondral ossification. Intramembranous ossification is the process in which precursor cells, mesenchymal stem cells (MSC), differentiate directly into osteoblasts and begin secreting bone matrix. What appears as thin and disorganized trabeculae soon mineralizes, entrapping osteoblasts to form osteocytes. MSCs continue to differentiate to form woven bone. This woven bone also has the potential to become a primitive cortical bone if the mineral matrix grows at the expense of connective tissue. Intramembranous ossification is commonly found in the regeneration of certain bones of the skull [1,15,17,18].

Endochondral ossification represents a different mechanism from that of the intramembranous. As the name suggests this process starts by the deposition of a primitive cartilaginous tissue. Endochondral ossification usually takes place when there is a need for rapid growth. When the neocartilage is formed, new cells can be

easily incorporated into the tissue, expanding both its volume and length rapidly. This mechanism is also observed in embryonic bone formation, where an avascular cartilaginous model is created with the shape of the bone. Ossification follows with three processes occurring simultaneously [11,18,19]:

1. Formation of a collagen type I rich osteon outside the cartilage core, which later mineralizes to create a periosteal collar
2. Hypertrophy of chondrocytes in the center with enlargement of their lacunae and calcification of the remaining tissue
3. The cartilage core is penetrated by new blood vessels coming from the periosteum, bringing along hematopoietic and osteoprogenitor cells that eventually calcify the entire cartilage volume

Once the bone is formed, it undergoes a process of modeling and remodeling by which the skeleton is continuously renewed so as to maintain its mechanical properties, prevent the accumulation of fatigue, and minimize micro fractures, among other things. Remodeling is a surface process that begins by osteoclastic resorption of the existing organic and mineral components, forming a cavity. After reaching a certain depth, osteoclast activity ceases and they are replaced by macrophage-like cells that deposit an early, immature tissue. Osteoblasts later start forming a new osteon within the cavity [1,11,16,20].

2.2 The need for bone tissue engineering

Every year there are more than 8.6 million procedures related to bone injury worldwide, a great portion of these require the use of an implant in order to recuperate bone functionally in the affected area. In 2001, expenditures related to bone implants surpassed $1 billion [21]. Cases where implants are necessary are usually related to the destruction of a large portion of the bone, infections, or in any other circumstance where the body can not regenerate the damaged osseous tissue, causing the disability of the patient. This type of therapy is needed in any part of the skeleton; however, usually the most affected areas are long bones, spinal cord, and maxillofacial bones. The estimated expenditures due to bone grafts needed for these surgeries is about $500 million with over 605,000 procedures a year in the United States alone [21,22].

Traditional tissue replacement therapies consist of implants made out of synthetic materials such as titanium and ceramics that can meet the mechanical demands of the injury site, enabling temporal recovery of the functionality. Nonetheless, these implants, which to a certain degree are successful in reestablishing functionality, generally exert considerable stress on the surrounding tissue resulting in significant wear over time [23-26]. Thus, further surgeries on a regular basis become necessary, increasing not only the cost of the therapy but also the patient's discomfort. The use of constructs that can interact with the body, induce the formation of new tissue and be fully incorporated is the most desirable solution to this problem. Natural grafts would be ideal for this application because they possess part of the chemical and mechanical environment necessary for the optimal performance of the tissue. There are different kinds of natural grafts used to regenerate tissue *in vivo* [27-31].

Autografts: in this therapy, a piece of tissue is harvested from a healthy site of the same patient's skeleton and implanted at the area of injury. This therapy does not pose any problems of host acceptance; nevertheless, the surgical procedure would be considerably invasive and painful for the patient and morbidity of the site of harvesting is a major concern. Additionally, the amount of harvested tissue is limited and thereby off-the-shelf availability is very challenging [28,29,32,33].

Allografts: these grafts are harvested from another individual of the same species, usually a cadaver. The limitations in terms of the amount of tissue being harvested still remain, and host acceptance may arise, causing undesired immune reactions and potential disease transmission [29,34].

Xenografts: these grafts are harvested from a member of a different species. For human tissue regeneration, this therapy mitigates the problems of availability encountered with the autografts and allografts. Nevertheless, in addition to the risk of a strong immune reaction, there exists a great possibility of transmission of animal viruses [30,35].

All the limitations encountered with these different technologies have led researchers to the development of new approaches based on the combination of different bioactive components. The goal of tissue engineering is then to create artificial constructs that induce the formation of new tissue at the site of injury by activating a cascade of events related to wound healing and the process bone formation. Tissue engineering is based on the principle that new tissue formation can be guided through the use of cells, biomaterials and bioactive molecules [36]. Ultimately, recovery of total functionality is the ultimate goal of this field. The most common strategy employed in tissue engineering consists on the extraction of a

biopsy of autologous tissue without compromising the functionality of the harvesting site (Figure 2.2). Cells extracted from this piece of tissue are then cultured and expanded in a three dimensional scaffold that supports their growth and differentiation [36]. Furthermore, the *in vitro* creation of an efficient construct can be accelerated by applying certain stimuli, chemical or mechanical, that can elicit specific responses to the cells.

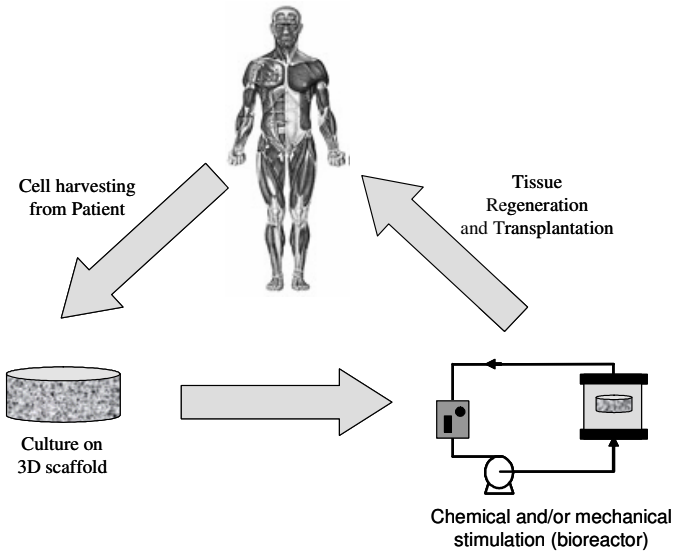


Figure 2.2. The tissue engineering paradigm. Cells are harvested from the patient for expansion in a three dimensional scaffold; they are later mechanically stimulated in a bioreactor for implantation and regeneration of the damaged or lost tissue [37]

2.3. Cell Source for Bone Tissue Engineering

The type of cells utilized in a specific tissue engineering application is of extreme importance. Cells cultured *in vitro* will generate an initial, immature tissue by depositing an extracellular matrix (ECM) rich in tissue-specific proteins and growth

factors. These cells will strongly interact with the scaffolding material and respond to any environmental stimulus both *in vitro* and early after implantation in the body. Consequently, choosing the right cell type will affect the development of the *in vitro* culture and the efficient tissue regeneration both early and later after implantation. One of the first cell-based approaches for bone tissue engineering was the use of fresh, unfractioned bone marrow, which is rich on osteogenic precursors [38-40]. The bone marrow is usually extracted from a healthy site of the patient, i.e. the iliac crest, and implanted in the defect site thereby preventing immune rejection. However, the greatest limitation to this approach is the lack of availability of sufficient marrow aspirate for transplantation [41]. Stem cells, such as mesenchymal stem cells (MSC), are pluripotent cells found in the bone marrow. They have the potential for differentiation into different lineages (Figure 2.3) in addition to the ability of being cultured and greatly expanded *in vitro* without differentiation and without loosing the potential for differentiation. Their potential for clinical application has been shown in different *in vivo* studies, where regeneration of bone has been observed [42-46].

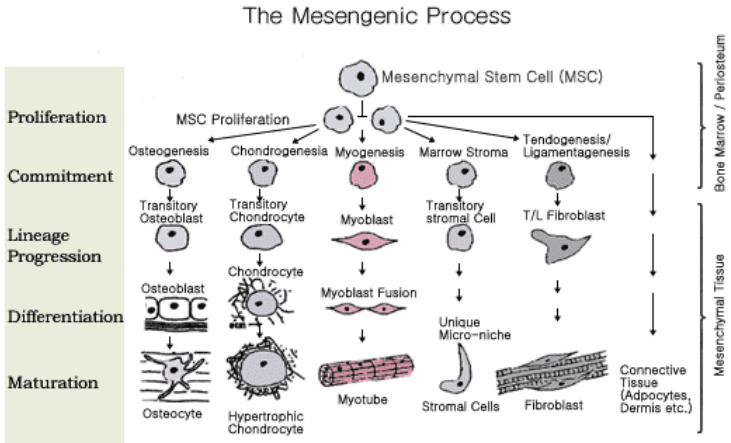


Figure 2.3. Differentiation potential of adult bone marrow mesenchymal stem cells. Several steps are involved in the mesengenic process as stem cells differentiate into tissue specific cells [47].

Specific stem cell differentiation can be achieved through the use of growth and differentiation factors or by the application of certain mechanical stimuli that will be discussed later in this chapter [16,48-52]. MSC harvested from the bone marrow can be differentiated into the osteoblastic lineage by being cultured in the presence of β-glycerophosphate, dexamethasone and ascorbic acid [48]. When cultured under these conditions, MSCs undergo a cascade of morphological and functional changes that lead up to their transformation into osteoblasts. Usually, MSC which are fibroblastic in appearance, assume a cuboidal shape and tend to form communities that will eventually form hydroxyapatite- mineralized nodules late in the differentiation cascade. Other events that take place during osteogenic differentiation include the transient up-regulation of alkaline phosphatase (AP) activity, while at the late states collagen type I is down-regulated, and the production of ECM proteins such as osteopontin, osteocalcin and bone sialoprotein are up-regulated [47,48,53].

2.4. Scaffold Technologies in Bone Tissue Engineering

The biochemical and physical interactions of the cells with the scaffold are of crucial importance in the process of tissue regeneration. The deposition of extracellular matrix by the osteoblastic cells on the surface of the scaffolds improves the osteoinductive potential of the construct once implanted *in vivo*. Thus, strong cell-matrix interactions between the cultured cells and the scaffold will result in greater expression of extracellular matrix components. The scaffold has to thereby support the adhesion of the cells, as wells as their growth, migration and differentiation towards a specific phenotype, in this case, osteoblasts [54,55].

Certain mechanical and morphological requirements must be met by the scaffold in order to achieve a more efficient regeneration process [56]. The scaffolding material needs to have mechanical properties that can meet the demands of the defect site, especially when the injury occurs in a load-bearing zone. Sufficient porosity, an optimum pore size and pore interconnectivity are necessary for the nutrition of the cells. It is important to achieve the formation of neotissue and a vascular network that will guarantee the survival of the newly formed tissue. Ideally, the scaffold should be biodegradable so as to permit further formation of tissue as it degrades. However, this process needs to occur without compromising the mechanical demands at the site of implantation. [29,56-58]

Scaffolds for tissue engineering have been created using a wide variety of techniques and materials, both synthetic and natural. Collagen is the most widely used material for the creation of scaffolds in numerous tissue engineering applications ranging from cardiovascular tissue to bone [59-68]. Other important natural materials include glycosaminoglycans, which are traditionally used for cartilage reconstruction; however, crosslinked heparin and hyaluronic acid have been found to support the deposition of mineral matrix [69-73]. Some popular choices for synthetic materials include ceramics, metals such as titanium, poly-ethylene glycol and biodegradable polymers [74,75]. Poly(α-hydroxy esters) are widely used biodegradable polymers for bone and other tissue engineering therapies due to their well known degradation characteristics and the fact that they are approved by the Food and Drug Administration, particularly poly(lactic acid), poly(glycolic acid) and their copolymers. Both types of materials present advantages and disadvantages. Generally being part of the ECMs of different tissues, natural materials can be chosen to possess the right chemical composition to allow strong cell-matrix interactions and thereby

provide the appropriate environment for the cells to attach, migrate and proliferate. Nonetheless, most of these materials present poor mechanical properties, posing a limitation for the regeneration of certain tissues such as bone in load bearing zones. Greater mechanical properties can be acquired through the right modulation of synthetic materials in terms of their chemistries and morphologies. The disadvantage of synthetic materials is often due to the lack of functional groups that the cells are known to interact with.

Scaffolds for tissue engineering can be injectable or preformed. Injectable materials are *in situ* polymerizable and generally come in the form of hydrogels and ceramic pastes, which can be made of different synthetic and natural materials. Poly(ethylene glycol) and modifications of it are some of the most widely used hydrogels. Injectable scaffolds are able to fit injuries with odd shapes and they also require implantation procedures with a minimal level of invasiveness [76,77]. They also have drawbacks such as potentially poor mechanical properties and inability to work for large defects, but most importantly, they may result in high levels of cytotoxicity negatively affecting the surrounding tissue. Preformed scaffolds, as the name suggests, are scaffolds formed *in vitro* prior to implantation. Many different techniques have been used to create them: fiber bonding, solvent-casting, particulate leaching, micro-printing, melt molding, etc [78-83]. All these techniques are capable of producing porous scaffolds that can sustain cell attachment and growth, and provide open spaces for nutrient transport. Most of these scaffolds minimize risks of cytotoxicity and have better mechanical properties than preformed scaffolds, but their implantation can be rather invasive.

Most biodegradable polymers used in preformed scaffolds are able to support cell adhesion and growth to a certain extent, yet they possess a hydrophobic and inert nature that limits cell-matrix interactions [84]. Consequently, the creation of a construct that can mimic the *in vivo* molecular environment and enhance cell-matrix interactions is imperative in the process of creating efficient constructs [60,85]. The development of these biomimetic scaffolds involves the bulk or surface modification of the base biomaterial with growth and differentiation factors that can improve cell attachment, proliferation, and migration, as well as eliciting other specific cellular responses and biological signals to the surrounding extra cellular matrix (ECM) of the tissue *in vivo* such as development of angiogenesis [36,60].

The most common way to modify biodegradable polymers is by chemically grafting them with a bioactive molecule [60,86-88]. Shan-hui H et al improved cell attachment by cross linking poly (lactic-*co* glycolic acid) (PLGA) with collagen type II [89]. Cook et al also increased the number of cells attached to the surface and improved cell spreading by covalently attaching arginine-glycine-aspartic acid (RGD) peptides to PLGA [90].

Physisorption is another technique that has been utilized for surface modification of tissue engineering scaffolds [91,92]. Yang et al induced adsorption poly(L-lysine)-GRGDS conjugates to the surface of poly(L-lactic acid) (PLLA) films and porous scaffolds, affecting the osteoblasts' response not only in terms of cell adhesion but also on differentiation and the long term deposition of extracellular matrix [88]. However, this methodology poses the risk of desorbing the incorporated bioactive molecules. Cui et al entrapped gelatin in the surface of PLLA films and enhanced the attachment of chondrocytes, overcoming, at the same time, the problem

of desorption of the bioactive molecule [93]. In our studies we have used partial dissolution and entrapment of bioactive molecules for the creation of biomimetic scaffolds that can be further functionalized for specific applications.

2.5. Bioreactors in Bone Tissue Engineering

A bioreactor is described as a simulator, a device in which biological and/or biochemical processes can be carried out [57]. In tissue engineering, bioreactors are used to impart certain forces that imitate different mechanical stimuli that simulate those occurring in the body. However, these devices are not limited to the sole application of mechanical stimuli; they must meet other requirements in order to create grafts that, when implanted, will lead to the regeneration of damaged organs. A bioreactor must efficiently transport nutrients and oxygen to the construct, maintaining an appropriate concentration in solution. In most tissue engineering applications, a scaffold is seeded with cells that supports the formation of extracellular matrix (ECM). Consequently, the bioreactor has to induce a homogeneous cell distribution throughout these structures in order to generate a uniformly distributed ECM. Tissue engineering bioreactors can be used for cell seeding and/or long term cultures.

2.5.1. Common Bioreactors Designs in Tissue Engineering

The choice of a bioreactor to cultivate three dimensional constructs depends upon the tissue to be engineered and its functional biomechanical environment. Emulation of physiological conditions is the main objective when developing these

kinds of systems, and this issue has been addressed in different ways. The incorporation of convective forces has become a common characteristic among most bioreactors. Some bioreactors that meet some these characteristics and are often used in many different applications are:

Spinner Flask: The spinner flask (Figure 2.4b) represents one of the simplest bioreactor models. It was first designed with the idea to use convection in order to maintain a well mixed system. The scaffolds are threaded into needles connected to the cover of the flask, and submerged in the culture medium. Convection is generated through the usage of a magnetic stir bar or a shaft that continuously mixes the media surrounding the scaffolds, providing a practically homogenous distribution of oxygen and nutrients [52,94]. The fluid dynamic environment at the external surface of the scaffolds is turbulent and characterized by the existence of eddies that may enhance the transport of nutrients into the porosity, and locally expose cells residing at the exterior of the construct to relatively high shear forces. The magnitude of the shear stresses can vary significantly between different locations; therefore, not all the cells are exposed to the same shear stresses. The presence of convective forces external to the scaffolds may not suppress concentration gradients appearing deep inside large three dimensional constructs, where diffusion is the controlling mechanism of nutrient transport [95,96].

Rotating-Wall Vessels: Initially designed by NASA as a microgravity environment for cell culture, the rotating wall bioreactor (Figure 2.4c) is now widely used in the formation of engineered bone, cartilage, and other tissues [52,94,97,98]. This device consists of two concentric cylinders whose annular space contains the cell culture medium [99]. The inner cylinder is static and permeable to allow gas exchange

for oxygen supply. The outer cylinder, on the other hand, is impermeable and horizontally rotates at a speed that causes centrifugal forces that can balance, if tuned properly, the gravitational forces; thus, generating a pseudo microgravity environment [52,99,100]. Unlike the spinner flask, in the rotating wall vessel the fluid flow is mostly laminar and the range of shear forces experienced by the cells at the outer surface is relatively narrow, with the existence of a stagnation zone at the upstream edge. As reported by Williams et al, shear stresses decrease in the direction of flow, and no significant variations from scaffold to scaffold are observed [101]. Medium can be recirculated between the annular space and an external gas membrane. A modification of the original design, called rotating-wall perfused-vessel bioreactor, includes the rotation of the inner cylinder. In this model, media is perfused from the vessel's end cap to the pores of the inner cylinder [100].

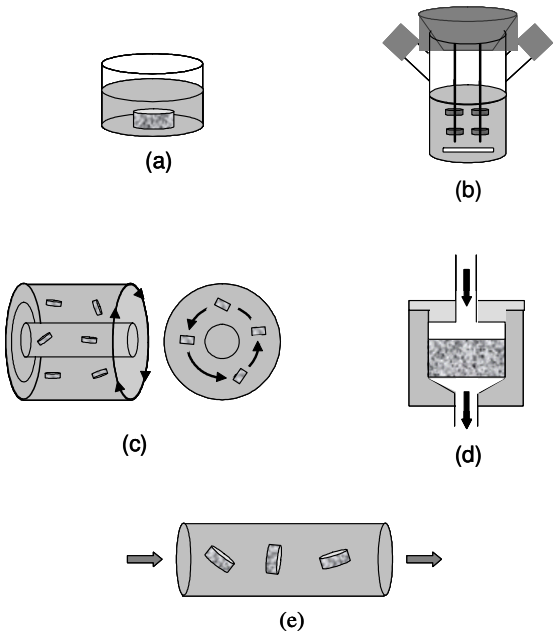


Figure 2.4. Common bioreactors used in tissue engineering. (a) Static culture (b) Spinner flask (c) Rotating wall (d) Perfusion system (e) Perfused column [37]

Perfusion Chambers and Flow Perfusion Systems: Flow perfusion bioreactors provide continuous flow through chambers where the scaffolds are located. The perfusion column (Figure 2.4e) was one of the first designs of this kind of bioreactors. Culture medium is continuously recirculated through the chamber, thus improving the transport of nutrients and oxygen to the constructs [62,102,103]. Nevertheless, the flow of medium in these chambers is distributed between the inner network of the construct and its surroundings, minimizing convective flow through the scaffold [79,104,105]. To ensure that the flow of medium occurs exclusively through the porosity of the material, new designs of flow perfusion bioreactors include the confining of the construct in chambers (figure 2.4d). In this way, a more controllable flow is achieved and nutrient transport limitations are virtually eliminated. Internal flow can also expose the cells inside the scaffold to fluid shear forces that have been known to be stimulatory for some cell types such as osteoblasts and endothelial cells [51,105,106]. A standard design of this kind of reactors does not exist, but all of them are based on the same principle. A more detailed description of a perfusion system will be given later in this chapter.

2.5.2. Cell Seeding in Bioreactors

The first step to culturing cells in a three dimensional environment is the seeding of scaffolds [107]. Along with the characteristics of the material, this process plays a crucial role in the development of efficient constructs for tissue engineering. Seeding of scaffolds determines the initial number of cells in the construct, as well as their spatial distribution throughout the matrix. Consequently, proliferation, migration and the specific phenotypic expression of the engineered tissue will be affected by the

seeding technique utilized [102]. In the case of tissues that require a fibrous or porous material, static seeding has been the most widely used method of cell seeding (see Figure 2.4a). Burg et al., compared different seeding techniques using rat aortic cells in poly(glycolide) fibrous meshes. Static seeding produced the poorest cellular distribution [108]. In addition to preventing a homogeneous spatial distribution of the cells, static seeding also produces a low yield [57,108]. Holy et al., reported a 25% efficiency of attac hment after seeding 0.5 to $10x10^6$ cells on porous PLGA 75/25 scaffolds [57]. A low yield diminishes the development of specific functions related to cell-cell interactions and increases the amount of cells necessary; therefore, the usage of new seeding techniques becomes imperative.

In order to address these issues, researchers have incorporated convection into the process of cell seeding, suppressing some of the mass transfer limitations encountered in the static procedure. Spinner flask bioreactors (figure 2b) have been implemented to create convection and, thereby, hydrodynamic forces that could help increase mass transport. Poly(glycolic acid) (PGA) scaffolds were threaded onto needles, and chondrocytes suspensions with a total number of cells between $2x10^6$ and $10x10^6$ were used. A yield of 60% was obtained after 2 hours of seeding. A more uniform distribution of the cells in the scaffold was seen (compared to the static seeding); nonetheless, the concentration of cells in the outer layer of the construct was 60-70% higher than that in the bulk [109]. This behavior may be due to the poor convection to the interior of the scaffold, making migration the only way for cells to reach the interior of the scaffold.

It has been reported that, in the spinner flask, the shear forces at the external surface of the scaffold are highly non-uniform. Such variability may influence the homogeneity of the seeded cells even when considering only the external surface area [96]. However, despite the high efficiency of seeding achieved with the spinner-flask bioreactor, a more homogeneous distribution of the cells throughout the construct volume is still desired.

One way to guarantee mass transfer to the interior of the scaffold and a better distribution of cells is by applying perfusion [79,108,110]. In this technique, the construct is press fitted into a chamber, and the cell suspension is flowed through it (figure 2c). Li et al., used a depth filtration system to seed poly(ethylene terephthalate) matrices at a rate of 1ml/min. The cell suspension was recycled to increase the yield. Cell density increased along with the inoculation cell number, with an efficiency of about 65%, while with the static seeding, the yield stayed constant and lower than that achieved with perfusion [102]. Similarly, Kim et al seeded hepatocytes on polymeric matrices using a flow perfusion system. A suspension of rat hepatocytes at a density of $5x10^6$ cells/ml was pumped through bone matrices at a flow rate of 1.5 ml/min for 4 h. A total of approximately $4.4x10^6$ cells were attached to the matrix, which was considered successful. Furthermore, scanning electron microscopy and histology confirmed a uniform distribution of hepatocytes throughout the scaffold.

Wendt et al., monitored seeding efficiency and uniformity of static, spinner flask and perfusion systems [110]. Using the same inoculation concentrations, there was not statistical significance among the efficiencies of the static and perfused techniques, both producing a larger yield than the spinner flask. Uniformity, however,

was optimized by the perfusion apparatus, while the static and the spinner flask generated cell-scaffold constructs with low spatial uniformity [110].

2.5.3. Development of Bone-Like Extracellular Matrix in Bioreactor Systems

Bone is a hard connective tissue that provides mechanical support to the human body and is a frame for locomotion. Bone grafts have been generated under a wide variety of culturing conditions, including static and dynamic systems. Among the most popular dynamic systems are spinner flasks, rotating wall vessels and perfusion systems [106,109,111]. Like for every tissue engineering approach, before deciding upon the kind of bioreactor to be used, considerations concerning the carrier matrix, cells (osteoblasts, mesenchymal stem cells, etc.) and growth factors must be taken into account. In the case of bone, the matrix to be used must be osteoconductive, provide mechanical support, deliver cells and allow their attachment, growth, migration and osteoblastic differentiation. Synthetic and natural polymers have been implemented. Among the synthetic polymers poly(α-hydroxy esters), poly(ε-caprolactone), poly(propylene fumarate), poly(sebacic acid) and their copolymers have been widely used. Materials such as ceramics and titanium have been also used for bone replacement [74,75]. Cell number and calcium deposition are good markers to evaluate the evolution of bone matrix. Furthermore, alkaline phosphatase activity (ALP) is used to assess early differentiation activity of osteoblastic cells. Production of extracellular matrix proteins such as osteocalcin, osteopontin and bone sialoprotein is also taken into consideration [112].

As mentioned earlier, static culture was one the first attempts to produce bone matrix. Ishaug et al., seeded marrow stromal cells on top of poly (DL-lactic-co-glycolic acid) foams of different pore sizes at different densities. Cell proliferation was supported by the scaffold, and high level of ALP activity and calcium matrix deposition were observed. It was found that the depth of mineralized tissue increased over time, but the maximum penetration was only around 240μm, resulting in a non homogeneous cell and matrix distribution [84].

Improvement in the development of bone matrix *in vitro* has been achieved with the addition of convection in the *in vitro* culture stage, which ultimately translates in a better transport of nutrients and gases. After statically seeding $1x10^6$ marrow stromal cells on PLGA scaffolds, Sikavitsas et al., cultured these constructs under three different conditions: statically, in a spinner flask and in a rotating-wall vessel [52]. The culture was carried out for 21 days, and samples were analyzed at 7, 14 and 21 days. Scaffolds cultured in the spinner flask bioreactor showed the largest number of cells at all time points, followed by the static culture. At the end of the culture period, constructs in the spinner flask presented higher calcium contents than those encountered in the static and rotating wall vessel [52].

Shea et al., also utilized a spinner flask to culture poly(lactic acid) foams seeded with MC3T3-E1 pre-osteoblasts and evaluated their differentiation [59]. Cells were seeded statically and cultured for 12 weeks. Proliferation was observed over time; however, their distribution throughout the scaffold lacked homogeneity. Cells were densely located only at a thin layer of 200μm near the scaffold's surface. The density dramatically decreased deeper into the construct. The same behavior was seen for the formation of extracellular matrix and calcium deposition.

It has been shown that mechanical stimulation augments the production of alkaline phosphatase, osteoblast proliferation, and mineral deposition in osteoblastic cells seeded on different scaffolding materials [113]. Osteoblastic cells have been shown to be responsive to shear stress induced by fluid flow. The stimulatory effect of shear stresses has shown to induce an increase in the release of important regulatory factors such as nitric oxide and prostaglandin E2 [16,114]. Interestingly, osteoblasts have been found to be more responsive to fluid shear forces than mechanical strain [115]. A question arises then, what is the physiological relevance of the stimulatory effect of fluid flow on bone cells? It has been hypothesized that mechanical strains on bone tissue cause fluid flow in the lacunar-canalicular porosity of bone [116-118]. Consequently, the incorporation of fluid flow through the porous network is desired in order to stimulate a faster and more efficient formation of bone matrix. This goal has been reached with the implementation of flow perfusion bioreactors [92,106,119].

Bancroft et al., developed a perfusion system (figure 2.4) where medium is pumped through the scaffold, thereby maintaining mechanical stimulation and transport of nutrients through the pores [94]. The scaffolds are tightly fit into cassettes in order to ensure fluid flow exclusively through the porous network. Constructs are later placed in flow chambers that are capped and secured with o-rings to restrict the flow around them (figure 2.5a). The medium is pumped from a flask to the top of the chamber and sent to another reservoir from the bottom. This direction of flow helps avoiding the entrance of air bubbles into the flow chamber. Both flasks are connected so that the medium is in continuous recirculation. The main body of the reactor consists of a total of six chambers and is made out of Plexiglas to allow the visualization and monitoring of the flow inside the chambers. Each chamber corresponds to an independent circuit using one of the heads of a peristaltic pump that

produces flow rates from 0.1 to 10 ml/min (Figure 2.5b). The tubing permits the exchange of carbon dioxide and oxygen with the atmosphere in the incubator. A complete change of medium can be done due to the two-reservoir set up [51,104].

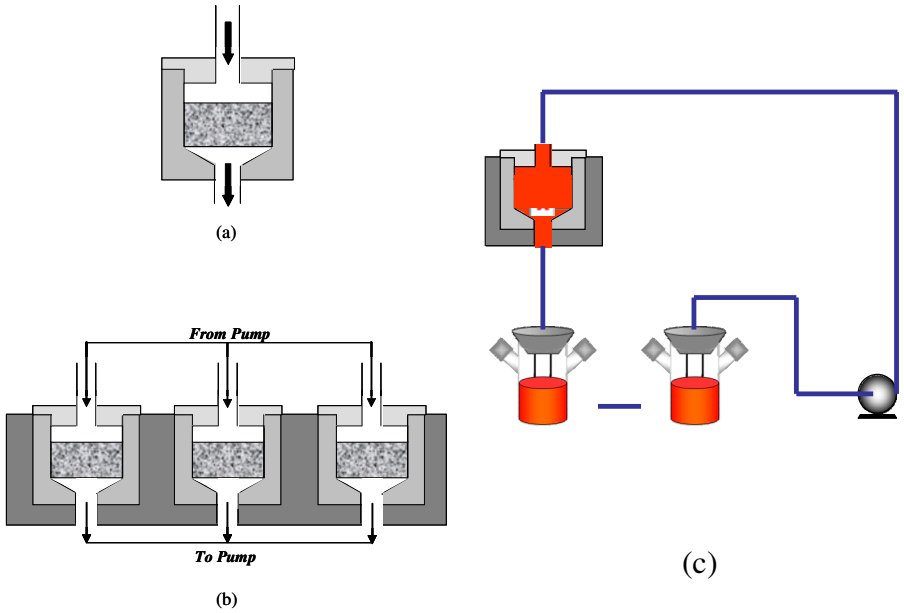


Figure 2.5. Schematics of a flow perfusion bioreactor (a) Close up of the perfusion chamber where the scaffold is press fitted (b) Lateral view of the main body of the bioreactor (c) Schematics of the system

To study how the shear rate affects the growth of bone matrix *in vitro*, Bancroft et al., varied the flow rate when culturing titanium fiber meshes seeded with rat marrow stromal cells for 16 days [51,105]. Controls had been cultured under static conditions, and the flow rates used in the perfusion culture were 0.3, 1.0 and 3.0 ml/min. It was found that the deposition of calcium was greatly increased in the flow perfusion culture as compared with the static conditions. It was also observed that increased medium flow improves the distribution of extracellular matrix throughout the construct volume [51,105]. The increased calcium deposition could have been due to the increased shear forces or increased chemotransport in the porosity of the scaffolds when higher flow rates were employed. To isolate the effects of shear forces from the mass transport effects, the shear forces were changed by varying the viscosity of the

culture medium under constant flow rate [51]. An increase in viscosity, which translates into greater shear forces, was found to enhance the deposition of mineral matrix and the ECM distribution throughout the construct, demonstrating the importance of fluid flow induced shear forces on the creation of bone tissue-engineered grafts.

Mainel et al., cultured human mesenchymal stem cells on silk scaffolds for five weeks in a flow perfusion chamber (at 0.2 ml/min) and a spinner flask. Scaffolds cultured under flow perfusion showed a more homogenous distribution of the mineralized matrix throughout the construct although those cultured in the spinner flask produced a greater amount of deposited calcium [119].

The use of flow perfusion greatly enhances the formation of bone matrix, activating mechanisms related to the differentiation of osteoblastic cells. Great challenges are still encountered however. What are the actual mechanisms that transduce the external shear forces and influence the cellular behavior? Currently, only estimates of the shear rates at the interior of three dimensional scaffolds have been provided, and detailed mathematical modeling needs to be conducted. Using larger scaffolds can represent another problem; is it possible to achieve a completely homogeneous distribution of matrix in larger constructs? What would be the necessary culturing conditions to achieve this? And how long and under what conditions must the cells be pre-cultured prior to the application of mechanical forces to avoid their detachment? By answering these questions, the field of tissue engineering could be enriched and take a more feasible route towards achieving practical applications.

In bone tissue, cells experience a degree of shear stress due to interstitial fluid flow. The shear stress was estimated by Weinbaum et al assuming peak physiological loading regimes, with values of 8-30 dynes/cm^2. This effect is mimicked in the flow perfusion bioreactor; therefore, it is important to estimate the values of average shear stresses experienced by the cells due to perfused flow.[120]

The mechanotransduction mechanisms by which the activity of bone cells is increased are still being investigated. However, it has been shown that different osteoblast and osteocytes receptors, such as integrins and CD44, that are located on their membrane, are stimulated by shear forces and convert the mechanical stimuli into different intracellular signaling pathways. Prostaglandins have also been shown to be involved in osteoblastic behavior in the presence of shear stress. Moreover, nitric oxide (NO) production increases in the presence fluid flow. NO is a mediator of many intracellular processes, and it is suggested that it maybe one of the major mediators of the response of osteoblasts to stress.[6]

The characterization of shear forces on the surface of tissue engineering scaffolds in the presence of perfusion has proven very challenging. Scaffolds generally possess non-uniform pore distribution. In the present work, the scaffolds used were prepared through two different techniques:

1. Porous foams by particulate leaching
2. Fibrous matrices by melt blowing

In the first case, foams made by particulate leaching, the pores represent a tortuous path with very irregular structures generated by the initial presence of sodium

chloride crystals (refer to Chapter 3 for more details on slat leaching). Thus, the estimation of shear stresses at different points of the scaffold's surface can be made by three dimensional computational modeling, usually based on the Lattice-Boltzman method. For the fibrous matrices prepared by melt blowing, the scenario is very similar since the fibers are randomly oriented.[121,122]

In the field of tissue engineering, the need for characterizing the distribution of shear stresses throughout the scaffold has been recognized. This analysis would allow for a detailed study of cell-matrix interactions due to fluid flow. Nevertheless, for the studies comprising the present doctoral research project, it was important to at least know the magnitude of the shear stresses. Models for the estimation of shear stress on scaffolds in the presence of flow perfusion are based on Newton's Law of Viscosity. Figure 2.6 shows a fluid placed between two parallel, infinite plates. At a certain time (t = 0) the lower plate is set in motion in the x direction at a constant velocity v. After some time, the linear steady state velocity profile is reached. It is assumed here that the flow is laminar, moving in parallel layers. Newton's law of viscosity establishes that the constant force, F, required to maintain the steady state motion is proportional to the area, A, and velocity, and inversely proportional to the distance, y. This is summarized in equation 2.1:

$$\tau = \frac{F}{A} = -\mu \frac{dv_x}{dy} \tag{2.1}$$

where τ is the shear stress, defined as the applied force per unit area necessary to deform the fluid. The symbol μ is the viscosity, and it is the proportionality constant between the shear stress and the shear rate (dv_x/dy). [123]

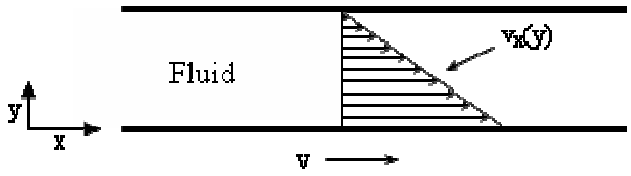


Figure 2.6. Steady state linear velocity profile of a Newtonian fluid between two plates.

For porous foams, it is assumed that the flow is uniformly distributed across a foam surface of diameter, D. The mean velocity, V_m, through the porous media is then calculated as [95]:

$$V_m = \frac{Q}{\phi\pi(D/2)^2} \tag{2.2}$$

where Q is the flow rate, and ϕ is the porosity of the scaffold. The shear stress, τ, at the pore walls can be estimated by assuming flow through parallel cylindrical pores of diameter d. [95]

$$\tau = \frac{8\mu V_m}{d} \tag{2.3}$$

For the fibrous matrices, the Stokes-Olsen model for flow around a cylinder can be applied [124]. This model was developed for creeping flow around a single cylinder. In the scaffolds used for the study presented in Chapter 3, fibers were separated by at least 150μm, which is considerably greater than the fiber size (20-50 μm). In addition to that, Reynolds numbers were very small at the conditions of flow used (Re < 1). Thus, this model was appropriate for estimating the magnitude of the shear stresses experienced by the cells under those conditions of flow perfusion. According to this model, the drag coefficient is expressed as follows [124]:

$$C_D = \frac{D}{\rho U^2 r} = \frac{8\pi}{\mathrm{Re} * \log\left(7.4/\mathrm{Re}\right)} \tag{2.4}$$

where D is the drag force per unit length, ρ is the density of the fluid, U is the velocity, r is the radius of the cylinder, and Re is the Reynolds number. Shear stress is defined as:

$$\tau = \frac{D}{A} \tag{2.5}$$

where A is the area of the cylinder, which is defined as A= 2πrL. Then considering the area per unit length, and knowing that the Reynolds number for flow around a cylinder is:

$$\mathrm{Re} = \frac{2r\rho U}{\mu} \tag{2.6}$$

where μ is the fluid's viscosity, equations 2.4, 2.5 and 2.6 are combined to obtain an expression for shear stress on the walls of the cylinder [124]:

$$\tau = \frac{2U\mu}{r * \log\left(7.4/\mathrm{Re}\right)} \tag{2.7}$$

2.6. References

1. Buckwalter, JA, Glimcher, MJ, Cooper, RR, Recker, R. Bone biology. II: Formation, form, modeling, remodeling, and regulation of cell function. Instr Course Lect. 1996;45:387-399.
2. Buckwalter, JA, Glimcher, MJ, Cooper, RR, Recker, R. Bone biology. I: Structure, blood supply, cells, matrix, and mineralization. Instr Course Lect. 1996;45:371-386.
3. Ducy, P, Schinke, T, Karsenty, G. The osteoblast: a sophisticated fibroblast under central surveillance. Science. 2000;289:1501-1504.
4. Owen, M. Histogenesis of bone cells. Calcif Tissue Res. 1978;25:205-207.
5. Walsh, WR, Walton, M, Bruce, W, Yu, Y, Gillies, R, Svehla, M. Cell Structure and Biology of Bone and Cartilage. In: An YH, Martin KL, eds. Handbook of Histology Methods for Bone and Cartilage. Totowa: Humana Press; 2003:35-58.
6. Nijweide, PJ, Burger, EH, Nulend, JK, Van der Plas, A. The Osteocyte. In: Bilezikian JP, Raisz LG, Rodan GA, eds. Principles of Bone Biology. 1 ed. New York: Academic Press; 1996:115-126.
7. Aarden, EM, Burger, EH, Nijweide, PJ. Function of osteocytes in bone. J Cell Biochem. 1994;55:287-299.
8. Bianco, P, Riminucci, M, Silvestrini, G, et al. Localization of bone sialoprotein (BSP) to Golgi and post-Golgi secretory structures in osteoblasts and to discrete sites in early bone matrix. J Histochem Cytochem. 1993;41:193-203.

9. Maillard, C, Berruyer, M, Serre, CM, Dechavanne, M, Delmas, PD. Protein-S, a vitamin K-dependent protein, is a bone matrix component synthesized and secreted by osteoblasts. Endocrinology. 1992;130:1599-1604.

10. Hauschka, PV, Mavrakos, AE, Iafrati, MD, Doleman, SE, Klagsbrun, M. Growth factors in bone matrix. Isolation of multiple types by affinity chromatography on heparin-Sepharose. J Biol Chem. 1986;261:12665-12674.

11. Steiniche, T, Hauge, EM. Normal Structure and Function of Bone. In: An YH, Martin KL, eds. Handbook of Histology Methods for Bone and Cartilage. Totowa: Humana Press; 2003:59-72.

12. Vesterby, A, Kragstrup, J, Gundersen, HJ, Melsen, F. Unbiased stereologic estimation of surface density in bone using vertical sections. Bone. 1987;8:13-17.

13. Yaszemski, MJ, Payne, RG, Hayes, WC, Langer, R, Mikos, AG. Evolution of bone transplantation: molecular, cellular and tissue strategies to engineer human bone. Biomaterials. 1996;17:175-185.

14. Spence, AP, Mason, EB. *Human anatomy and physiology*. 4th ed. St. Paul: West Pub Co.; 1992:xxv, 956, [994] p.

15. Caplan, AI. Bone development. Ciba Found Symp. 1988;136:3-21.

16. Sikavitsas, VI, Temenoff, JS, Mikos, AG. Biomaterials and bone mechanotransduction. Biomaterials. 2001;22:2581-2593.

17. Bruder, SP, Caplan, AI. Cellular and molecular events during embryonic bone development. Connect Tissue Res. 1989;20:65-71.

18. Fawcett, DW, Bloom, W, Fawcett, DW, Raviola, E. *Bloom and Fawcett, a textbook of histology*. 12th ed. New York: Chapman & Hall; 1994:xx, 964 p.

19. Pechak, DG, Kujawa, MJ, Caplan, AI. Morphological and histochemical events during first bone formation in embryonic chick limbs. Bone. 1986;7:441-458.

20. Parfitt, AM. Bone remodeling, normal and abnormal: a biological basis for the understanding of cancer-related bone disease and its treatment. Can J Oncol. 1995;5 Suppl 1:1-10.

21. Hing, KA. Bone repair in the twenty-first century: biology, chemistry or engineering? Philos Transact A Math Phys Eng Sci. 2004;362:2821-2850.

22. Reports, C. Orthopaedics: key markets and emerging technologies: PJB Publications; 2002.

23. Laurencin, CT, Ambrosio, AM, Borden, MD, Cooper, JA, Jr. Tissue engineering: orthopedic applications. Annu Rev Biomed Eng. 1999;1:19-46.

24. Chuang, HC, Cho, DY, Chang, CS, et al. Efficacy and safety of the use of titanium mesh cages and anterior cervical plates for interbody fusion after anterior cervical corpectomy. Surg Neurol. 2006;65:464-471; discussion 471.

25. Eingartner, C. Current trends in total hip arthroplasty. Ortop Traumatol Rehabil. 2007;9:8-14.

26. Goodman, SB, Ma, T, Chiu, R, Ramachandran, R, Smith, RL. Effects of orthopaedic wear particles on osteoprogenitor cells. Biomaterials. 2006;27:6096-6101.

27. Brown, KL, Cruess, RL. Bone and cartilage transplantation in orthopaedic surgery. A review. J Bone Joint Surg Am. 1982;64:270-279.

28. Freeland, AE, Rehm, JP. Autogenous bone grafting for fractures of the hand. Tech Hand Up Extrem Surg. 2004;8:78-86.

29. Bostrom, RD, Mikos, AG. Tissue Engineering of Bone. In: Atala A, Mooney DJ, eds. Synthetic biodegradable polymer scaffolds. Boston: Birkhäuser; 1997:215.

30. Cascalho, M, Ogle, BM, Platt, JL. The future of organ transplantation. Ann Transplant. 2006;11:44-47.

31. Kretlow, JD, Mikos, AG. Review: mineralization of synthetic polymer scaffolds for bone tissue engineering. Tissue Eng. 2007;13:927-938.

32. Kessler, P, Thorwarth, M, Bloch-Birkholz, A, Nkenke, E, Neukam, FW. Harvesting of bone from the iliac crest--comparison of the anterior and posterior sites. Br J Oral Maxillofac Surg. 2005;43:51-56.

33. Nkenke, E, Weisbach, V, Winckler, E, et al. Morbidity of harvesting of bone grafts from the iliac crest for preprosthetic augmentation procedures: a prospective study. Int J Oral Maxillofac Surg. 2004;33:157-163.

34. Strong, DM, Friedlaender, GE, Tomford, WW, et al. Immunologic responses in human recipients of osseous and osteochondral allografts. Clin Orthop Relat Res. 1996:107-114.

35. Yang, YG, Sykes, M. Xenotransplantation: current status and a perspective on the future. Nat Rev Immunol. 2007;7:519-531.

36. Bonassar, LJ, Vacanti, CA. Tissue engineering: the first decade and beyond. J Cell Biochem Suppl. 1998;30-31:297.

37. Alvarez-Barreto, JF, Sikavitsas, VI. Tissue Engineering Bioreactors. In: Boronzino JD, ed. Tissue Engineering and Artificial Organs. Vol 3. 3 ed. Boca Raton: Taylor & Francis Group; 2006:44-41.

38. Connolly, JF, Guse, R, Tiedeman, J, Dehne, R. Autologous marrow injection as a substitute for operative grafting of tibial nonunions. Clin Orthop Relat Res. 1991:259-270.

39. Werntz, JR, Lane, JM, Burstein, AH, Justin, R, Klein, R, Tomin, E. Qualitative and quantitative analysis of orthotopic bone regeneration by marrow. J Orthop Res. 1996;14:85-93.

40. Jackson, IT, Scheker, LR, Vandervord, JG, McLennan, JG. Bone marrow grafting in the secondary closure of alveolar-palatal defects in children. Br J Plast Surg. 1981;34:422-425.

41. Bruder, SP, Fox, BS. Tissue engineering of bone. Cell based strategies. Clin Orthop Relat Res. 1999:S68-83.

42. Castano-Izquierdo, H, Alvarez-Barreto, J, van den Dolder, J, Jansen, JA, Mikos, AG, Sikavitsas, VI. Pre-culture period of mesenchymal stem cells in osteogenic media influences their *in vivo* bone forming potential. J Biomed Mater Res A. 2007;82:129-138.

43. Bruder, SP, Kraus, KH, Goldberg, VM, Kadiyala, S. The effect of implants loaded with autologous mesenchymal stem cells on the healing of canine segmental bone defects. J Bone Joint Surg Am. 1998;80:985-996.

44. Bruder, SP, Kurth, AA, Shea, M, Hayes, WC, Jaiswal, N, Kadiyala, S. Bone regeneration by implantation of purified, culture-expanded human mesenchymal stem cells. J Orthop Res. 1998;16:155-162.

45. Kadiyala, S, Young, RG, Thiede, MA, Bruder, SP. Culture expanded canine mesenchymal stem cells possess osteochondrogenic potential *in vivo* and *in vitro*. Cell Transplant. 1997;6:125-134.

46. Vilquin, JT, Rosset, P. Mesenchymal stem cells in bone and cartilage repair: current status. Regen Med. 2006;1:589-604.

47. Bruder, SP, Caplan, AI. Bone Regeneration Through Cellular Engineering. In: Lanza RP, Langer R, Vacanti J, eds. Principles of Tissue Engineering. 2 ed. New York: Academic Press; 2000:682-696.

48. Jaiswal, N, Haynesworth, SE, Caplan, AI, Bruder, SP. Osteogenic differentiation of purified, culture-expanded human mesenchymal stem cells *in vitro*. J Cell Biochem. 1997;64:295-312.

49. Satija, NK, Gurudutta, GU, Sharma, S, et al. Mesenchymal stem cells: molecular targets for tissue engineering. Stem Cells Dev. 2007;16:7-23.

50. Sumanasinghe, RD, Bernacki, SH, Loboa, EG. Osteogenic differentiation of human mesenchymal stem cells in collagen matrices: effect of uniaxial cyclic tensile strain on bone morphogenetic protein (BMP-2) mRNA expression. Tissue Eng. 2006;12:3459-3465.

51. Sikavitsas, VI, Bancroft, GN, Holtorf, HL, Jansen, JA, Mikos, AG. Mineralized matrix deposition by marrow stromal osteoblasts in 3D perfusion culture increases with increasing fluid shear forces. Proc Natl Acad Sci U S A. 2003;100:14683-14688.

52. Sikavitsas, VI, Bancroft, GN, Mikos, AG. Formation of three-dimensional cell/polymer constructs for bone tissue engineering in a spinner flask and a rotating wall vessel bioreactor. J Biomed Mater Res. 2002;62:136-148.

53. Caplan, AI. Mesenchymal stem cells. J Orthop Res. 1991;9:641-650.

54. Saltzman, MW. Cell Interactions with Polymers. In: Lanza R, Langer R, Vacanti J, eds. Principles of Tissue Engineering. 2 ed. San Diego: Academic Press; 2000:221.

55. Vacanti, JP, Langer, R, Upton, J, Marler, JJ. Transplantation of cells in matrices for tissue regeneration. Adv Drug Deliv Rev. 1998;33:165-182.

56. Temenoff, JS, Lu, L, Mikos, AG. Bone Tissue Engineering Using Synthetic Biodegradable Polymer Scaffolds. In: Davies JE, ed. Bone Engineering. Toronto: University of Toronto; 2000:454.

57. Holy, CE, Shoichet, MS, Davies, JE. Engineering three-dimensional bone tissue *in vitro* using biodegradable scaffolds: investigating initial cell-seeding density and culture period. J Biomed Mater Res. 2000;51:376-382.

58. Whang, K, Healy, KE, Elenz, DR, et al. Engineering bone regeneration with bioabsorbable scaffolds with novel microarchitecture. Tissue Eng. 1999;5:35-51.

59. Shea, LD, Wang, D, Franceschi, RT, Mooney, DJ. Engineered bone development from a pre-osteoblast cell line on three-dimensional scaffolds. Tissue Eng. 2000;6:605-617.

60. Shin, H, Jo, S, Mikos, AG. Biomimetic materials for tissue engineering. Biomaterials. 2003;24:4353.

61. Nerem, RM, Seliktar, D. Vascular tissue engineering. Annu Rev Biomed Eng. 2001;3:225-243.

62. Mizuno, S, Allemann, F, Glowacki, J. Effects of medium perfusion on matrix production by bovine chondrocytes in three-dimensional collagen sponges. J Biomed Mater Res. 2001;56:368-375.

63. Langelier, E, Rancourt, D, Bouchard, S, et al. Cyclic traction machine for long-term culture of fibroblast-populated collagen gels. Ann Biomed Eng. 1999;27:67-72.

64. Zhu, Y, Wu, Z, Tang, Z, Lu, Z. HeLa cell adhesion on various collagen-grafted surfaces. J Proteome Res. 2002;1:559-562.

65. Seliktar, D, Black, RA, Vito, RP, Nerem, RM. Dynamic mechanical conditioning of collagen-gel blood vessel constructs induces remodeling *in vitro*. Ann Biomed Eng. 2000;28:351-362.

66. Feng, Z, Yamato, M, Akutsu, T, Nakamura, T, Okano, T, Umezu, M. Investigation on the mechanical properties of contracted collagen gels as a scaffold for tissue engineering. Artif Organs. 2003;27:84-91.

67. Ker, RF. The design of soft collagenous load-bearing tissues. J Exp Biol. 1999;202:3315-3324.

68. Chen, G, Sato, T, Ushida, T, Ochiai, N, Tateishi, T. Tissue engineering of cartilage using a hybrid scaffold of synthetic polymer and collagen. Tissue Eng. 2004;10:323-330.

69. Sagnella, S, Anderson, E, Sanabria, N, Marchant, RE, Kottke-Marchant, K. Human endothelial cell interaction with biomimetic surfactant polymers containing Peptide ligands from the heparin binding domain of fibronectin. Tissue Eng. 2005;11:226-236.

70. Farrell, E, Byrne, EM, Fischer, J, et al. A comparison of the osteogenic potential of adult rat mesenchymal stem cells cultured in 2-D and on 3-D collagen glycosaminoglycan scaffolds. Technol Health Care. 2007;15:19-31.

71. Benoit, DS, Anseth, KS. Heparin functionalized PEG gels that modulate protein adsorption for hMSC adhesion and differentiation. Acta Biomater. 2005;1:461-470.

72. Cristino, S, Grassi, F, Toneguzzi, S, et al. Analysis of mesenchymal stem cells grown on a three-dimensional HYAFF 11-based prototype ligament scaffold. J Biomed Mater Res A. 2005;73:275-283.

73. Lisignoli, G, Cristino, S, Piacentini, A, et al. Cellular and molecular events during chondrogenesis of human mesenchymal stromal cells grown in a three-dimensional hyaluronan based scaffold. Biomaterials. 2005;26:5677-5686.

74. Hollinger, JO, Battistone, GC. Biodegradable bone repair materials. Synthetic polymers and ceramics. Clin Orthop Relat Res. 1986:290.

75. Nam, YS, Yoon, JJ, Park, TG. A novel fabrication method of macroporous biodegradable polymer scaffolds using gas foaming salt as a porogen additive. J Biomed Mater Res. 2000;53:1.

76. Gomes, ME, Reis, RL, Mikos, AG. Injectable Polymeric Scaffolds for Bone Tissue Engineering. In: Reis RL, Roman JS, eds. Biodegradable Systems in Tissue Engineering and Regenerative Medicine. Boca Raton: CRC Press; 2005:29-38.

77. Nguyen, TK, West, JL. Photopolymerizable hydrogels for tissue engineering. Biomaterials. 2002;23:4307-4314.

78. Tuzlakoglu, K, Reis, RL. Formation of bone-like apatite layer on chitosan fiber mesh scaffolds by a biomimetic spraying process. J Mater Sci Mater Med. 2007;18:1279-1286.

79. Alvarez-Barreto, JF, Linehan, SM, Shambaugh, RL, Sikavitsas, VI. Flow Perfusion Improves Seeding of Tissue Engineering Scaffolds with Different Architectures. Ann Biomed Eng. 2007.

80. Mikos, AG, Bao, Y, Cima, LG, Ingber, DE, Vacanti, JP, Langer, R. Preparation of poly(glycolic acid) bonded fiber structures for cell attachment and transplantation. J Biomed Mater Res. 1993;27:189.

81. Mikos, AG, Lyman, MD, Freed, LE, Langer, R. Wetting of poly(L-lactic acid) and poly(DL-lactic-co-glycolic acid) foams for tissue culture. Biomaterials. 1994;15:55.

82. Butler, MJ, Sefton, M. Poly(butyl methacrylate-co-methacrylic acid) tissue engineering scaffold with pro-angiogenic potential *in vivo*. J Biomed Mater Res A. 2007;82:265-273.

83. Mapili, G, Lu, Y, Chen, S, Roy, K. Laser-layered microfabrication of spatially patterned functionalized tissue-engineering scaffolds. J Biomed Mater Res B Appl Biomater. 2005;75:414-424.

84. Ishaug, SL, Crane, GM, Miller, MJ, Yasko, AW, Yaszemski, MJ, Mikos, AG. Bone formation by three-dimensional stromal osteoblast culture in biodegradable polymer scaffolds. J Biomed Mater Res. 1997;36:17.

85. Hubbell, JA. Bioactive biomaterials. Curr Opin Biotechnol. 1999;10:123.

86. Elbert, DL, Hubbell, JA. Conjugate addition reactions combined with free-radical cross-linking for the design of materials for tissue engineering. Biomacromolecules. 2001;2:430.

87. Rowley, JA, Madlambayan, G, Mooney, DJ. Alginate hydrogels as synthetic extracellular matrix materials. Biomaterials. 1999;20:45.

88. Yang, XB, Roach, HI, Clarke, NM, et al. Human osteoprogenitor growth and differentiation on synthetic biodegradable structures after surface modification. Bone. 2001;29:523.

89. Hsu, SH, Tsai, CL, Tang, CM. Evaluation of cellular affinity and compatibility to biodegradable polyesters and Type-II collagen-modified scaffolds using immortalized rat chondrocytes. Artif Organs. 2002;26:647.

90. Cook, AD, Hrkach, JS, Gao, NN, et al. Characterization and development of RGD-peptide-modified poly(lactic acid-co-lysine) as an interactive, resorbable biomaterial. J Biomed Mater Res. 1997;35:513.

91. Schense, JC, Hubbell, JA. Cross-linking exogenous bifunctional peptides into fibrin gels with factor XIIIa. Bioconjug Chem. 1999;10:75-81.

92. van den Dolder, J, Bancroft, GN, Sikavitsas, VI, Spauwen, PH, Jansen, JA, Mikos, AG. Flow perfusion culture of marrow stromal osteoblasts in titanium fiber mesh. J Biomed Mater Res A. 2003;64:235-241.

93. Cui, YL, Hou, X, Qi, AD, et al. Biomimetic surface modification of poly (L-lactic acid) with gelatin and its effects on articular chondrocytes *in vitro*. J Biomed Mater Res. 2003;66A:770.

94. Darling, EM, Athanasiou, KA. Articular cartilage bioreactors and bioprocesses. Tissue Eng. 2003;9:9-26.

95. Goldstein, AS, Juarez, TM, Helmke, CD, Gustin, MC, Mikos, AG. Effect of convection on osteoblastic cell growth and function in biodegradable polymer foam scaffolds. Biomaterials. 2001;22:1279.

96. Sucosky, P, Osorio, DF, Brown, JB, Neitzel, GP. Fluid mechanics of a spinner-flask bioreactor. Biotechnol Bioeng. 2004;85:34-46.

97. Vunjak-Novakovic, G, Obradovic, B, Martin, I, Freed, LE. Bioreactor studies of native and tissue engineered cartilage. Biorheology. 2002;39:259-268.

98. Saini, S, Wick, TM. Concentric cylinder bioreactor for production of tissue engineered cartilage: effect of seeding density and hydrodynamic loading on construct development. Biotechnol Prog. 2003;19:510-521.

99. Vunjak-Novakovic, G, Searby, N, De Luis, J, Freed, LE. Microgravity studies of cells and tissues. Ann N Y Acad Sci. 2002;974:504-517.

100. Begley, CM, Kleis, SJ. The fluid dynamic and shear environment in the NASA/JSC rotating-wall perfused-vessel bioreactor. Biotechnol Bioeng. 2000;70:32-40.

101. Williams, KA, Saini, S, Wick, TM. Computational fluid dynamics modeling of steady-state momentum and mass transport in a bioreactor for cartilage tissue engineering. Biotechnol Prog. 2002;18:951-963.

102. Li, Y, Ma, T, Kniss, DA, Lasky, LC, Yang, ST. Effects of filtration seeding on cell density, spatial distribution, and proliferation in nonwoven fibrous matrices. Biotechnol Prog. 2001;17:935.

103. Navarro, FA, Mizuno, S, Huertas, JC, Glowacki, J, Orgill, DP. Perfusion of medium improves growth of human oral neomucosal tissue constructs. Wound Repair Regen. 2001;9:507-512.

104. Bancroft, GN, Sikavitsas, VI, Mikos, AG. Design of a flow perfusion bioreactor system for bone tissue-engineering applications. Tissue Eng. 2003;9:549.

105. Bancroft, GN, Sikavitsas, VI, van den Dolder, J, et al. Fluid flow increases mineralized matrix deposition in 3D perfusion culture of marrow stromal osteoblasts in a dose-dependent manner. Proc Natl Acad Sci U S A. 2002;99:12600.

106. Cartmell, SH, Porter, BD, Garcia, AJ, Guldberg, RE. Effects of medium perfusion rate on cell-seeded three-dimensional bone constructs *in vitro*. Tissue Eng. 2003;9:1197.

107. Martin, I, Wendt, D, Heberer, M. The role of bioreactors in tissue engineering. Trends Biotechnol. 2004;22:80-86.

108. Burg, KJ, Holder, WDJ, Culberson, CR, et al. Comparative study of seeding methods for three-dimensional polymeric scaffolds. J Biomed Mater Res. 2000;52:576.

109. Vunjak-Novakovic, G, Obradovic, B, Martin, I, Bursac, PM, Langer, R, Freed, LE. Dynamic cell seeding of polymer scaffolds for cartilage tissue engineering. Biotechnol Prog. 1998;14:193.

110. Wendt, D, Marsano, A, Jakob, M, Heberer, M, Martin, I. Oscillating perfusion of cell suspensions through three-dimensional scaffolds enhances cell seeding efficiency and uniformity. Biotechnol Bioeng. 2003;84:205.

111. Botchwey, EA, Pollack, SR, Levine, EM, Laurencin, CT. Bone tissue engineering in a rotating bioreactor using a microcarrier matrix system. J Biomed Mater Res. 2001;55:242-253.

112. Nefussi, JR, Brami, G, Modrowski, D, Oboeuf, M, Forest, N. Sequential expression of bone matrix proteins during rat calvaria osteoblast differentiation and bone nodule formation *in vitro*. J Histochem Cytochem. 1997;45:493-503.

113. Pavlin, D, Dove, SB, Zadro, R, Gluhak-Heinrich, J. Mechanical loading stimulates differentiation of periodontal osteoblasts in a mouse osteoinduction model: effect on type I collagen and alkaline phosphatase genes. Calcif Tissue Int. 2000;67:163-172.

114. Klein-Nulend, J, Helfrich, MH, Sterck, JG, et al. Nitric oxide response to shear stress by human bone cell cultures is endothelial nitric oxide synthase dependent. Biochem Biophys Res Commun. 1998;250:108-114.

115. Owan, I, Burr, DB, Turner, CH, et al. Mechanotransduction in bone: osteoblasts are more responsive to fluid forces than mechanical strain. Am J Physiol. 1997;273:C810-815.

116. Burger, EH, Klein-Nulend, J. Mechanotransduction in bone--role of the lacuno-canalicular network. FASEB J. 1999;13 Suppl:S101-112.

117. Cowin, SC. Bone poroelasticity. J Biomech. 1999;32:217-238.

118. Knothe Tate, ML, Knothe, U, Niederer, P. Experimental elucidation of mechanical load-induced fluid flow and its potential role in bone metabolism and functional adaptation. Am J Med Sci. 1998;316:189-195.

119. Meinel, L, Karageorgiou, V, Fajardo, R, et al. Bone tissue engineering using human mesenchymal stem cells: effects of scaffold material and medium flow. Ann Biomed Eng. 2004;32:112-122.

120. Weinbaum, S, Cowin, S.C, Zeng, Y. A model for the excitation of osteocytes be mechanical loading-induced bone fluid shear stresses. J Biomech. 1994; 27: 339-360.

121. Porter, B, Zauel, R, Stockman, H, et al. 3-D computational modeling of media flow through scaffolds in a perfusion bioreactor. J Biomech. 2005; 38: 543-549.

122. Ethier, C.R. Flow through mixed fibrous porous materials. AIChE J. 1991; 37(8):1227-36

123. Bird, B.R, Steward, W.E., Lightfoot, E.N. Transport Phenomena. 2ed. John Wiley & Sons. New York, 2002, 11-13

124. Batchelor, G.K. An Introduction to Fluid Dynamics. Great Britain: Cambridge University Press; 1991:245-246.

Chapter 3

Oscillating Flow perfusion improves seeding of different tissue engineering scaffolds

Chapter Abstract

Scaffold seeding determines initial cellularity and cell spatial distribution throughout the scaffold, and affects cell-matrix interactions. Static seeding often yields low seeding efficiencies and poor cell distributions; thus creating a need for techniques that can improve these parameters. We have evaluated the effect of oscillating flow perfusion on seeding efficiency and spatial distribution of MC3T3-E1 pre-osteoblastic cells in fibrous polystyrene matrices (20, 35 and 50-μm fibers) and foams prepared by salt leaching, using as controls statically seeded scaffolds. An additional control was investigated where static seeding was followed by unidirectional perfusion. Oscillating perfusion resulted in the most efficient technique yielding higher seeding efficiencies, more homogeneous distribution and stronger cell-matrix interactions. Cell surface density increased with inoculation cell number and then reached a maximum, but significant detachment occurred at greater flow rates. Oxygen plasma treatment of the fibers greatly improved seeding efficiency. Having similar porosity and dimensions, fibrous matrices yielded higher cell surface densities than foams. Perfusion seeding produced more homogeneous cell distribution, with fibrous matrices presenting greater uniformity than the foams.

3.1 Introduction

The main goal of bone tissue engineering is to create artificial constructs that could repair or simply replace lost or damaged osseous tissue. Common tissue engineering strategies involve the extraction of cells from a small biopsy of tissue for *in vitro* expansion. This culture can be carried out in a three dimensional scaffold that allows and induces the formation of new tissue after implantation [1-4]. Most approaches in this field are based on common bioactive factors, consisting of cells (generally stem or tissue specific cells), a scaffolding material and growth and differentiation factors [5]. Furthermore, the *in vitro* creation of an efficient construct can be improved by applying certain stimuli that can elicit specific responses to the cells. Stimulation can be done in two major ways: chemically and mechanically [6-9].

The need for *in vitro* mechanical stimulation in tissue engineering is drawn from the fact that most tissues function under specific biomechanical environments *in vivo* that play a key role in tissue remodeling and regeneration [10,11]. These mechanical stimuli can be classified into different kinds of forces that range from load bearing to hydrodynamic forces due to fluid flow [9,11]. Thus, the mechanochemical microenvironment that progenitor cells grow into is expected to control the fate of these cells and influence their differentiation.

In many tissue engineering applications, bioreactors are used to impart certain forces that imitate different mechanical stimuli occurring in the body, thereby enhancing the formation of an extracellular matrix (ECM) similar to the *in vivo* matrix [12-19]. However, these devices are not limited to the sole application of mechanical stimuli; they must meet other requirements in order to create grafts that, when

implanted, will lead to the regeneration of damaged organs. A bioreactor must efficiently transport nutrients and oxygen to the construct. In most tissue engineering approaches, a scaffold is seeded with cells and supports the formation of extracellular matrix (ECM). Consequently, the bioreactor has to induce a cell distribution throughout these structures that is as homogeneous as possible in order to generate a uniformly distributed ECM. Tissue engineering bioreactors can be used for cell seeding and/or long term cultures [19-29].

The first step to culturing cells in a three dimensional environment is the seeding of scaffolds with cells appropriate for the desired application [20]. Scaffold seeding determines the initial number of cells in the construct, as well as their spatial distribution throughout the matrix. Therefore, proliferation, migration and the specific phenotypic expression of the engineered tissue will be affected by the utilized seeding technique [30]. In the case of tissues that require fibrous or porous materials, static seeding has been the most widely used method of cell seeding; however, poor cellular distribution and a low seeding efficiency are obtained with this technique [26,31]. A low seeding efficiency diminishes the development of specific functions related to cell-cell interactions and requires a greater amount of cells suspended prior to seeding; therefore, the usage of new and improved seeding techniques becomes imperative [32].

In order to address these issues, researchers have incorporated convection into the process of cell seeding to overcome some of the limitations encountered in the static procedure. Spinner flask bioreactors have been utilized to create convective flow and deliver hydrodynamic forces that may help increase mass transport into the scaffold. In these systems, higher seeding efficiencies are obtained, and the cells are

more uniformly distributed when compared with static seeding; however, a more homogeneous cell distribution is still desired [19,33]. This behavior may be due to the poor convection through the interior of the scaffold, making migration the only way for cells to reach the interior.

One way to improve cell penetration into the interior of the scaffold and a better distribution of cells is by applying perfusion [14,24,34-36]. In this technique, the construct is press fit into a chamber, and the cell suspension is perfused through it. Different systems that operate based on the concept of flow perfusion have been utilized to seed polymeric scaffolds. Dramatic increases in the seeding efficiency have been found in all these systems, and more homogeneous cell distributions throughout the scaffolds have been achieved, compared with static and other dynamic systems [30,34,37].

Therefore, it can be hypothesized that scaffolds seeded in a flow perfusion system, using oscillatory flow, will present higher seeding efficiencies and more homogeneous cell distributions than scaffolds seeded statically. In this study, we evaluate the effect of flow perfusion on seeding efficiency and cell spatial distribution on fibrous polystyrene matrices and foams using MC3T3-E1 pre-osteoblastic cells, using a flow perfusion system also suitable for long-term cultures. To asses the potential applicability of this seeding technique as a first step for long term cultures or as the last step prior to implantation of cell/scaffold constructs, oscillatory flow was followed by unidirectional flow and the scaffold cellularity (total number of cells attached per scaffold) was determined afterwards. The effects of fiber size and surface modification by oxygen plasma on polystyrene fibers were also evaluated, as well as

the assessment of cell distribution on poly(L-lactic acid) (PLLA) foams in order to demonstrate that the employed methodology is not material dependant. The results yielded by oscillatory flow perfusion seeding are compared to those achieved with static seeding and static seeding followed by unidirectional flow perfusion.

3.2 Materials and Methods

3.2.1 Scaffolds

Fibrous meshes and porous foams are among the most popular scaffold architectures employed in the regeneration of bone and other tissues [13,38-45]. These two different morphologies were utilized in this study and seeded with MC3T3-E1 pre-osteoblastic cells under static and dynamic conditions in a flow perfusion bioreactor[14]. Scaffolds were prepared as follows:

a) Fibrous meshes. Non-woven polystyrene fibrous matrices were produced by spunbonding [46,47]. The apparatus consisted of a Brabender™ single screw extruder, a spin pack equipped with a gear pump, and a spinneret. The extruder barrel was 19.0 mm (0.75 in.) in diameter and 381 mm (15 in) in length and had a compression ratio of 3:1. The spin pack contained a Zenith™ gear pump that metered and pressurized the molten polymer. A single-hole spinneret was used for the production of fibers. The single-hole spinneret had a diameter of 0.407 mm (0.016 in) and a length 2.97 mm (0.1169 in). The Brabender extruder was kept at 265^{o}C, the spin pack was kept at 275^{o}C, and the spinneret was kept at 280^{o}C. Fiber diameters were 20, 35 and 50μm. The fibers were used as produced and also treated with oxygen-plasma in order to incorporate hydroxyl groups on the surface of the fibers and; both, plain and treated

surfaces were compared. Oxygen-plasma treatment was carried out for 1 min at medium intensity and a pressure of 200mmHg in a plasma cleaner/sterilizer (Model PDC-32G, Harrick). Fibrous scaffolds were punched from the resulting mesh. These fibrous matrices had an approximate porosity of 95%, and dimensions of 8 mm in diameter and 3 mm in thickness. The porosity was determined as the percentage ratio of the weight of the scaffold to the weight of a solid polystyrene disc with the same dimensions.

b) Porous foams. Polystyrene foams were prepared by particulate leaching, using sodium chloride (NaCl) as the porogen [48-50]. The grain size of the NaCl was between 300-450μm. Briefly, polystyrene (average MW 100,000) was dissolved in chloroform at a concentration of 5% w/v. The solution was then poured on a sodium chloride bed, and the solvent was allowed to evaporate for 24 h. The solid salt-polymer composite, which was 95 wt% NaCl, was pressed in a cylindrical mold with an inner diameter of 8 mm at 500 psig, using a hydraulic press, with simultaneous heating at 130^{o}C for 30 min. The resulting pellet was cut into discs of 3 mm in thickness using a low speed diamond wheel saw (Model 650, South Bay Technology, Inc). Salt leaching was carried out using deionized water for 3 days while the water was changed at least twice a day. The scaffolds had a porosity of 95% determined as the percentage ratio of the weight of the scaffold to the weight of a solid polystyrene disc with the same dimensions.

3.2.2. Cell Source

Preosteoblastic MC3T3-E1 cells were cultured in T-75 flasks (Corning) using Dulbeco's modified essential medium (D-MEM, 10% fetal bovine serum) (Atlanta Biologicals), in a humid atmosphere at 37ºC and 5% CO_2. Media was changed every other day. Prior to seeding, cell cultures were rinsed with PBS (Atlanta Biologicals) and lifted from the culture flask using 0.25% trypsin/EDTA (Gibco). Cells were centrifuged at 400g for 5 min and re-suspended in fresh D-MEM. Seeding densities were $1.25x10^5$, $2.50x10^5$, $5x10^5$ and $1x10^6$ cells in 250µl of D-MEM.

3.2.3. Seeding Techniques

Three different seeding techniques were compared to evaluate scaffold initial cellularity, seeding efficiency and cell spatial distribution.

Static Seeding: Scaffolds were pre-wet with 200-proof alcohol by applying manual vacuum, rinsed in a series of solutions of decreasing concentrations of alcohol in phosphate buffered saline (PBS), press fit into cassettes designed for static seeding and placed in a low-attachment 6-well plate prior to seeding. Cells suspended in 250µl of D-MEM were slowly distributed on top of the scaffolds and allowed to attach for 4h. The wells were then filled with medium and cells were allowed to condition for 8h, in an incubator at 37^{o}C and under 5% CO_2.

Oscillatory perfusion (Dynamic) seeding: a modified flow perfusion system utilized in other studies was used in this set of experiments [14]. Briefly, scaffolds were confined in cassettes so as to force the flow throughout the porous network and restrict it from going around the scaffold. The cassettes were placed into the perfusion

chambers of the main body of the bioreactor, which consists of a total of six chambers. Culture media was pumped to the top of the chambers using a peristaltic pump (Cole-Parmer) from a media reservoir and returned to a second reservoir, allowing media recirculation.

Prior to seeding, the flow system was cured with D-MEM for 2 h. Pre-wet scaffolds were press-fit into cassettes and placed in the flow perfusion chambers of the bioreactor. Cell suspensions (in 250μl of D-MEM) were poured on top of the scaffolds, and the chambers were filled up with fresh media to avoid the presence of air bubbles. Oscillating flow was then applied for 2 h at 0.15 ml/min by manually changing the direction of the pump every 5 min. Cell conditioning, without flow, was allowed for a period of 2h, after which unidirectional flow was incorporated at 0.15 ml/min for 8h.

Statically seeding followed by shearing: Scaffolds were seeded statically for 4h, using flow perfusion cassettes as described earlier in this chapter. After that, the cassettes with the statically seeded scaffolds were placed in the bioreactor chambers, and unidirectional flow was applied at 0.15 ml/min for 8h.

3.2.4. Cell detachment

Scaffolds were seeded statically or dynamically for 2h as explained previously. After the additional 2h conditioning period (absence of any type of flow), unidirectional flow was applied for 8h at rates of 0.15, 0.5 and 1 ml/min, using the flow perfusion bioreactor.

3.2.5 Cell number quantification

After completing of the seeding process that lasted 12h for all groups, the constructs were quickly rinsed in PBS, suspended in 3 ml of water, and broken down into small pieces. Samples were later submitted to three cycles of freezing and thawing in order to lyse the cells. A picogreen® DNA quantification assay (Invitrogen) was carried out to obtain the number of cells attached to the scaffolds. A standard curve was made using known-concentration solutions of λ-DNA. Sample and standard aliquots of 43μl were accommodated in a 96-well plate, along with 107μl of reaction buffer (20mM Tris-HCl, 1 mM EDTA, pH 7.5) and 150μl of the Picogreen® Dye. Fluorescence was measured at 490 nm in excitation and 520 nm in emission, using a Synergy HT plate reader (Bio-Tek). The number of cells was calculated using the total amount of DNA determined in the sample divided by the amount of DNA contained in one cell, which was estimated in our laboratory to be 3 pg/cell.

The data were reported in two ways: total scaffold cellularity, which is the total number of cells attached to the scaffold; and cell surface density, which is defined as the cellularity divided by the total surface area available for cell attachment. Surface area in the foams was estimated using mercury porosimetry. The surface area of the fibrous matrices was calculated as follows[51]:

First, the total volume of the fibers (V) was computed by:

$$V = m/\rho = \frac{\pi}{4} L D^2 \qquad (3.1)$$

Where L is the total length of the fibers, D is the fiber diameter, m is the mass of the fibrous matrix, and ρ is the polystyrene density. Then, the total surface area of the fibers is given by:

$$A = \pi DL \tag{3.2}$$

By combining equations 3.1 and 3.2, the surface area available for attachment in a fibrous matrix is estimated by the following expression:

$$A = \frac{4m}{\rho D} \tag{3.3}$$

3.2.6. Assessment of cell spatial distribution throughout the scaffold surface

3.2.6.a. Fluorescence microscopy

After seeding with all of the methodologies previously described, cells were fluorescently tagged with BODIPY® FL phallacidin (Invitrogen), a high affinity probe for F-actin. Briefly, seeded scaffolds were fixed in 3.7% formalin for 10 min. Rinsing with 0.1% Triton-X and PBS followed. Constructs were then incubated for 20 min in the dye solution, with a concentration of 200units/ml. They were finally rinsed with 0.1% Triton-X and PBS. Top and bottom sections were analyzed for cell distribution, with the top section corresponding to the surface on which the cell suspension was originally placed. In fibrous matrices, the middle portion of the construct was also assessed for cellularity by manually sectioning the matrices along the axial direction. Fluorescence microscopy was performed using a Nikon Epifluorescence microscope, and image analysis was carried out with MetaMorph 6.2 (Universal Imaging Corporation). The excitation and emission wavelengths were 558nm and 569nm respectively.

3.2.6.b. Histological Analyses

Histology of 20-μm plasma treated fibers seeded both statically and dynamically with MC3T3-E1 pre-osteoblastic cells was carried out. Seeded scaffolds were fixed in 3.7% formalin overnight, dehydrated using a series of ethanol solutions of increasing concentration, and embedded in paraffin. Embedded samples were sectioned using an MT 6000 microtome (RMC). Sections were mounted on glass slides and stained with Safranin-O (Electron Microscopy Sciences).

Histology of porous foams seeded both statically and dynamically was also carried out. The material used in this section of the study was poly(L-lactic acid) (PLLA) (Birmigham polymers, average MW: 100,000). Foams were prepared by particulate leaching, using sodium chloride as the porogen (as previously explained for polystyrene foams). Seeded scaffolds were fixed in 3.7% formalin overnight, dehydrated, and embedded using a low viscosity embedding media Spurr's kit (Electron Microscopy Sciences, RT 14300). Infiltration of the samples with the embedding medium was done by starting with and ethanol-PBS solution (1:1), followed by a 1:3 mixture, and finally pure PBS. Each infiltration step lasted 2h. Fresh embedding media was aggregated and allowed to polymerize overnight at 60^{o}C. Embedded samples were sectioned in the direction of the flow, mounted on glass slides and stained with toluidine blue (Electron Microscopy Sciences). Microscopy was performed using a Nikon Epifluorescence microscope. Eight images were taken per each cross-section with a 10X objective.

The images were segmented in three different areas: an upper zone close to the surface on which the cell suspension was placed (0-1mm), a middle zone (1-2 mm), and a lower zone (2-3 mm). Cell nuclei were counted per zone. The distribution of cell coverage along the direction of the flow was determined by calculating cell coverage fractions. The cell coverage fraction was defined as the ratio of the number of cells counted in one zone to the total number of cells in the entire cross section.

To obtain a quantitative measurement of cell uniformity, we utilized the method proposed by Zhao et. al. and Wendt et. al.[56,65]. Six histological sections were obtained for each scaffold. Each cross section was divided into five areas in the direction of the flow starting from the top. Each area was imaged and the number of cells per image was quantified. The average number of cells for a cross section ($\bar{x}$) along with the standard deviation (s) were determined. Percent uniformity for a cross section was calculated by the following equation [56,52]:

$$\%Uniformity = 100 * \left(1 - \left(\frac{s}{\bar{x}}\right)\right) \tag{3.4}$$

3.2.7. Statistical analysis

For all the experiments, three to five samples were used (n = 3-5) in all the experiments, unless otherwise specified. Values were reported as the average of all the samples, and the error was reported as the standard error of the mean. The data were analyzed by using ANOVA, and multiple pair-wise comparisons were carried out using the Tukey-HSD method at a confidence level of 95%.

3.3. Results

3.3.1 Effect of the seeding technique and fiber diameter on initial scaffold cellularity and seeding efficiency in fibrous scaffolds

In Figure 3.1, the three different seeding techniques are compared in terms of scaffold initial cellularity (total number of cells attached per scaffold) at different fiber sizes and at an inoculation number of $2.5x10^5$ cells. At fiber sizes of 20 and 35 μm, oscillatory flow perfusion seeding (also called dynamic seeding) yielded the highest cellularity. In all cases, the shearing of statically seeded scaffolds yielded the lowest scaffold cellularity.

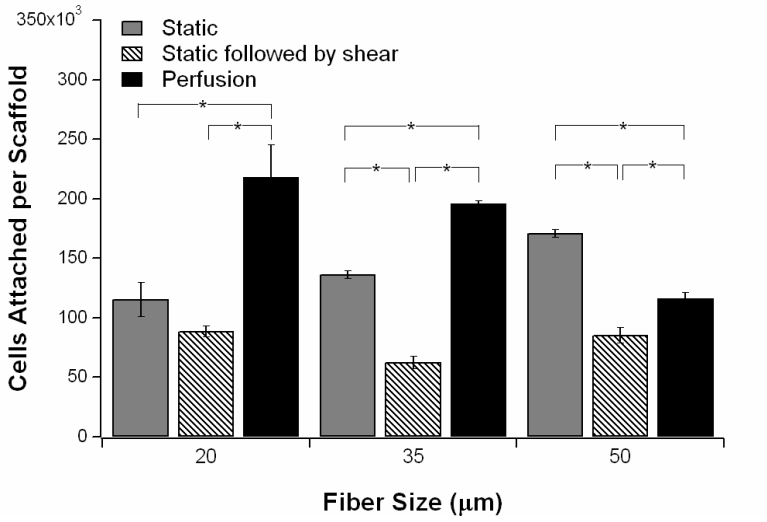


Figure 3.1. Effect of seeding technique and fiber size on the number of cells attached per scaffold using an inoculation number of $2.5x10^5$ cells. All scaffolds were oxygen plasma treated. (*) $p<0.05$

The efficiency of seeding (percentage ratio of the initial scaffold cellularity to the number of cells suspended), is shown in Figure 3.2 for the different seeding techniques. As a general trend, it was observed that seeding efficiency decreased at

higher suspension cell numbers. Dynamic seeding yielded the highest efficiency in most cases, with a maximum value of about (56±5)%; nonetheless, differences among the different seeding techniques were not clearly appreciated on untreated fibers (Figure 3.2a). In oxygen-plasma treated fibrous scaffolds, the differences on efficiency among the different seeding techniques were more obvious (Figure 3.2b). The tendency of the dependence of seeding efficiency on inoculation number was preserved, with values of up to (87±6)%. In most cases, the plasma treatment significantly increased seeding efficiency when compared with untreated fibers (Figures 3.2, 3.3 and 3.4).

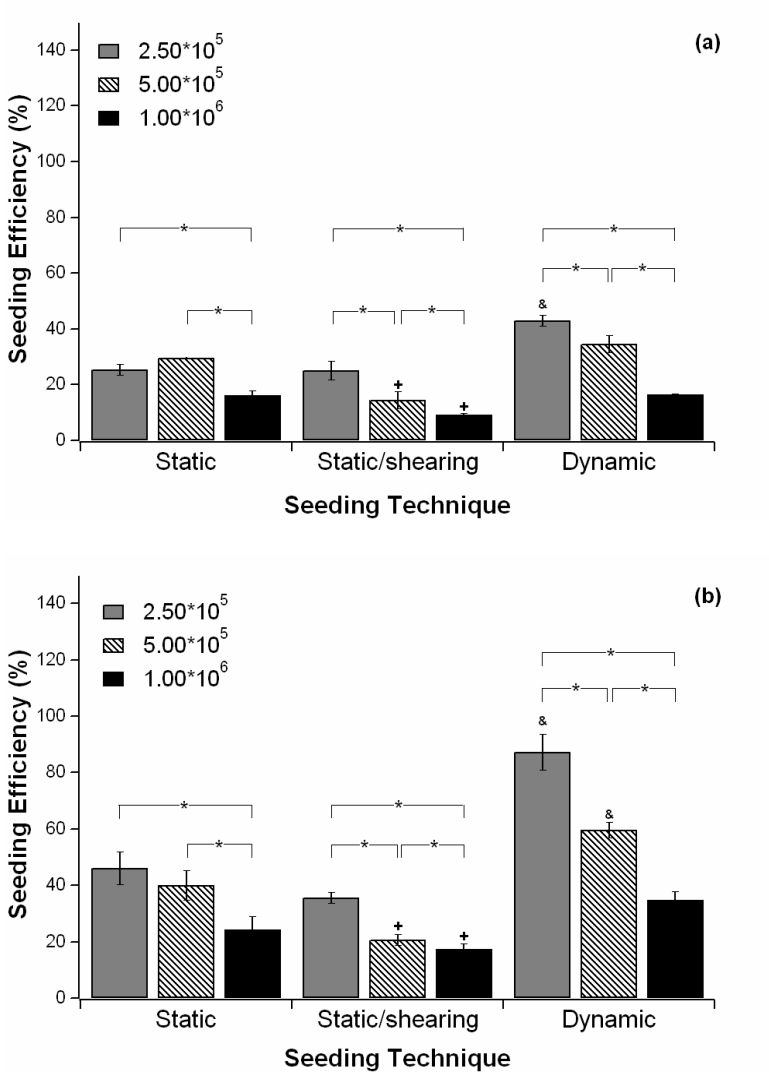


Figure 3.2. Effect of cell inoculation number on the seeding efficiency of (a) untreated scaffolds and (b) oxygen-plasma-treated scaffolds at different seeding techniques. All scaffolds had a fiber size of 20 μm. Multiple pair-wise comparisons have been carried out using the Tukey-HSD methodology at a confidence level of 95%.The ampersand symbol (&) denotes the seeding technique that yielded the highest seeding efficiency at the same inoculation number. The plus symbol (+) represents the seeding technique that yielded the lowest seeding efficiency at the same inoculation cell number. (*) $p<0.05$

The dependence of the scaffold cellularity on the inoculation cell number after dynamic seeding is presented in Figure 3.3. Similar trends were noticed for all fiber

sizes; cell attachment increased with the inoculation cell number, but it reached a plateau at an inoculation number of $5x10^5$ cells. In untreated fibers, there was not a significant difference between fiber sizes of 20 and 35μm; however, fibrous matrices with 50 μm fibers had a significantly lower number of cells attached. Plasma-treated scaffolds presented a similar trend in terms of cellularity related to the inoculation cell number and fiber size (Figure 3.3b). However, at higher inoculation numbers ($5x10^5$ and $1x10^6$ cells in the inoculum), the number of cells attached to the plasma treated scaffolds dramatically changed, presenting a 2-fold increase for fiber diameters of 20 and 35 μm, and a 5-fold increase for 50 μm, with respect to untreated scaffolds.

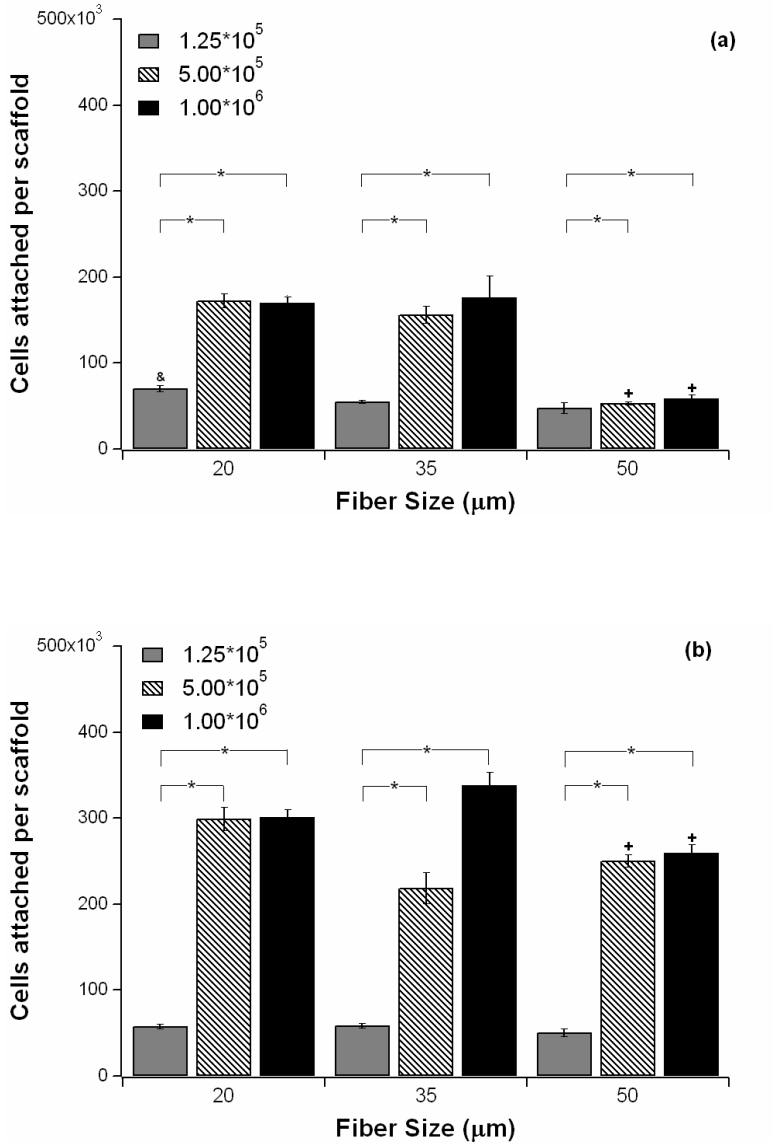


Figure 3.3. Dependence of the number of cells attached per scaffold (cellularity) on the cell inoculation number and fiber size of (a) untreated scaffolds, and (b) oxygen-plasma-treated scaffolds after flow perfusion seeding. Multiple pair-wise comparisons have been carried out using the Tukey-HSD methodology at a confidence level of 95%. The ampersand symbol (&) denotes the fiber size that presented the highest cellularity at the same inoculation number. The plus symbol (+) represents the fiber size that yielded the lowest cellularity at the same inoculation cell number. (*) $p<0.05$

Scaffold cellularity was normalized with the surface area available for cell attachment (Figure 3.4). This normalization is referred to as cell surface density.

Scaffold surface areas were estimated to be (11.8 ± 2.1), (5.2 ± 0.8), and (4.2 ± 0.4) cm^2 for fibers of 20, 35 and 50 μm respectively, and (18.7 ± 1.5) cm^2 for porous foams. Cell surface density kept a similar dependence on the inoculation cell number to that obtained in Figure 3.3, reaching a plateau when the number of cells in the inoculum was $5x10^5$. No clear trend on cell surface density was observed with respect to fiber sizes when untreated meshes were used, but, in plasma treated fibers, the surface density in the 20-μm fibers was significantly lower than those yielded by larger fiber sizes (35 and 50 μm).

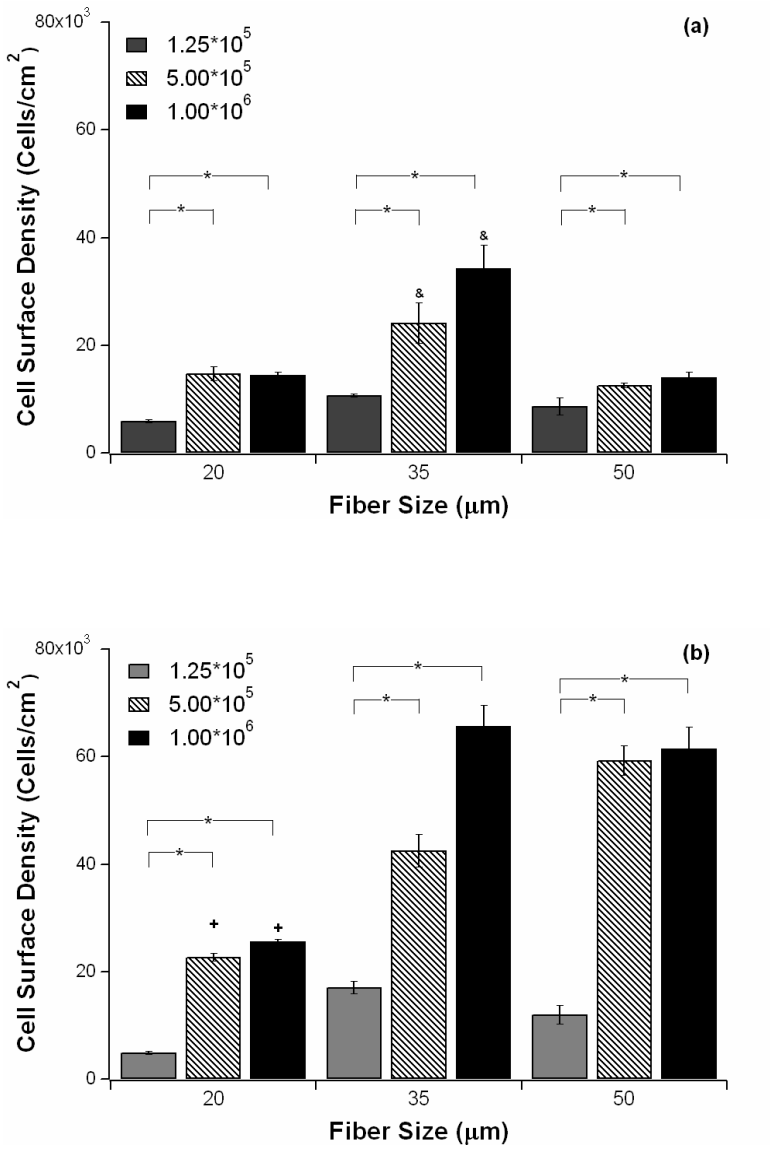


Figure 3.4. Dependence of cell surface density on cell inoculation number and fiber size of (a) untreated scaffolds, and (b) oxygen-plasma-treated scaffolds after flow perfusion seeding. Multiple pair-wise comparisons have been carried out using the Tukey-HSD methodology at a confidence level of 95%. The ampersand symbol (&) denotes the fiber size that presented the highest cell surface density at the same inoculation number. The plus symbol (+) represents the fiber size that yielded the lowest cell surface density at the same inoculation cell number. (*) $p<0.05$

The effect of scaffold architecture on cell surface density is shown in Figure 3.5. Both kinds of scaffolds, fibrous matrices and porous foams, had the same dimensions, 8 mm in diameter by 3 mm in thickness, and a porosity of 95%.

Untreated, 20 μm fibers were compared to untreated foams prepared by salt leaching. In both architectures, cell surface density increased with the inoculation number but reached a plateau at an inoculation of $5x10^5$ cells. The cell surface density of the foams was lower than that of the fibrous meshes at higher cell inoculation numbers ($5x10^5$ and $1x10^6$ cells).

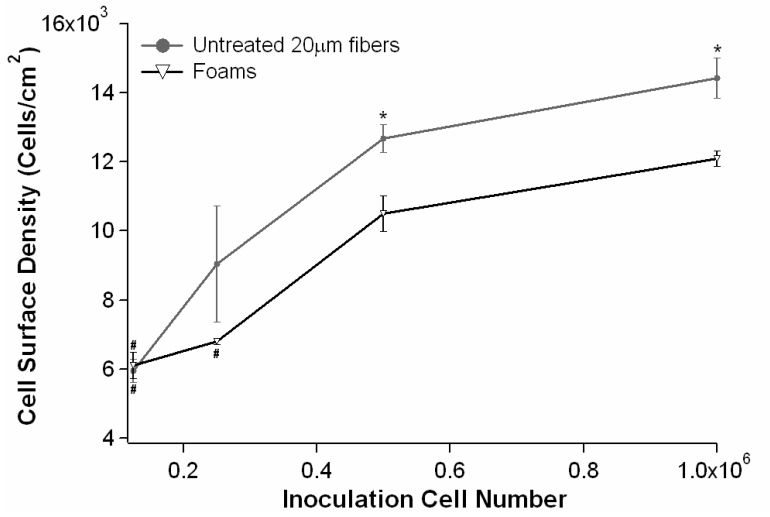


Figure 3.5. Effect of scaffold morphology on cell surface density after seeding in a flow perfusion system. Both scaffolds had a diameter of 8 mm, thickness of 3 mm and a porosity of approximately 95%. The symbol (*) denotes significantly higher cell surface density when comparing the different scaffold architectures at the same cell inoculation number. The symbol (#) represents cell inoculation number that yielded significantly lower cell surface densities than those yielded by inoculation cell numbers of $5x10^5$ and $1x10^6$ at the same scaffold morphology.

Figure 3.6 shows the effect of the seeding technique on the seeding efficiency on porous foams. As observed with the fibrous matrices, the oscillatory flow perfusion seeding yielded the highest seeding efficiency, while the static followed by

shearing yielded the lowest ($p<0.01$). Approximately, 40% of the cells seeded statically were detached when unidirectional flow perfusion was applied.

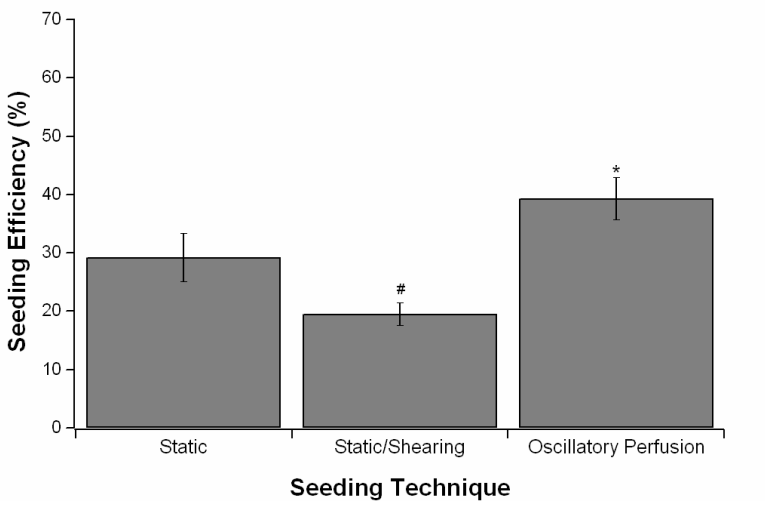


Figure 3.6. Effect of seeding technique on the cell seeding efficiency of prous scaffold scaffolds made by particulate leaching using an inoculation number of $5x10^5$ cells. (*) denotes the seeding technique that yielded the highest efficiency. (#) denotes the seeding technique that yielded the lowest seeding efficiency.

3.3.2. Cell detachment after seeding

Perfusion seeding consists of three stages: oscillating flow, cell conditioning without flow, and unidirectional media recirculation at a specific flow rate. In the detachment studies, three different flow rates were tested in the recirculation phase, 0.15, 0.5 and 1.0 ml/min. Figure 3.7 shows the detachment curves in plasma-treated fibrous meshes with a fiber size of 20 μm, seeded using an inoculation of $2.5x10^5$ cells. Scaffold cellularity remained unchanged at different stages of the perfusion seeding, oscillating flow for 2h, cell conditioning for 2fh without flow, and unidirectional media recirculation for 8h, both at a flow rate of 0.15ml/min. Nonetheless, the number of cells attached to the scaffolds seeded dynamically

decreased when higher rates of media recirculation were tested. At 0.5 and 1.0 ml/min unidirectional flow, the cellularity of the mesh was respectively about 50 and 35% of that obtained at 0.15 ml/min.

In the case of statically seeded scaffolds, the cellularity was decreased when unidirectional flow was incorporated, and lower cellularities were obtained compared to the dynamically seeded scaffolds experiencing the same unidirectional flow for the same period of time. Statically seeded scaffolds that were subjected to 0.15 ml/min presented about 70% of the initial cellularity, yielding the same cellularity as the dynamically seeded scaffolds exposed to 1.0 ml/min in the recirculation phase. After applying flow rates of 0.5 and 1 ml/min to statically seeded scaffolds, the total scaffold cellularity was between 38 and 31% of the initial cellularity, respectively.

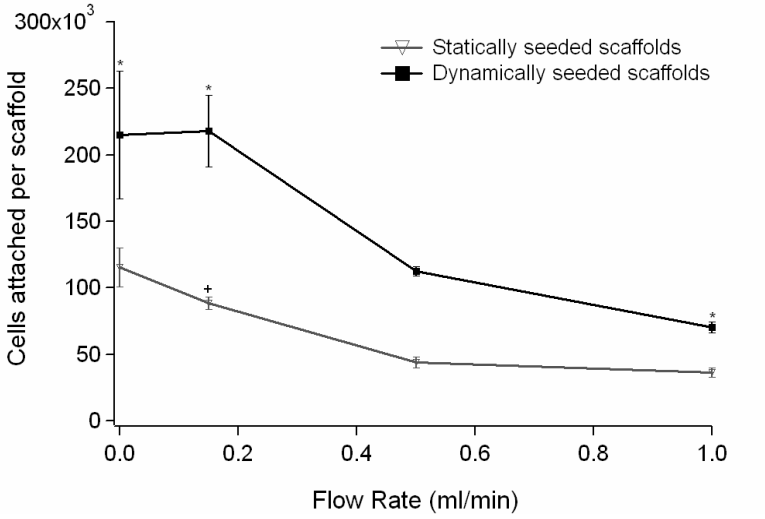


Figure 3.7. Detachment curve of cells seeded both statically and dynamically on oxygen plasma treated fibrous meshes with a fiber size of 20 μm. Inoculation cell number of $2.50x10^5$ cells. (*) $p<0.05$ with respect to 0.5 ml/min; (+) $p<0.05$ with respect to 0 ml/min. Both curves were significantly different at every point of flow rate ($p<0.05$).

3.3.3. Assessment of cell spatial distribution

Fluorescence microscopy was used to assess cell distribution. In Figure 3.8, the different seeding techniques for the fibrous matrices were compared by fluorescence microscopy. Scaffolds were separated in three general regions: top, middle and bottom, with the top being the surface on which the cell suspension was initially placed. In the statically seeded scaffolds, cells were clustered around the fibers at the top of the matrix, forming large cellular networks. Middle and bottom sections of these scaffolds showed significantly fewer cells, and no clusters were found. A closer look at the cells, using a higher magnification, revealed that a great number of single cells attached to the fibers had a rounded shape, while others were slightly stretched (Figure 3.9a). In the dynamically seeded fibers, the top surface also appeared to have more cells than the other regions of the scaffold, but the difference in depth was less pronounced than that observed under static conditions. Clusters were occasionally found in some areas of the upper scaffold section, but they were smaller than those seen in statically seeded scaffolds and localized. Unlike cells attached under static conditions, most of the dynamically seeded cells stretched along the surface of the fibers (Figure 3.9b).

Cells seeded on porous foams were located along the edges of the pores at the outer scaffold surface, as shown in Figure 3.10. In both seeding techniques, the top presented an appreciable number of cells. The bottom, on the other hand, showed very few cells in dynamically seeded scaffolds and virtually no cells in those scaffolds seeded statically.

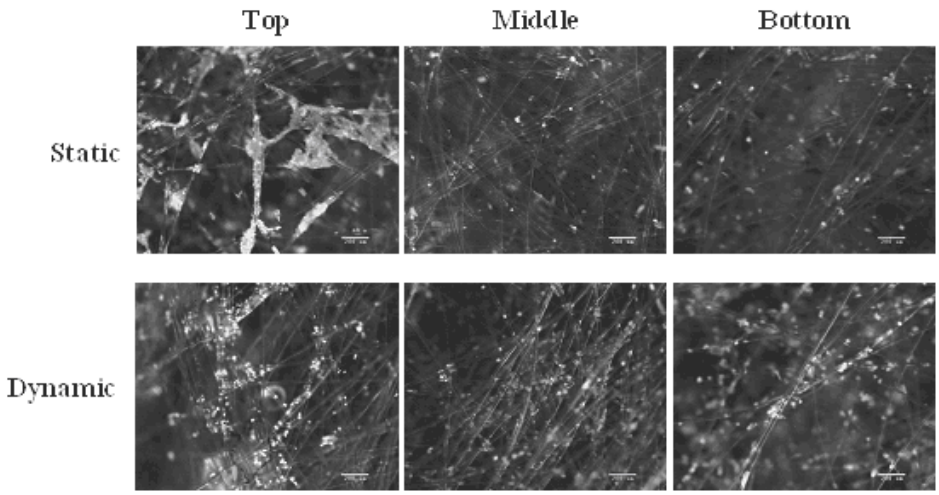


Figure 3.8. Fluorescent micrographs of the top, middle and bottom portions of fibrous matrices (20-μm fibers) seeded statically and dynamically in the flow perfusion bioreactor. Cells were tagged with BODIPY® FL phallacidin. Calibration bar: 200 μm.



Figure 3.9. Cell stretching on fibrous matrices (20-μm fibers) seeded (a) statically, and (b) dynamically in the flow perfusion bioreactor. Calibration bar: 50 μm.

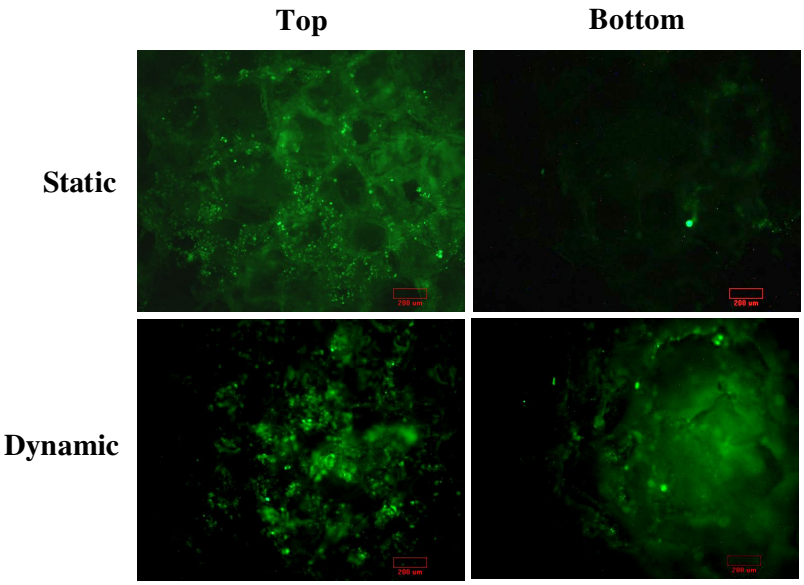


Figure 3.10. Fluorescent micrographs of the top and bottom portions of polystyrene porous foams seeded statically, and dynamically, in the flow perfusion bioreactor. Cells appear as brighter dots. Calibration bar: 200 μm.

Histology of porous poly(L-lactic acid) (PLLA) foams was used to assess cell distribution in the direction of the flow. Histological sections of statically seeded PLLA scaffolds (Figure 3.11) are in accordance with the fluorescence microscopy on polystyrene foams; most of the cells are observed close to the top surface, and very few cells are located in the bottom portions after static seeding. Under flow perfusion however, a greater number of cells was observed in all the sections of the scaffold. We also compared scaffold cellularities of PLLA and polystyrene foams under flow perfusion seeding for identical inoculation densities but did not find a significant difference between the two values (data not shown).

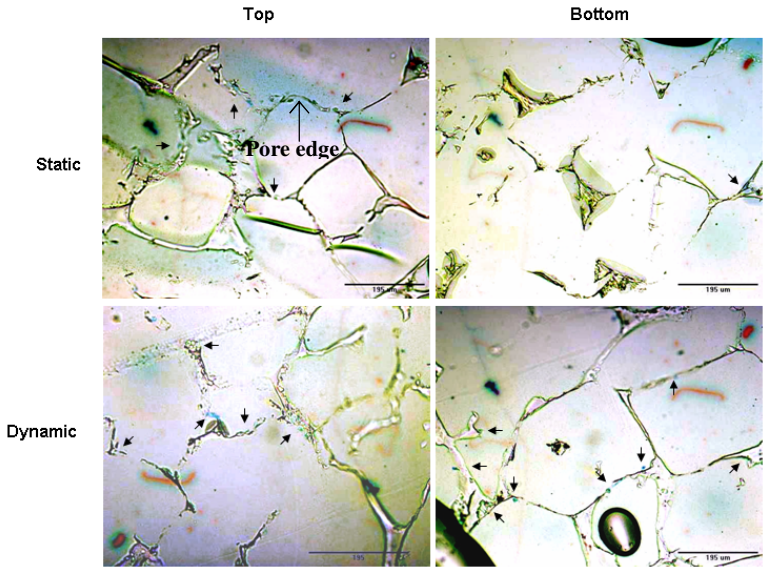


Figure 3.11. Axial histological sections of PLLA foams seeded statically and dynamically, in the flow perfusion bioreactor. Top and bottom portions of both scaffolds are represented. Cells were stained with toluidine blue. Arrows point the areas were cells were observed. Calibration bar: 195 μm.

From the histology analyses, both of the foams and the fibers, it was possible to calculate the percent uniformity defined by equation 3.4. The percent uniformities for 20-μm fibers (plasma treated) seeded statically and dynamically are compared in Figure 3.12, in which a significant difference was observed among the two different techniques, with the dynamic seeding yielding higher uniformity. Moreover, Table 3.1 shows that in dynamically seeded scaffolds cells showed increased homogeneity in the direction of the flow than in statically seeded scaffolds. This phenomenon was found in fibrous matrices and porous foams. In the foams, the percent uniformity after oscillatory seeding was (65 ± 4) %, while in the statically seeded scaffold it was (20 ± 2) %.

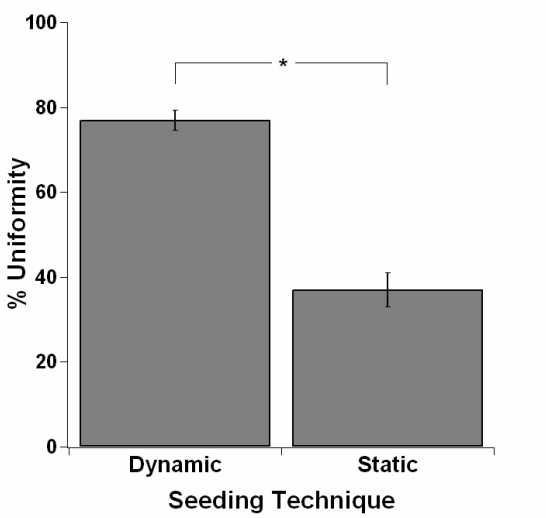


Figure 3.12. Percent uniformity of scaffold dynamic and static seeding. Oxygen plasma-treated fibrous meshes were used with a fiber size of 20 μm. A cell suspension number of $1x10^6$ was utilized. ($_*p<0.05$)

Table 3.1. Cell coverage fractions of statically and dynamically seeded scaffolds. Oxygen plasma-treated fibrous meshes were used with a fiber size of 20 μm. A cell suspension number of $1x10^6$ was utilized. Histological sections were segmented in three zones along the direction of the flow: a top zone close to the surface on which the cell suspension was originally placed (0-1 mm), a middle zone (1-2 mm), and a ottom zone (2-3 mm).

	Cell Coverage Fraction	
Technique / Zone	**Static Seeding**	**Dynamic Seeding**
0-1 mm	(0.56 ± 0.01)	(0.37 ± 0.02)
1-2 mm	(0.28 ± 0.01)	(0.39 ± 0.02)
2-3 mm	(0.16 ± 0.01)	(0.25 ± 0.01)

3.4. Discussion

The purpose of this study was to use oscillatory flow in a flow perfusion system suitable for long term cultures as an alternative technique for scaffold seeding. We also aimed to evaluate the effects of this seeding technique on seeding efficiency and cell spatial distribution on scaffolds with different architectures and materials. We compared the results obtained from this technique with those found when scaffolds were seeded statically, and when statically seeded scaffolds were submitted to unidirectional flow in the perfusion bioreactor.

Most experiments performed in flow perfusion systems utilized for long term cell culture have used static seeding and later incorporated these cell-scaffold constructs into the bioreactor [36,53-59]. However, static seeding is not an ideal method due to low efficiencies and poor cell distribution throughout the scaffold's porous network [30,34,37]. Consequently, it was important to evaluate the effects of flow perfusion in the seeding of polymeric scaffolds for tissue engineering. Performing the seeding in the flow perfusion system provided an obvious advantage since scaffold handling would be minimized. Seeding scaffolds statically and transporting them into the bioreactor poses great risks of contamination due to excessive manipulation.

The effects of the incorporation of flow perfusion in scaffold seeding can be examined by considering: 1) the influence of different seeding techniques (static, static followed by flow shearing, and oscillating flow perfusion) on seeding efficiency; 2) the relation between cell attachment and scaffold architecture, with two different kinds of scaffolds, fibrous meshes and porous foams, as well as, the effect of

fiber size, and 3) the influence of the seeding technique on the initial cell spatial distribution throughout the entire scaffold surface.

3.4.1. Influence of the seeding technique on seeding efficiency.

Previous studies have used systems similar to the flow perfusion bioreactor that we have employed. Li et. al., used a depth filtration system to seed poly (ethylene terephthalate) (PET) matrices at a rate of 1ml/min. The cell suspension was recycled to increase the yield. Cell density increased along with the suspension cell number, with an efficiency of about 65%, while the static seeding yielded lower efficiencies [30]. Similarly, Kim et. al. seeded hepatocytes on polymeric matrices using a flow perfusion system. A suspension of rat hepatocytes at a density of $5x10^6$ cells/ml was pumped through decellularized bone matrices at a flow rate of 1.5 ml/min for 4 h. A total of approximately $4.4x10^6$ cells were attached to the matrix, and a uniform distribution of the hepatocytes throughout the scaffold surface was achieved [27]. These studies are in agreement with our findings. Higher efficiencies were achieved using oscillating flow perfusion compared to static seeding. Furthermore, the seeding efficiencies yielded in our study by the oscillating flow perfusion reached values close to 100% in some instances.

Wendt et. al. monitored seeding efficiency and uniformity within static, spinner flask and perfusion systems. There was no difference among the efficiencies of the static and perfusion techniques, both producing a larger yield than the spinner flask. Uniformity, however, was optimized by the perfusion apparatus, while the static and the spinner flask generated cell-scaffold constructs with low spatial uniformity [34]. Zhao et. al. used a flow perfusion system to seed PET fibers by continuously

recirculating a cell suspension through the system confirming the results from other studies [37]. We have also demonstrated that dynamic seeding, in this case, oscillatory flow perfusion seeding improves cell spatial distribution when compared to static techniques.

In this study, not only did we compare dynamic and static seeding, but we also considered the effects of exposing statically seeded scaffolds to unidirectional flow. Efficiencies yielded by static seeding were in some instances comparable to those encountered dynamically, with values reaching 50% sometimes. Despite these efficiency values, there were poor cell matrix interactions since many of the cells attached under static conditions were washed away when subjected to shear forces in the flow perfusion system. A reason for this behavior can be found in Figures 3.8 and 3.9, in which large clusters are shown around the statically seeded fibers. These clusters were either attached to the scaffold in multiple locations or bonded through a single cell with the rest floating in the surrounding media. The latter type of clusters is expected to be more prone to detachment from the matrix in the presence of shear forces.

Under dynamic conditions of seeding, we were able to maintain higher efficiencies; an effect that can be attributed to several factors. The oscillation provided during the first stage of the perfusion seeding gives more chances for cells to attach. Furthermore, it is possible that, by applying these different cycles in the oscillation, the cells could attach to places that were more energetically favorable for them to interact with, thereby resulting in stronger cell-matrix interactions. Microscopy results corroborate this hypothesis by showing an absence of large cell

clusters and higher spreading of the cells attached to the fibers. In spite of these advantages, it was interesting to observe a decrease in the efficiency when larger numbers of cells were present in the suspension. This decrease can be explained by a possible saturation of the surface with cells (see the cell attachment curve in Figures 3.2 and 3.3). Thus, the trend of cell attachment with respect to the inoculation number presents a behavior that resembles a protein adsorption isotherm.

Changing the conditions of flow, depicted in the detachment curve, gives us an insight into the cell attachment behavior. The fact that the cellularity of dynamically seeded scaffolds remained unchanged when recirculation at 0.15 ml/min was applied, combined with the fact that the cellularity of statically seeded scaffolds significantly declined after applying flow, implies that flow perfusion induced stronger cell attachment. A sign of the strength of attachment was the spreading of the cells, shown in Figure 8. The incorporation of unidirectional flow at higher rates, which resulted in stronger shear forces, showed that the profile of cell detachment for dynamically and statically seeded scaffolds is very similar. Even though the profile for cell detachment for dynamically and statically seeded scaffolds was very similar, dynamically seeded scaffolds retained a significantly greater number of cells even at 1.0 ml/min. Shear stresses under the different conditions of cell detachment were estimated by using Stokes-Oseen equation (see Apendix II) [60]. This equation assumes creeping, transversal flow around a single cylinder, based on the determination of the drag coefficient. For our estimations, we have used the corrected Stokes-Oseen equation for a parallel array of cylinders [61,62]. The calculated values of shear stress were between 0.04 and 0.4 dyn/cm^2 for the range of flow rates utilized.

3.4.2. Relation between cell attachment and scaffold architecture

3.4.2.a. Dependence on fiber size

When the total number of cells attached was compared at different fiber sizes, it was noted that meshes with larger fibers displayed lower cellularity. This behavior further elucidated when the cell attachment was normalized by the available surface area per scaffold. In the latter case, scaffolds with smaller fibers had the smaller cell surface density. MC3T3-E1 pre-osteoblastic cells have a comparable size to the smaller fibers used in this study, which enables them to attach more easily to larger fibers; such is the case of 35 and 50-μm fibers.

3.4.2.b. Dependence of scaffold morphology on initial cell surface density

Scaffold morphology varies greatly in different tissue engineering applications. Our results demonstrate that cell attachment, among other factors, is affected by the architecture of the cell carrier matrix. Parameters such as scaffold diameter, thickness and porosity were kept constant for both architectures, but it was not possible to maintain the surface area available for cell attachment and the distribution of the void spaces constant as well. Inside the fibrous matrices, the flow is relatively undisturbed compared to the tortuous paths encountered in the foams. This difference may have played a role in the fluid dynamic environment the cells encountered within the scaffolds. In the case of the foams, sudden changes in pore diameter are capable of generating eddies followed by localized areas of significantly higher shear which can detach the cells.

3.4.3. Influence on the initial cell spatial distribution throughout the entire scaffold surface

Other groups have reported poor uniformity in cell spatial distribution throughout tissue engineering scaffolds when they are seeded under static conditions. Dynamic systems such as spinner flask bioreactors and rotating wall vessels have been implemented to create convection and, thereby, hydrodynamic forces that could increase mass transport to the interior of the scaffold. However, a higher cell density is still observed close to the outer surfaces of the construct but very few cells at its center [63]. Our findings, as well as previous experiments, confirm that flow perfusion guarantees fluid flow to the interior of the scaffold and a more uniform cell distribution [30,34,53-55,64].

It is implied from these findings that, in the absence of flow, the cells cannot easily penetrate the scaffold (especially ones with high tortuosity), and thereby the majority of them stay at the upper surface. Capillary forces may also generate barriers for the migration of the cells to the inner sections of scaffolds. Additionally, being anchorage dependent, MC3T3-E1 will bind to the first surface available, and ultimately form large cell cluster networks. The incorporation of flow perfusion into the seeding seems to greatly abate part of these problems since it forces fluid flow throughout the porous network. Consequently, the cell suspension is forced into the scaffolds, giving cells the possibility to attach to the deeper regions of the void spaces. Possible cell clusters present in the suspension break down due to the shear forces. These features are common for both scaffold morphologies; nevertheless, the porous foams exhibited a very small amount of cells at the bottom of the constructs, as compared to the fibers.

The distribution of the void spaces in these two architectures is dramatically different. The void space in the non-woven fibrous matrices is less tortuous when compared with the foams, allowing the cell suspension to readily penetrate the porous network. Higher tortuosity and decreased pore interconnectivity in the foams prepared by particulate leaching [65] obstruct the efficient penetration of the cell suspension into interior sections of the foam.

Morphology was not the only factor that was important for us to evaluate in this study. Polystyrene is one of many available biomaterials. To confirm the applicability of oscillating perfusion seeding beyond polystyrene, we have tested PLLA foams prepared in an almost identical way as the polystyrene foams used in this study. Therefore, we also explored whether the behavior observed in cell spatial distribution was maintained on PLLA foams. This fact is demonstrated by the histological analysis, which showed that flow perfusion yielded more homogeneous cell distributions than static seeding in PLLA foams.

3.5. Conclusions

In the present study, we have evaluated the effect of different seeding techniques on the initial scaffold cellularity and cell distribution, as well as the effects of scaffold morphology and the nature of their surface on cell attachment under different conditions of seeding. Flow perfusion yields higher seeding efficiencies and more homogeneous cell spatial distribution than static seeding. At the same time, oscillatory flow perfusion seeding results in stronger cell attachment. Moreover, scaffold architecture and the nature of the scaffold surface affect cell-matrix interactions. In general, flow perfusion seeding is more convenient for many tissue engineering applications, especially if a long term culture is to be carried out in a similar system.

3.6. References

1. Bonassar, L.J., and Vacanti, C.A. Tissue engineering: the first decade and beyond. J Cell Biochem Suppl 30-31, 297-303, 1998.
2. Alsberg, E., Anderson, K.W., Albeiruti, A., Rowley, J.A., and Mooney, D.J. Engineering growing tissues. Proc Natl Acad Sci U S A 99, 12025-12030, 2002.
3. Griffith, L.G., and Naughton, G. Tissue engineering--current challenges and expanding opportunities. Science 295, 1009-1014, 2002.
4. Laurencin, C.T., Ambrosio, A.M., Borden, M.D., and Cooper, J.A.J. Tissue engineering: orthopedic applications. Annu Rev Biomed Eng 1, 19-46, 1999.
5. Boden, S.D. Bioactive factors for bone tissue engineering. Clin Orthop, S84-94, 1999.
6. Lieberman, J.R., Daluiski, A., and Einhorn, T.A. The role of growth factors in the repair of bone. Biology and clinical applications. J Bone Joint Surg Am 84-A, 1032-1044, 2002.
7. Wang, E.A., Rosen, V., D'Alessandro, J.S., et al. Recombinant human bone morphogenetic protein induces bone formation. Proc Natl Acad Sci U S A 87, 2220-2224, 1990.
8. Trivedi, N., Steil, G.M., Colton, C.K., Bonner-Weir, S., and Weir, G.C. Improved vascularization of planar membrane diffusion devices following continuous infusion of vascular endothelial growth factor. Cell Transplant 9, 115-124, 2000.

9. Stoltz, J.F., Dumas, D., Wang, X., Payan, E., Mainard, D., Paulus, F., Maurice, G., Netter, P., and Muller, S. Influence of mechanical forces on cells and tissues. Biorheology 37, 3-14, 2000.

10. Sikavitsas, V.I., Temenoff, J.S., and Mikos, A.G. Biomaterials and bone mechanotransduction. Biomaterials 22, 2581-2593, 2001.

11. Hillsley, M.V., and Frangos, J.A. Bone tissue engineering: the role of interstitial fluid flow. Biotechnol Bioeng 43, 573-581, 1994.

12. Hoerstrup, S.P., Sodian, R., Sperling, J.S., Vacanti, J.P., and Mayer, J.E.J. New pulsatile bioreactor for *in vitro* formation of tissue engineered heart valves. Tissue Eng 6, 75-79, 2000.

13. Altman, G.H., Horan, R.L., Martin, I., Farhadi, J., Stark, P.R., Volloch, V., Richmond, J.C., Vunjak-Novakovic, G., and Kaplan, D.L. Cell differentiation by mechanical stress. FASEB J 16, 270-272, 2002.

14. Bancroft, G.N., Sikavitsas, V.I., and Mikos, A.G. Design of a flow perfusion bioreactor system for bone tissue-engineering applications. Tissue Eng 9, 549-554, 2003.

15. Dumont, K., Yperman, J., Verbeken, E., Segers, P., Meuris, B., Vandenberghe, S., Flameng, W., and Verdonck, P.R. Design of a new pulsatile bioreactor for tissue engineered aortic heart valve formation. Artif Organs 26, 710-714, 2002.

16. Garvin, J., Qi, J., Maloney, M., and Banes, A.J. Novel system for engineering bioartificial tendons and application of mechanical load. Tissue Eng 9, 967-979, 2003.

17. Marlovits, S., Tichy, B., Truppe, M., Gruber, D., and Vecsei, V. Chondrogenesis of aged human articular cartilage in a scaffold-free bioreactor. Tissue Eng 9, 1215-1226, 2003.

18. Meinel, L., Karageorgiou, V., Fajardo, R., Snyder, B., Shinde-Patil, V., Zichner, L., Kaplan, D., Langer, R., and Vunjak-Novakovic, G. Bone tissue engineering using human mesenchymal stem cells: effects of scaffold material and medium flow. Ann Biomed Eng 32, 112-122, 2004.

19. Sikavitsas, V.I., Bancroft, G.N., and Mikos, A.G. Formation of three-dimensional cell/polymer constructs for bone tissue engineering in a spinner flask and a rotating wall vessel bioreactor. J Biomed Mater Res 62, 136-148, 2002.

20. Martin, I., Wendt, D., and Heberer, M. The role of bioreactors in tissue engineering. Trends Biotechnol 22, 80-86, 2004.

21. Darling, E.M., and Athanasiou, K.A. Articular cartilage bioreactors and bioprocesses. Tissue Eng 9, 9-26, 2003.

22. Pazzano, D., Mercier, K.A., Moran, J.M., Fong, S.S., DiBiasio, D.D., Rulfs, J.X., Kohles, S.S., and Bonassar, L.J. Comparison of chondrogensis in static and perfused bioreactor culture. Biotechnol Prog 16, 893-896, 2000.

23. Pei, M., Solchaga, L.A., Seidel, J., Zeng, L., Vunjak-Novakovic, G., Caplan, A.I., and Freed, L.E. Bioreactors mediate the effectiveness of tissue engineering scaffolds. FASEB J 16, 1691-1694, 2002.

24. Burg, K.J., Holder, W.D.J., Culberson, C.R., et al. Comparative study of seeding methods for three-dimensional polymeric scaffolds. J Biomed Mater Res 52, 576, 2000.

25. Carrier, R.L., Papadaki, M., Rupnick, M., Schoen, F.J., Bursac, N., Langer, R., Freed, L.E., and Vunjak-Novakovic, G. Cardiac tissue engineering: cell seeding, cultivation parameters, and tissue construct characterization. Biotechnol Bioeng 64, 580-589, 1999.

26. Holy, C.E., Shoichet, M.S., and Davies, J.E. Engineering three-dimensional bone tissue *in vitro* using biodegradable scaffolds: investigating initial cell-seeding density and culture period. J Biomed Mater Res 51, 376-382, 2000.

27. Kim, S.S., Sundback, C.A., Kaihara, S., Benvenuto, M.S., Kim, B.S., Mooney, D.J., and Vacanti, J.P. Dynamic seeding and *in vitro* culture of hepatocytes in a flow perfusion system. Tissue Eng 6, 39-44, 2000.

28. Sodian, R., Lemke, T., Fritsche, C., Hoerstrup, S.P., Fu, P., Potapov, E.V., Hausmann, H., and Hetzer, R. Tissue-engineering bioreactors: a new combined cell-seeding and perfusion system for vascular tissue engineering. Tissue Eng 8, 863-870, 2002.

29. Vunjak-Novakovic, G., Obradovic, B., Martin, I., and Freed, L.E. Bioreactor studies of native and tissue engineered cartilage. Biorheology 39, 259-268, 2002.

30. Li, Y., Ma, T., Kniss, D.A., Lasky, L.C., and Yang, S.T. Effects of filtration seeding on cell density, spatial distribution, and proliferation in nonwoven fibrous matrices. Biotechnol Prog 17, 935-944, 2001.

31. Burg, K.J., Holder, W.D.J., Culberson, C.R., et al. Comparative study of seeding methods for three-dimensional polymeric scaffolds. J Biomed Mater Res 51, 642-649, 2000.

32. Alvarez-Barreto, J.F., and Sikavitsas, V.I. Tissue Engineering Bioreactors. In: Boronzino JD, ed. Tissue Engineering and Artificial Organs. Vol 3. 3 ed. Boca Raton: Taylor & Francis Group, pp. 44-41 - 44-18, 2006.

33. Vunjak-Novakovic, G., Obradovic, B., Martin, I., Bursac, P.M., Langer, R., and Freed, L.E. Dynamic cell seeding of polymer scaffolds for cartilage tissue engineering. Biotechnol Prog 14, 193-202, 1998.

34. Wendt, D., Marsano, A., Jakob, M., Heberer, M., and Martin, I. Oscillating perfusion of cell suspensions through three-dimensional scaffolds enhances cell seeding efficiency and uniformity. Biotechnol Bioeng 84, 205-214, 2003.

35. Cartmell, S.H., Porter, B.D., Garcia, A.J., and Guldberg, R.E. Effects of medium perfusion rate on cell-seeded three-dimensional bone constructs *in vitro*. Tissue Eng 9, 1197-1203, 2003.

36. Goldstein, A.S., Juarez, T.M., Helmke, C.D., Gustin, M.C., and Mikos, A.G. Effect of convection on osteoblastic cell growth and function in biodegradable polymer foam scaffolds. Biomaterials 22, 1279-1288, 2001.

37. Zhao, F., and Ma, T. Perfusion bioreactor system for human mesenchymal stem cell tissue engineering: dynamic cell seeding and construct development. Biotechnol Bioeng 91, 482-493, 2005.

38. Nam, Y.S., and Park, T.G. Porous biodegradable polymeric scaffolds prepared by thermally induced phase separation. J Biomed Mater Res 47, 8-17, 1999.

39. Ratner, B.D., and Bryant, S.J. Biomaterials: where we have been and where we are going. Annu Rev Biomed Eng 6, 41-75, 2004.

40. Watanabe, J., Eriguchi, T., and Ishihara, K. Cell adhesion and morphology in porous scaffold based on enantiomeric poly(lactic acid) graft-type phospholipid polymers. Biomacromolecules 3, 1375-1383, 2002.

41. Zhang, J., Doll, B.A., Beckman, E.J., and Hollinger, J.O. A biodegradable polyurethane-ascorbic acid scaffold for bone tissue engineering. J Biomed Mater Res 67A, 389-400, 2003.

42. Cooper, J.A., Lu, H.H., Ko, F.K., Freeman, J.W., and Laurencin, C.T. Fiber-based tissue-engineered scaffold for ligament replacement: design considerations and *in vitro* evaluation. Biomaterials 26, 1523-1532, 2005.

43. Durselen, L., Dauner, M., Hierlemann, H., Planck, H., Claes, L.E., and Ignatius, A. Resorbable polymer fibers for ligament augmentation. J Biomed Mater Res 58, 666-672, 2001.

44. Sikavitsas, V.I., van den Dolder, J., Bancroft, G.N., Jansen, J.A., and Mikos, A.G. Influence of the *in vitro* culture period on the *in vivo* performance of cell/titanium bone tissue-engineered constructs using a rat cranial critical size defect model. J Biomed Mater Res 67A, 944-951, 2003.

45. Badami, A.S., Kreke, M.R., Thompson, M.S., Riffle, J.S., and Goldstein, A.S. Effect of fiber diameter on spreading, proliferation, and differentiation of osteoblastic cells on electrospun poly(lactic acid) substrates. Biomaterials 27, 596-606, 2006.

46. de Rovere, A., and Shambaugh, R.L. Melt-Spun Hollow Fibers for Use in Nonwoven Structures. Ind. Eng. Chem. Res. 40, 176-187, 2001.

47. de Rovere, A., and Shambaugh, R.L. Melt Spun Hollow Fibers: Modeling and Experiments. Polym. Eng. Sci. 41, 1206-1219, 2001.

48. Hou, Q., Grijpma, D.W., and Feijen, J. Porous polymeric structures for tissue engineering prepared by a coagulation, compression moulding and salt leaching technique. Biomaterials 24, 1937-1947, 2003.

49. Lu, L., Peter, S.J., Lyman, M.D., Lai, H.L., Leite, S.M., Tamada, J.A., Vacanti, J.P., Langer, R., and Mikos, A.G. *In vitro* degradation of porous poly(L-lactic acid) foams. Biomaterials 21, 1595-1605, 2000.

50. Vehof, J.W., Fisher, J.P., Dean, D., van der Waerden, J.P., Spauwen, P.H., Mikos, A.G., and Jansen, J.A. Bone formation in transforming growth factor beta-1-coated porous poly(propylene fumarate) scaffolds. J Biomed Mater Res 60, 241-251, 2002.

51. Shambaugh, R.L. A Macroscopic View of the Melt Blowing Process for Producing Microfibers. Ind. Eng. Chem. Res. 27, 2363, 1988.

52. Zhong, J., Asker, C.L., and Salerud, E.G. Imaging, image processing and pattern analysis of skin capillary ensembles. Skin Res Technol 6, 45-57, 2000.

53. Bancroft, G.N., Sikavitsas, V.I., van den Dolder, J., Sheffield, T.L., Ambrose, C.G., Jansen, J.A., and Mikos, A.G. Fluid flow increases mineralized matrix deposition in 3D perfusion culture of marrow stromal osteoblasts in a dose-dependent manner. Proc Natl Acad Sci U S A 99, 12600-12605, 2002.

54. Gomes, M.E., Sikavitsas, V.I., Behravesh, E., Reis, R.L., and Mikos, A.G. Effect of flow perfusion on the osteogenic differentiation of bone marrow stromal cells cultured on starch-based three-dimensional scaffolds. J Biomed Mater Res 67A, 87-95, 2003.

55. Sikavitsas, V.I., Bancroft, G.N., Holtorf, H.L., Jansen, J.A., and Mikos, A.G. Mineralized matrix deposition by marrow stromal osteoblasts in 3D perfusion culture increases with increasing fluid shear forces. Proc Natl Acad Sci U S A 100, 14683-14688, 2003.

56. Gomes, M.E., Bossano, C.M., Johnston, C.M., Reis, R.L., and Mikos, A.G. *In vitro* localization of bone growth factors in constructs of biodegradable

scaffolds seeded with marrow stromal cells and cultured in a flow perfusion bioreactor. Tissue Eng 12, 177-188, 2006.

57. Datta, N., Holtorf, H.L., Sikavitsas, V.I., Jansen, J.A., and Mikos, A.G. Effect of bone extracellular matrix synthesized *in vitro* on the osteoblastic differentiation of marrow stromal cells. Biomaterials 26, 971-977, 2005.

58. Hosseinkhani, H., Inatsugu, Y., Hiraoka, Y., Inoue, S., and Tabata, Y. Perfusion culture enhances osteogenic differentiation of rat mesenchymal stem cells in collagen sponge reinforced with poly(glycolic Acid) fiber. Tissue Eng 11, 1476-1488, 2005.

59. Kreke, M.R., Badami, A.S., Brady, J.B., Akers, R.M., and Goldstein, A.S. Modulation of protein adsorption and cell adhesion by poly(allylamine hydrochloride) heparin films. Biomaterials 26, 2975-2981, 2005.

60. Batchelor, G.K. An Introduction to Fluid Dynamics. Great Britain: Cambridge University Press; 1991:245-246.

61. Ford, A.N., and Papavassiliou, D.V. Flow around Surface-Attached Carbon Nanotubes. Ind. Eng. Chem. Res. 45, 1797-1804, 2006.

62. Walther, J.H., Werder, T., Jaffe, R.L., and Koumoutsakos, P. Hydrodynamic properties of carbon nanotubes. PHYSICAL REVIEW E 69, 062201, 2004.

63. Klein-Nulend, J., Helfrich, M.H., Sterck, J.G., MacPherson, H., Joldersma, M., Ralston, S.H., Semeins, C.M., and Burger, E.H. Nitric oxide response to shear stress by human bone cell cultures is endothelial nitric oxide synthase dependent. Biochem Biophys Res Commun 250, 108-114, 1998.

64. van den Dolder, J., Bancroft, G.N., Sikavitsas, V.I., Spauwen, P.H., Jansen, J.A., and Mikos, A.G. Flow perfusion culture of marrow stromal osteoblasts in titanium fiber mesh. J Biomed Mater Res 64A, 235-241, 2003.

65. Moore, M.J., Jabbari, E., Ritman, E.L., Lu, L., Currier, B.L., Windebank, A.J., and Yaszemski, M.J. Quantitative analysis of interconnectivity of porous biodegradable scaffolds with micro-computed tomography. J Biomed Mater Res A 71, 258-267, 2004.

Chapter 4

Preparation of a functionally flexible, three-dimensional, biomimetic poly (L-lactic acid) scaffold with improved cell adhesion

Chapter Abstract

Poly(L-lactic acid) (PLLA) is widely used in tissue engineering applications due to its degradation characteristics and mechanical properties but possesses an inert nature, affecting cell-matrix interactions. It is desirable to modify the surface of PLLA to create biomimetic scaffolds that will enhance tissue regeneration. We prepared a functionally flexible, biomimetic scaffold by derivatizing the surface of PLLA foams into primary amines, activated pyridylthiols, or sulfhydryl groups, allowing a wide variety of modifications. Poly (L-lysine) (PolyK) was physically entrapped uniformly throughout the scaffold surface and in a controllable fashion by soaking the foams in an acetone-water mixture and later in a polyK solution in dimethylsulfoxide. RGDC adhesion peptide was linked to the polyK via creating disulfide bonds introduced through the use of the linker N-succinimidyl-3-(2-pyridylthiol)-propionate (SPDP). Presence of RGDC on the surface of PLLA 2-D disks and 3-D scaffolds increased the number of adherent mesenchymal stem cells. We have proposed a methodology for creating biomimetic scaffolds that is easy to execute, flexible, and nondestructive.

4.1. Introduction

In most tissue engineering applications, the biochemical and physical interactions of the cells with the scaffolding material are of crucial importance. The deposition of extracellular matrix by specific functional or progenitor cells (e.g., mesenchymal stem cells) on the surface of the scaffolds provides a tissue-inductive nature to the construct that can enhance the regeneration of the damaged or lost tissue. Thus, strong cell-matrix interactions will benefit the expression of extracellular matrix proteins [1,2]. The scaffold has to thereby support the adhesion of the cells, as well as their growth, migration and differentiation toward a specific phenotype [3-5].

The scaffold needs to possess certain mechanical and morphological characteristics so as to achieve a more efficient regeneration process [6-9]. The material must have mechanical properties that can meet the demands of the defect site, especially when the injury occurs in a mechanically demanding zone. Sufficient porosity, an optimum pore size and pore interconnectivity are necessary for the nutrition of the cells, the formation of new tissue and the establishment of a vascular network that will guarantee the survival of the *de novo* tissue. Ideally, the scaffold should be biodegradable and permit progressive tissue formation without compromising the fulfillment of the mechanical requirements at the site of implantation [8,10-12].

Scaffolds for tissue engineering have been created using a wide variety of techniques and materials, both synthetic and natural [13-27]. Collagen, ceramics, and biodegradable polymers are among the most popular choices in different approaches

[21,28,29]. Poly(α-hydroxy esters) represent the most common biodegradable polymers for this purpose due to their well known degradation mechanisms, and good mechanical properties, particularly poly(lactic acid), poly(glycolic acid) and their copolymers are widely employed. Nevertheless, these polymers can only support cell adhesion and growth to a certain extent [30,31]. These polymers can be modified with active biomolecules to create scaffolds that enhance cell-matrix interactions or elicit other specific cellular responses according to the application [29,32].

The development of these biomimetic scaffolds involves the bulk or surface modification of a base biomaterial with growth and differentiation factors that can improve cell attachment, proliferation, and migration, as well as eliciting other specific cellular responses both *in vitro* and *in vivo* [2,6,32]. The most common way to modify the bulk of biodegradable polymers is by chemically cross-linking polymer chains with a bioactive molecule; this technique is popular in the preparation of hydrogels for cartilage repair [32-39]. A challenge encountered with the current bulk modification techniques, when applied to a porous preformed scaffold, is the modification of its mechanical properties and degradation characteristics.

Surface modification can also be carried out both physically and chemically. Physical adsorption, a common and easy way to modify materials, consists of simply incubating the surface of the polymer in a solution with the modifying biomolecule and letting it adsorb onto the surface; however, this methodology poses the risk of desorbing the incorporated modifying agent during their utilization [38,40,41]. The surface of the polymer can also be functionalized by hydrolysis or aminolysis by soaking the scaffold in reactive solutions. Nonetheless, the extent of modification with this

methodology is limited since the intrinsic inert nature of the polymer restricts the creation of active sites; in addition to that, the degradation properties of the polymer close to the surface could also be changed [42]. Physical entrapment of the bioactive molecule near the surface of the scaffold is an alternative that could overcome the restrictions regarding the generation of active sites as well as desorption of the modifying agent. Cui et al. entrapped gelatin in the surface of poly(L-lactic acid) (PLLA) films and enhanced the attachment of chondrocytes [43]. Furthermore, the degradation characteristics are preserved because the chemical structure and bulk composition of the polymer are not altered. In our studies, we have used a similar modification methodology to that used by Cui et al to create a functionally flexible, biomimetic scaffold that can be further functionalized for specific applications in tissue engineering.

The aim of this study was to modify the surface of PLLA foams using physical entrapment of poly(L-lysine) (PolyK) into their surface. This amine functionalized scaffold can be further modified by linking different molecules chosen accordingly in different tissue engineering applications through the use of amine coupling chemistries. Linking different bioactive molecules makes the scaffold functionally flexible since, through its appropriate modification, specific cellular responses can be attained depending on the desired application. The possibility of entrapping PolyK in a controllable fashion was considered. Moreover, we strived to estimate the amount of polyK available in the surface at different levels of entrapment. The stability of the modified surface and the effects of the modification technique on scaffold morphology were also studied. Further functionalization of the surface was demonstrated by improving cell adhesion. Arg-Gly-Asp (RGD), an adhesion peptide

found in fibronectin and other bioactive molecules that promote cell adhesion, was linked to the entrapped polyK, and the capacity for mesenchymal stem cell attachment at different levels of RGD modification was assessed on two-dimensional discs and three-dimensional tissue engineering scaffolds .

4.2. Materials and Methods

4.2.1 Materials

Poly(L-lactic acid) (PLLA, average MW 100,000) was purchased from Birmingham Polymers. Poly(L-lysine) (PolyK, MW 1000-4000) and dimethyl sulfoxide (DMSO) were purchased from Sigma-Aldrich. Periodate-activated horseradish peroxidase (HRP) (E-Z link activated peroxidase), N-succinimidyl 3-(2-pyridylthiol) propionate (SPDP), dithiothreitol (DTT), and fluorescein-5-maleimide, were obtained from Pierce. Chloroform and acetone were purchased from Fisher Scientific. Sodium chloride, Triton X-100, and hydrogen peroxide (H_2O_2) were obtained from VWR. An ABTS kit for the detection of HRP activity, containing the ABTS reagent (2,2'-azino-di(3-ethylbenzthiazoline-6-sulfonate)), citrate buffer and hydrogen peroxide (H_2O_2), was purchased from Zymed Laboratories. An AMPLEX® Red kit, BODIPY® FL phalloidin, cell-loading pinocytic reagent and a PicoGreen® DNA quantification kit were purchased from Invitrogen. Phosphate buffered saline (PBS) and fetal bovine serum (FBS) from selected lots were purchased from Atlanta Biologicals. Alpha minimum essential medium (α-MEM) and trypsin-EDTA were obtained from Gibco. Arginine-glycine-aspartic acid-cysteine (RGDC) was purchased from American Peptide.

4.2.2 Determination of the optimal entrapment technique

PolyK has been incorporated in different biomaterial surfaces to enhance the adhesion of osteoblasts and other cells. PolyK molecules have shown great improvement on cell spreading and, in many cases, cell growth, demonstrating compatibility of the biomaterial with the cells [44-49]. The degree of adhesion has been shown to be directly proportional to the polyK molecular weight [50,51]. A small-size polyK (MW 1000-4000) was utilized in order to minimize its effect on cell adhesion and assess the effect of RGD only.

To determine the most efficient entrapment technique, two-dimensional PLLA films were created. PLLA was dissolved in chloroform at a concentration of 0.1g/ml and poured on glass Petri dishes, and the chloroform was allowed to evaporate overnight. Discs with 8 mm in diameter and 200 μm in thickness were punched. The following modification techniques were tested:

(a) Bulk modification. In this technique, the Poly(L-lysine) (polyK) was dispersed in the chloroform- PLLA solution at a concentration of 0.1mg polyK/ml, before pouring it on the Petri dishes.

(b) Acetone-polyK soaking. Prefabricated PLLA discs were incubated in 600μl of a suspension of polyK in acetone (0.1mg/ml) for 12 h.

(c) Acetone/DMSO soaking. Prefabricated PLLA discs were soaked in a 7:3 acetone-water mixture for 1h. They were then soaked in 600μl of a solution of polyK in dimethyl sulfoxide (DMSO) (0.1mg/ml) for 12 h.

Four discs were used to test each modification technique. To assess polyK incorporation, modified discs were reacted in 600 µl of 10^{-8} M periodate-activated horseradish peroxidase (Periodate-HRP) (pH 8) for 2 h. An ABTS kit was used to detect the presence of HRP. Briefly, equal amounts of the ABTS reagent and H_2O_2 were diluted in a citrate buffer, as specified by the manufacturer. Modified discs were incubated in 600µl of the ABTS/ H_2O_2 solution. HRP activity was measured by reading absorbance in a Synergy HT plate reader (Bio-Tek®) at 405nm. Levels of polyK entrapment were directly related to the absorbance signal; the higher the signal, the greater the amount of polyK entrapped.

PolyK surface distribution after entrapment: Fluorescence tagging of the polyK also allows for the evaluation of its distribution throughout the disc surface. Modified discs were incubated in 600µl of 1mM N-Succinimidyl 3-(2-pyridyldithio) propionate (SPDP) in HEPES buffer (pH 8.3) for 30 min., followed by rinsing and the unmasking of the thiol group in 600µl of 1mM dithiothreitol (DTT). The discs were then rinsed and incubated in 0.1mM fluorescein-5-maleimide in HEPES buffer (pH 8.3) for 2 hrs. Every rinsing step after modification consisted of one wash with 0.1% Triton X-100 and three washes with deionized water. Fluorescence microscopy of modified and unmodified discs was performed using a Nikon Epifluorescence microscope with excitation at 495nm and emission at 518 nm. Images were captured with MetaMorph 6.2 (Universal Imaging Corporation).

The presence of SPDP linked to the entrapped polyK was corroborated by measuring the absorbance generated by the release of pyridine-2-thione at a wavelength of 343 nm, after the reaction of SPDP with DTT. A standard curve was

generated by preparing SPDP solutions of known concentrations and incubating them with DTT for 30 min. Moles of reactive SPDP linked to the polyK in 2-D surfaces were estimated with this curve. The number of discs used in these quantifications was four.

4.2.3 Modification of 3-D PLLA scaffolds

Scaffold fabrication. PLLA foams were prepared by particulate leaching using sodium chloride (NaCl) as the porogen, with a grain size between 300-450μm 2,52,53. Briefly, PLLA was dissolved in chloroform at a concentration of 5% w/v. The solution was then poured on a sodium chloride bed, and the solvent was allowed to evaporate for 24 h. The solid salt-polymer composite, which was 95 wt% in NaCl, was pressed in a cylindrical mold with an inner diameter of 8 mm at 500 psig, using a hydraulic press, with simultaneous heating at 130^{o}C for 30 min. The resulting pellet was cut into discs of 3 mm in thickness using a low speed diamond wheel saw (Model 650, South Bay Technology, Inc). Salt leaching was carried out using deionized water for 3 days while the water was changed at least twice a day. Scaffold porosity was determined as the percentage ratio of the weight of the porous scaffold to the weight of a solid PLLA disc with the same dimensions.

Entrapment of polyK in 3-D scaffolds. Results from the modification of 2D discs indicated that the most efficient entrapment technique was Acetone\DMSO soaking (section 4.2.2.c); thus, this technique was used to modify three dimensional scaffolds. Foams were soaked in a 1:3 acetone-water mixture for 1 h. Then, they were placed in 1 ml of a solution of PolyK in dimethyl sulfoxide (DMSO) at 0.1 mg/ml for 12 h. Rinsing was carried out after that with 0.1% Triton X-100, followed by three

washes with deionized water. All the stages were carried out under vacuum and vigorous shaking so as to allow the penetration of the different solutions throughout the porous network of the scaffold.

Detection of entrapped PolyK. Modified foams were incubated in 600µl of 1mM SPDP in HEPES buffer (pH 8.3) for 30 min., followed by rinsing and unmasking of the thiol group of the SPDP in 600µl of 1mM DTT. Scaffolds were then incubated in 0.1mM fluorescein-5-maleimide for 2 hrs. All steps were carried out under vacuum and sufficient rinsing followed each incubation step as previously explained. Scaffolds were placed in 1-ml centrifuge tubes with deionized water and frozen in liquid nitrogen for later longitudinal sectioning using a low speed diamond wheel saw. The sections had a thickness of 1 mm. Fluorescence microscopy was performed on the transversal sections in a Nikon Epifluorescence microscope with excitation at 495nm and emission at 518 nm. Images were captured with MetaMorph 6.2. Controls included modification of the scaffolds in the following combinations: polyK-no SPDP, no polyK-SPDP, or plain. All scaffolds were treated with DTT and fluorescein-5-maleimide as explained above.

4.2.4 Varying the amount of entrapped polyK in PLLA foams

PLLA scaffolds were modified at polyK incubation concentrations of $1x10^{-8}$, $1x10^{-7}$, $1x10^{-6}$, $1x10^{-4}$, and 0.1 mg/ml. PolyK- modified scaffolds were incubated in 1 ml of 10^{-7} M periodate-HRP under vacuum for 2 hrs. After HRP linkage, they were rinsed in 0.1% Triton X-100 under vacuum, followed by three washes with deionized water. Each rinsing step was carried out for 15 min, and the vacuum was applied by covering the container with a sleeve stopper and suctioning the air with a syringe.

Estimation of the amount of entrapped polyK was achieved by using an AMPLEX® Red kit (Molecular Probes). Briefly, equal parts of 20mM H_2O_2 in reaction buffer (0.05 M sodium phosphate in Tris buffer, pH 7.4) and 100μM AMPLEX® Red (10-acetyl-3,7-dihydroxyphenoxazine) in DMSO were mixed. In a 96-well plate, the remaining activated HRP incubation solutions and washes were arranged in aliquots of 10 μl, along with 90 μl of PBS and 50μl of the working solution (AMPLEX® Red/H_2O_2) and incubated for 5 min. A standard curve was generated by reading the fluorescence of HRP solutions of known concentrations. Fluorescence was measured at an excitation of 530 nm and emission of 590 nm in a Synergy HT plate reader (Bio-Tek®). Fluorescence signals were converted to concentrations through the use of the standard curve. The moles of entrapped polyK were determined as the difference between the moles of HRP present in the original soaking solution and the moles measured in the remaining soaking solutions and washes. Amounts of entrapped polyK were calculated by subtracting the background signal emitted by the plain scaffolds. The number of scaffolds used in each group was four.

4.2.5. Stability of the modified surface

Modified 2-D discs were soaked in PBS for 10 days, at room temperature, under gentle shaking. After thorough rinsing, entrapped polyK was quantified at days 0, 4 and 10 with periodate-HRP linkage and AMPLEX® Red, as previously described (n = 4).

4.2.6. Effect of the acetone treatment on the porous architecture of 3-D foams

Micro-computed tomography was carried out by scanning the scaffold (treated with acetone) using the ultra-high-resolution tomography system with a 200-kV

microfocal X-ray source (Bio-Imaging Research, Inc.) at the University of Texas Computed Tomography Facility (UTCT, Austin, TX), using X-ray settings of 180 kV and 0.088 mA. The slice thickness and inter-slice spacing was 0.0193 mm. An 8.15 mm field of view was reconstructed on a 512x512 pixel field, resulting in a pixel spacing of 0.0162 mm. The data was analyzed using the software Blob3D developed at the UTCT facility. Values of scaffold porosity and interconnectivity of the void spaces were obtained from these analyses 54. (n=1)

4.2.7. Incorporation of RGDC peptides to the polyK modified surface

After entrapping polyK in the surface of PLLA discs and foams, RGDC was linked via a disulfide bond through the SPDP attached to the amine groups. PolyK-modified surfaces were incubated in 600µl of 1mM SPDP in HEPES buffer (pH 8.3) for 30 min. One cycle of rinsing with 0.1% Triton X-100 and three cycles with PBS were performed succeeding the reaction. Surfaces were incubated in 100µM RGDC for one hour and rinsed. When modifying the 3-D foams, vacuum was utilized at each stage of modification to mitigate mass transport limitations to the interior of the scaffold.

RGDC linkage to SPDP was corroborated on 2D discs by measuring the absorbance at 343nm corresponding to the release of pyridine-2-thione group during the reaction of the sulfhydryl group from the cysteine with the SPDP (see Apendix I). A standard curve was generated by preparing SPDP solutions of known concentrations and incubating them with RGDC for one hour. Moles of reactive SPDP linked to the polyK in 2-D surfaces were estimated with this curve (n = 4).

X-ray photoemission spectroscopy (XPS). XPS was also performed on the surface of RGDC-linked and unmodified disks to confirm the presence of the adhesion peptide on the surface. Another control also included polyK-treated disks incubated in RGDC, in the absence of SPDP. XPS data were recorded on a Physical Electronics PHI 5800 ESCA System with a background pressure of approximately 3.0X 10^{-9} Torr. The electron takeoff angle was 45^{o} with respect to the sample surface. A spot size of 800-μm and 23 eV pass energy were used for the analysis. The number of discs was used was four, and ten spots were taken on each sample. The binding energies were corrected by reference to the C1s line at 284.8 eV for hydrocarbon. Quantification of the surface composition was carried out by integrating the peaks corresponding to each element with aid of the Shirley background subtraction algorithm, and then converting these peak areas to atomic composition by using the sensitivity factors provided for the each element by the PHI 5800 system software.

4.2.8 Cell seeding on RGDC-modified surfaces

Adult mesenchymal stem cells (MSCs) were isolated from the bone marrow of eight-week-old male Wistar® rats (Harland Laboratories) using well established methods [38-40]. Briefly, rats were euthanized, and the tibiae and femura were extracted. The epiphyses were cut off, and the bone marrow was flushed and suspended in α-MEM supplemented with 10% fetal bovine serum (FBS). The suspension was then distributed in polystyrene culture flasks (75 cm^2). Cells were cultured at 37^{o}C and 5% CO_2. Non-adherent cells were discarded after two days of culture. MSCs were detached using trypsin, centrifuged at 400g for 5 min, resuspended in α-MEM and replated until the 4th passage.

Cell area measurements on 2D discs: Cells from the 4th passage (total of $5x10^4$ cells at a density of $2x10^5$ cells/ml) were seeded on the surface of polyK-SPDP-RGDC modified discs (at different levels of modification) and allowed to attach for 6 hours. Discs were then rinsed in PBS and fixated in 3.7% formalin for 10 min, and rinsed with 0.1% Triton-X-100 and PBS. Cells were labeled with 2 units of BODIPY® FL phalloidin, a high affinity probe for F-actin, for 10 min. After rinsing, fluorescence microscopy was performed using a Nikon Epifluorescence microscope. Image processing and measurements of cell area were carried out with MetaMorph 6.2 (Universal Imaging Corporation). The excitation and emission wavelengths were 558nm and 569 nm, respectively. Fifteen cells from four different samples were used in cell area measurements. Controls in this study included plain discs and plain discs incubated in an RGDC solution to assess the effect of RGDC physisorption.

Cell attachment on 3D scaffolds: MSCs from the 4th passage were also seeded on three-dimensional foams that were either unmodified or modified with RGDC at different levels of polyK-SPDP-RGDC modification (four scaffolds for each modification level). Scaffolds were press-fitted in cartridges designed for static seeding, and a cell suspension containing $5x10^5$ MSCs (at a density of $2x10^6$ cells/ml) was poured on top of the scaffolds. Cells were allowed to attach for 6 hours. Furthermore, cells seeded on RGDC-modified scaffolds were cultured for 24 and 48 h in order to assess any cytotoxic effects. After attachment, the seeded scaffolds were quickly rinsed in PBS, suspended in 3 ml of deionized water, and broken down into small pieces. Samples were later submitted to three cycles of freeze/thaw to lyse the cells. A picogreen® DNA quantification assay was performed to obtain the number of cells attached to the scaffolds. A standard curve was made using known-concentration

solutions of lambda virus DNA. Sample and standard aliquots of 43 µl were accommodated in a 96-well plate, along with 107 µl of reaction buffer (20mM Tris-HCl, 1 mM EDTA, pH 7.5) and 150 µl of the Picogreen® dye. Fluorescence was measured (490 nm excitation and 520 nm emission) using a Synergy HT plate reader. The number of cells was calculated using the total amount of DNA determined in the sample divided by the amount of DNA contained in one cell.

4.2.9 Statistical analysis

For most experiments, four samples were used (n = 4), unless otherwise specified. Values were reported as the average ± the standard error of the mean. The data were analyzed by using ANOVA, and multiple pair-wise comparisons were carried out using the Tukey-HSD method at a confidence level of 95%.

4.3. Results

4.3.1 Determination of the optimal polyK entrapment technique

Two dimensional discs were used to determine the most efficient surface modification protocol due to their regular morphology and ease of preparation and handling. The optimal technique characterized in the 2-dimensional surfaces was later utilized in the modification of 3-D foams. After entrapment, it was possible to attach HRP to the polyK, and quantitative absorbance or fluorescent assays involving the enzymatic reaction with hydrogen peroxide could be carried out.

Detection of entrapped polyK on the surface of PLLA discs using different entrapping techniques is shown in Figure 4.1. Bulk modification and acetone-polyK soaking yielded no significantly different absorbance signals from the unmodified surfaces (0.38 ± 0.06). The acetone/DMSO soaking, on the other hand, gave the significantly highest absorbance (1.16 ± 0.11). Thus, acetone soaking of the discs followed by incubation (room temperature) in a polyK/DMSO solution resulted in the most efficient method to entrap PolyK in the surface of the polymer and would be later used to modify three-dimensional scaffolds.

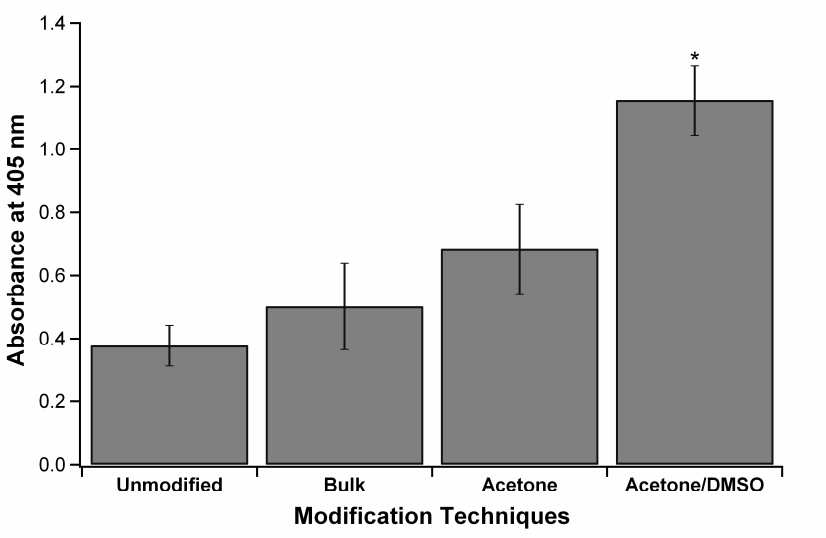


Figure 4.1. Detection of poly(L-lysine) entrapped in poly(L-lactic acid) discs with different techniques. Horse radish peroxidase was linked to the polyK and reacted with H_2O_2 in the presence of ABTS, developing a green color whose absorbance can be read at 405nm.The (*) represents the technique that yielded the significantly highest absorbance signal. (n = 4)

The reaction of SPDP with DTT results in the release of pyridine-2-thione, a group responsible for the generation of absorbance at 343 nm (Figure 4.2). The detection of this group can also provide an insight into the amount of reactive SPDP incorporated to the surface by using a standard curve prepared with SPDP solutions of known concentrations unmasked with excess DTT. The estimated amount of SPDP linked to disks modified with a polyK incubation concentration of 0.1 mg/ml was (36.0 ± 6) nmoles. The unmodified surface yielded a negligible absorbance signal ($p<0.05$).

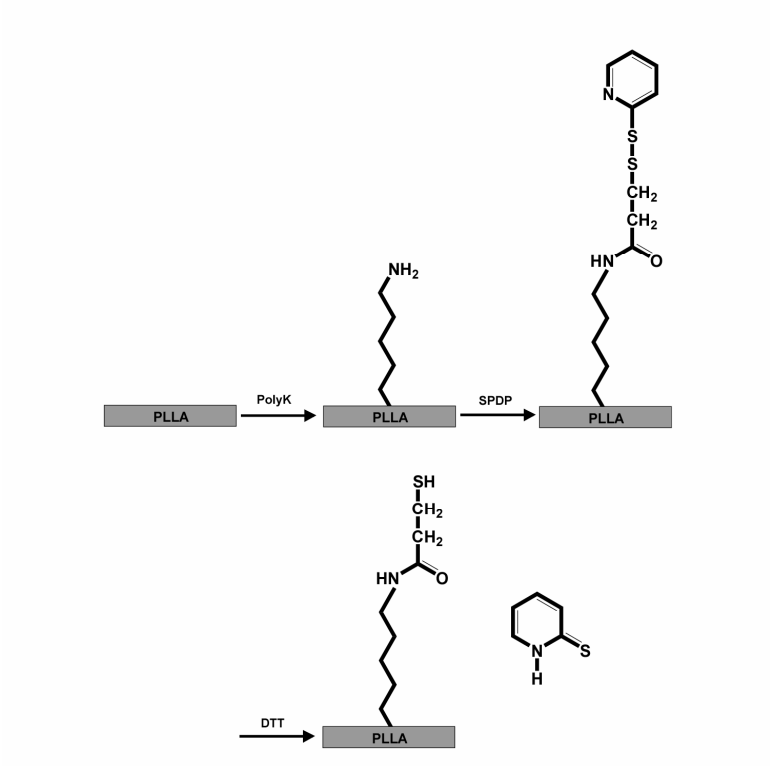


Figure 4.2. Physical entrapment of Poly(L-lysine) (PolyK) on the surface of poly (L-lactic acid) and further incorporation of SPDP, and the release of pyridine-2-thione due to the action of DTT

The distribution of the entrapped PolyK was assessed by linking Fluorescein-5-Maleimide to the sulfhydryl groups provided by the SPDP after DTT treatment. The distribution of the PolyK can be seen in Figure 4.3, where both modified and unmodified discs are shown. The modified disc exhibited greater fluorescence than the plain disc, and a uniform labeling pattern was observed throughout the modified surface.

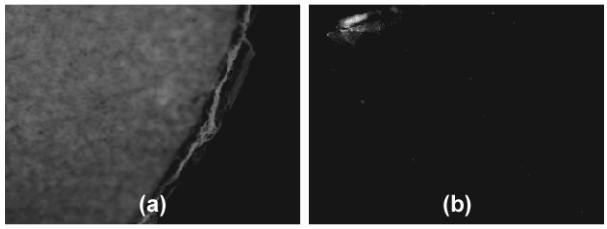


Figure 4.3. Fluorescent micrographs of the surface of (a) polyK-modified (using the acetone/DMSO procedure), SPDP-derivatized and (b) unmodified discs. Both discs were treated with Fluorescein-5-Maleimide.

4.3.2 Modification of 3-D porous foams

Acetone/DMSO soaking resulted in the most efficient polyK entrapment technique in PLLA discs; therefore, it was employed to modify three-dimensional porous foams. Fluorescein-5-Maleimide was used once again to evaluate the distribution of the PolyK throughout the porous network. In Figure 4.4, fluorescence micrographs of longitudinal transversal sections of three-dimensional foams prepared using different modification methodologies are shown. PolyK/SPDP modified foams presented a stronger fluorescence than the controls, which included scaffolds treated with polyK/no SPDP, no polyK/SPDP and plain discs; all scaffolds were treated with DTT and fluorescein-5-maleimide. A homogeneous intensity was observed throughout the transversal sections of polyK/SPDP-scaffold.

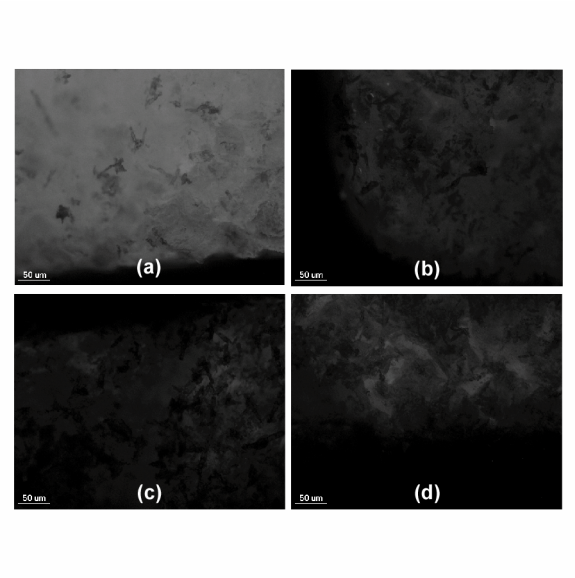


Figure 4.4. Demonstration of the presence of polyK on the surface of 3-D scaffolds modified with the acetone/DMSO procedure. Transversal sections of scaffolds treated differently are shown: (a) polyK/SPDP (b) polyK/no SPDP (c) no polyK/SPDP (d) plain. All scaffolds were treated with DTT followed by fluorescein-5-maleimide

4.3.3 Varying the amount of the entrapped polyK

To vary the amount of entrapped polypeptide added to the scaffolds, different concentrations of PolyK were incubated with the scaffolds during the period of entrapment. The quantification of the amount of entrapped polyK using periodate-HRP is presented in Figure 4.5. The amount of entrapped polyK directly depended on the polyK incubation concentration up to an incubation concentration of $1x10^{-4}$ mg/ml, after which the amount of polyK entrapped did not significantly change. A statistically significant lower amount was entrapped at an incubation concentration of $1x10^{-6}$ mg/ml (58.5 ± 0.5 pg). Low polyK incubation concentrations of $1x10^{-7}$ and $1x10^{-8}$ mg/ml yielded significant levels of entrapment, with amounts of entrapped polyK of (22.8 ± 1.4) and (12.6 ± 0.7) pg, respectively.

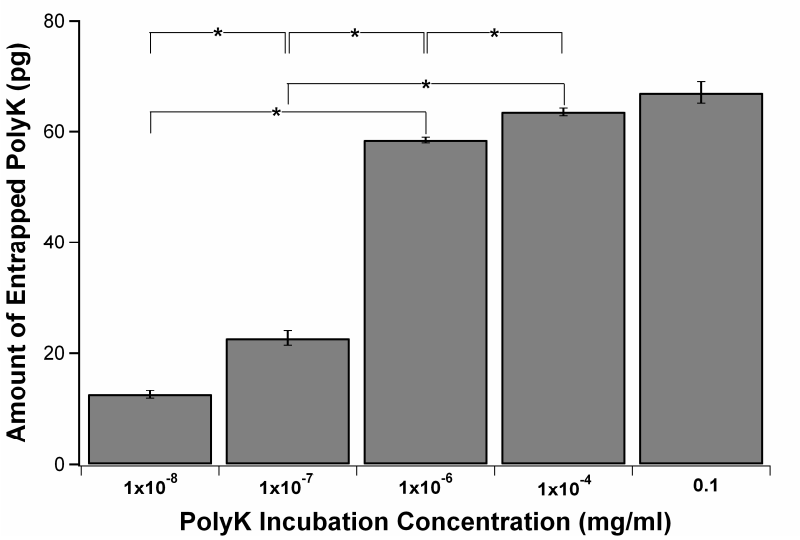


Figure 4.5. Quantification of the amount of entrapped polyK in the surface of PLLA foams at different concentrations of polypeptide in the stage of incubation after the soaking with acetone. (* $p<0.05$) (n = 4)

4.3.4. Effect of the acetone treatment on the porous architecture of 3-D foams.

Micro-computed tomography images (Figure 4.6) revealed that, after treatment, the scaffold presented a clear porous network, with a level of interconnectivity of 99.9% as reported by the microCT data analysis. This analysis also reported a porosity of 90% after treatment, which was in agreement with our estimations prior and after treatment, in which cases the porosity was calculated as the ratio of the scaffold weight to the weight of a solid PLLA disc with the same dimensions, resulting in 90% in both cases.

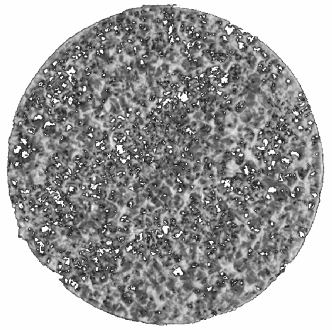


Figure 4.6. Micro-computed tomography scan of a PLLA foam after being treated with a mixture of acetone and water (7:3) for 1 hr.

4.3.5 Stability of the modified surface

The initial amount of entrapped polyK in 2-D discs, using the AMPLEX RED® quantification procedure, was estimated to be (1.1 ± 0.1) ng. After 10 days of incubation in PBS under gentle shaking, the estimated amount of polyK on the surface was (1.1 ± 0.2) ng, which was not statistically different from freshly modified surfaces.

4.3.6 Incorporation of RGDC peptides to the poly-modified surfaces

When RGDC is linked to polyK-SDPD-modified surfaces, the sulfhydryl group from the cysteine causes the release of the pyridine-2-thione group from the SPDP molecule (see Figure 4.7). The amount of released pyridine-2-thione, which is equivalent to the amount of SPDP that reacts with the RGDC, was estimated using a standard curve, as previously explained. PolyK/SPDP/RGDC-modified 2-D discs using a polyK incubation concentration of 0.1 mg/ml yielded (25 ± 8) nmoles.

When using an incubation concentration of 0.01mg/ml, there was no statistically significant difference with the higher polyK incubation concentration in the estimated amount of reactive SPDP (24 ± 8) nmoles. However, at an incubation concentration of $1x10^{-4}$ mg/ml, the amount of reactive SPDP was estimated to be (18 ± 6) nmoles, which was significantly lower than those obtained at higher incubation concentrations ($p<0.05$). The release of the pyridine-2-thione at polyK incubation concentrations lower than $1x10^{-4}$ mg/ml was below the lowest detection limit of the dose response curve, and no measurement could be done.

The presence of the RGDC peptide on the surface was confirmed by X-ray photoemission spectroscopy (XPS). Sulfur was chosen as the marker for comparison in this analysis since the sulfhydryl group from the cysteine is responsible for the reaction with the SPDP. Sulfur concentration on the polyK/SPDP/RGDC-modified surface (0.67 ± 0.25)% was significantly higher than in the polyK/RGDC-modified (without SPDP) and unmodified surfaces, (0.22 ± 0.05)% and (0.11 ± 0.01)% respectively.

With the quantification of the moles of SPDP present on the surface of the polyK-modified PLLA surface by the release of the pyridine-2-thion, it is now possible to estimate the area covered by the entrapped poly (L-lysine). In the same way, an estimation can be made based on the amount of HRP quantified through the AmplexRed procedure. The molecular coverage of the surface, A_{cov}, can be calculated through equation 4.1:

$$A_{\text{cov}} = nN_A a_{mol} \tag{4.1}$$

Where n is the number of moles, N_A is Avogadro's number (6.022×10^{23}), and a_{mol} is the area occupied by a single molecule, which was estimated assuming a circle with the molecular hydrodynamic radius. In the case of HRP, the radius was 30 Å. When using the SPDP data, a_{mol} was based on the spacer length of SPDP (6.8 Å) added to the size of a single lysine (10.2 Å). The available surface area for entrapment for a PLLA disc was 106 mm^2.

With the AmplexRed quantification done at a polyK incubation concentration of 0.1 mg/ml (the highest used in our studies), $2.8x10^{-12}$ moles of HRP/cm^2 were estimated on the surface of 2D discs. In this case, the area of coverage resulted in 123 mm^2. This value was obtained for the coverage of HRP on the PLLA surface. It needs to be noted that HRP is much larger than either polyK or SPDP, and under each HRP molecule, multiple polyK molecules can be found. Thus, in essence, we are just calculating the HRP coverage, which appears to cover the entire available area of the 2D surface. Clearly, a one to one stoichiometry of HRP to polyK would provide a lower limit on the polyK coverage ($2.8x10^{-12}$ moles/cm^2), while the actual value may be higher. This procedure will provide a more accurate estimate of polyK coverage when the HRP coverave is very sparce (less than 5% of the value observed here).

For the SPDP calculations, it was assumed that polyK had an average MW of 2500 (the manufacturer stated that the MW ranged from 1000 to 4000), and that 50% of the molecule was entrapped in the PLLA, leaving approximately 12 lysines active for reaction. If we assume that all the available lysines react with SPDP, the coverage obtained is 56 mm^2, implying 53% coverage of the PLLA surface with polyK. Clearly, this is a conservative estimate since the presence of unreacted lysines with SPDP could result in higher than 53% coverage. If the number of reactive lysines is decreased, we can achieve 100% coverage when 6 out of 12 lysines per polyK are reacted. Therefore, our surface coverage ranges between 50 and 100%, depending on the assumptions made, and the number of reacted lysines is at least 50% of the assumed 12 available reactive lysines per polyK molecule.

For a lower polyK incubation concentration ($1x10^{-4}$ mg/ml), and with the same assumptions stated in the previous paragraph (avg MW of polyK of 2500, and 12 lysines available for reaction), it was found that if all lysines react the surface coverage is 38%. Moreover, if the number of reactive lysines is decreased to 5, we get 100% coverage. Again, the lowest limit of polyK coverage can be established to be on the order of 35 to 100%, with a similar level of reactive lysines as in the highest polyK level.

4.3.7. Cell seeding on RGDC-modified surfaces

The RGDC incorporation steps can be seen in Figure 4.7. Figure 4.8 shows fluorescence micrographs of fluorescently tagged MSCs that were seeded on plain and modified discs. In polyK/SPDP/RGDC-modified discs, at polyK incubation concentrations of 0.1 and $1x10^{-4}$ mg/ml, cells greatly stretched once attached to the surface after six hours, with elongated extensions of the cell membrane and a uniform distribution throughout the disc surface, while at a polyK incubation concentration of $1x10^{-6}$ some cells started to display a rounded appearance, a behavior that was more pronounced on unmodified discs. Cell surface areas at different levels of surface modification are shown in Figure 4.9.

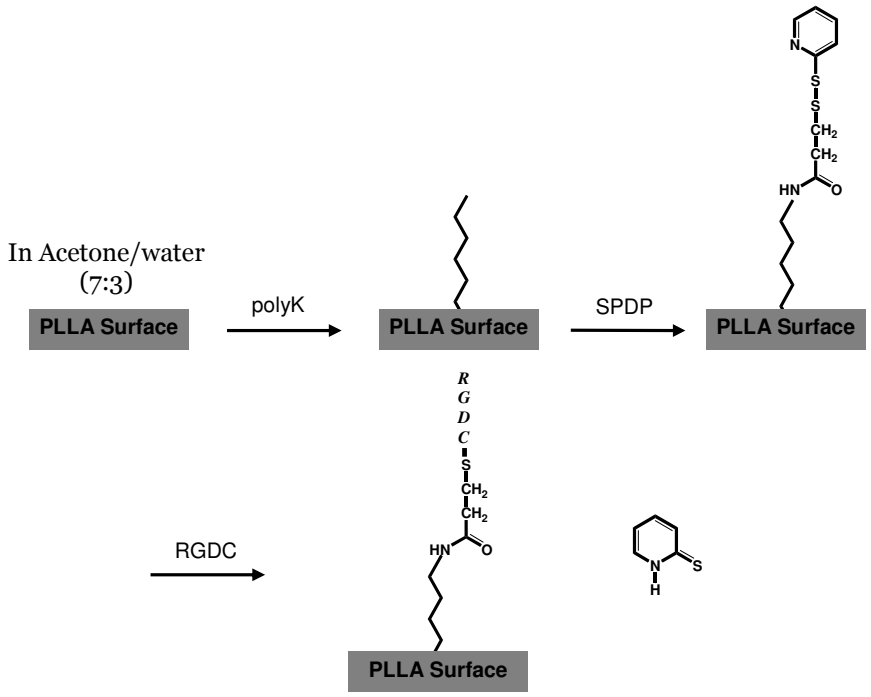


Figure 4.7. Incorporation of RGDC to the Poly-modified PLLA surface

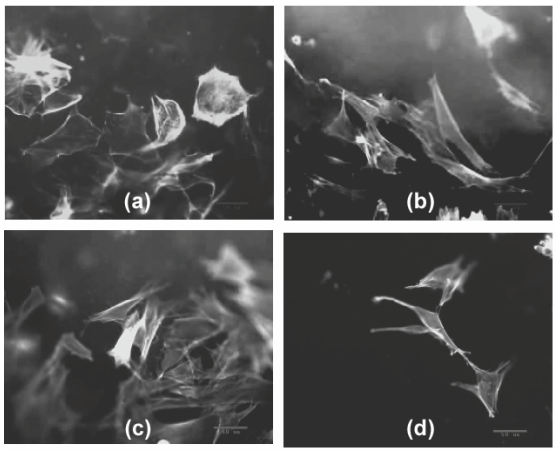


Figure 4.8. Cell adhesion test on RGDC-modified PLLA discs. The RGDC was linked to polyK through the creation of a disulfide bond using SPDP. Mesenchymal stem cells were seeded on the surface of disks modified with polyK at: (a) 0.1 mg/ml, (b) 10^{-4} mg/ml, (c) 10^{-6} mg/ml, or (d) plain surface.

Greater cell spreading area was obtained at polyK incubation concentrations of 0.1 and $1x10^{-2}$ mg/ml, without any significant difference between the two. Significant

declines were observed at polyK incubation concentrations of $1x10^{-4}$ and $1x10^{-6}$ mg/ml, but there was not a significant decrement when the incubation concentration was reduced to $1x10^{-7}$ mg/ml. Furthermore, polyK/SPDP/RGDC-modified surfaces provided greater cell surface areas than polyK-modified or polyK/RGDC-modified discs. Cell surface area was the lowest when cells were seeded on plain discs and plain discs incubated in an RGDC solution.

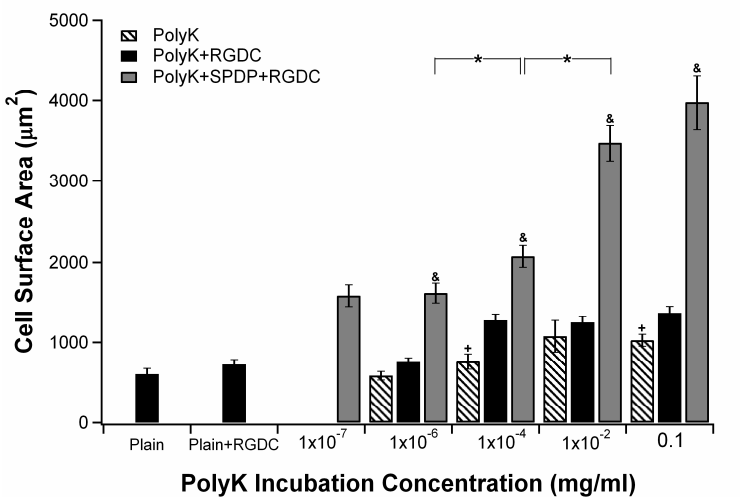


Figure 4.9. Effect of the extent of polyK entrapment on cell surface area after linkage of RGDC peptides to polyK entrapped in PLLA discs. Controls included polyK-modified and polyK/RGDC-modified surfaces, as well as plain discs and plain discs incubated in an RGDC solution. The (*) denotes statistical significance between two groups ($p<0.05$). The (&) denotes the modification sequence that yielded the highest cell surface area at a given polyK incubation concentration. The (+) denotes the modification sequence that yielded the lowest cell surface area at a given polyK incubation concentration. The (#) denotes significant difference ($p<0.05$) with respect to polyK-SPDP-RGDC at every polyK incubation concentration. (n=15 cells)

In the three-dimensional PLLA foams, the incorporation of small amounts of RGDC onto the surface (polyK incubation concentration of $1x10^{-7}$ mg/ml) increased cell attachment after 6 h ($2.7 \pm 0.1x10^{5}$ cells) (Figure 4.10), which was about three

times higher than that obtained in the unmodified scaffolds, ($0.9 \pm 0.2 \times 10^5$ cells). However, no significant difference in cell attachment was observed when scaffolds were modified with RGDC at a polyK incubation concentration of 0.1 mg/ml when compared to the lower polyK incubation concentrations. Cellularity of scaffolds modified at a polyK concentration of 0.1 mg/ml did not significantly change after 24 h ($2.9 \pm 0.1 \times 10^5$ cells), but there was a significant increase after 48 h ($3.4 \pm 0.1 \times 10^5$ cells) ($p<0.05$). At a polyK concentration of 1x10-7 mg/ml, scaffold cellularity was ($3.0 \pm 0.2 \times 10^5$) after 24 h, and a significantly higher cellularity of ($3.4 \pm 0.2 \times 10^5$) was found after 48 h ($p<0.05$).

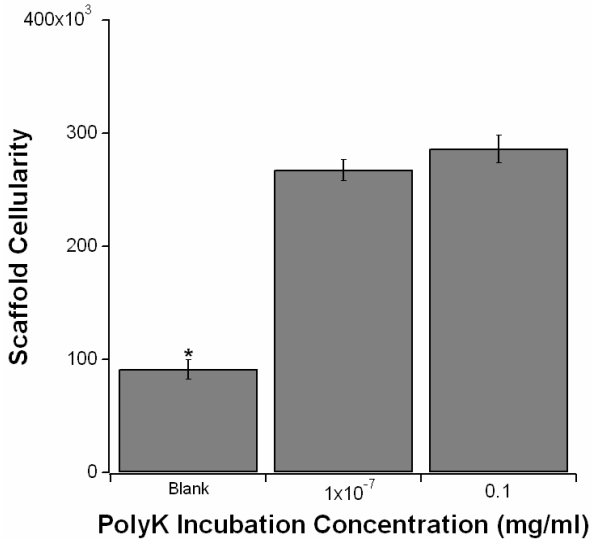


Figure 4.10. Effect of the extent of modification on the adhesion of cells to three-dimensional, porous PLLA foams. Two different extents of modification are represented by polyK incubation concentrations of 1×10^{-7} and 0.1 mg/ml; both scaffolds were treated with SPDP and RGDC. A plain scaffold was used a control. The (*) denotes the significantly lowest scaffold cellularity (number of cells attached per scaffold). (n = 4)

4.4. Discussion

Aiming to create a functionally flexible construct that can be utilized in different tissue engineering applications, we have physically entrapped poly(L-lysine) (polyK) in the surface of 3-D, poly(L-lactic acid) (PLLA) tissue engineering scaffolds. Thus, the main goal of this study was to demonstrate that 1) the entrapment could be done easily, efficiently and in a controllable fashion, 2) the modification procedure of three dimensional scaffolds, which consisted of soaking the scaffold in an acetone-water mixture and later incubating in a polyK solution in DMSO, was nondestructive, and the modified surface was stable, 3) the surface could be further functionalized (e.g. with pyridyl thiols, free thiols, or bioactive molecules) to induce particular responses from the cells, specially cell adhesion by the incorporation of RGDC peptides.

The quality and effectiveness of the final, biomimetically modified scaffold will greatly depend on the polyK entrapment technique. Therefore, the optimal entrapment methodology would be the one that not only yields the most suitable amounts of the entrapped polyK but is also easy to carry out and preserves the morphologic structure of the scaffold. In this study, we initially determined the optimal entrapment technique on two dimensional discs due to the ease of preparation and handling of the discs, and then confirmed its feasibility on three-dimensional scaffolds. In the latter, the additional application of vacuum to the scaffolds to thoroughly penetrate the porous structure was found to be critical because it mitigates any problems pose by transport limitations. The criteria used to determine the most efficient procedure included the highest amount of entrapped polyK, the homogeneity

of polyK distribution throughout the surface, and the preservation of the structure of the three-dimensional porous foams.

The total amount of polyK present in the incubation steps of all the assayed entrapment procedures was maintained constant so as to be able to make a fair comparison among those listed in section 4.2.2. In case a, when the polyK was suspended into the solution of PLLA in chloroform prior to making the disks (bulk modification), the presence of polyK on the disc's surface was minimal, as observed in Figure 1. In case b (acetone-polyK soaking), where the surface was incubated in a suspension of polyK in acetone, the amount of polyK available on the surface was not significantly different from that of the bulk modification. Case c (acetone/polyK in DMSO soaking), where the disc is soaked in acetone and later incubated in a solution of polyK in DMSO, resulted in the highest polyK entrapment.

The main improvement in technique c is the introduction of an intermediate stage, before rinsing, where the polyK is dissolved in DMSO. It is important to point out that polyK is not soluble in either acetone or chloroform; therefore, it is only possible to make polyK suspensions in these systems, and during the experimental trials, clusters of the polypeptide could be observed. This phenomenon poses great limitations in the efficiency of entrapment and the ability to achieve reproducible uniform distributions throughout the surface because not every site is exposed to polyK molecules that could be potentially entrapped. DMSO, on the other hand, is a solvent for polyK; as a result, every site on the surface of the disc is exposed to polyK molecules. Furthermore, the DMSO is responsible for slowing down the dissolution of the PLLA, simultaneously hardening the polymer surface and entrapping, at the

same time, some of the polyK in solution. A similar softening technique was implemented by Cui et al where two-dimensional PLLA surfaces were soaked in an acetone/water mixture (7:3) and later in a gelatinous solution, where the water is responsible for the unswelling or hardening of the polymer surface [43].

Even though case a (bulk modification) was less efficient than case c, quantities of entrapped polyK comparable to those obtained in case c can be reached by increasing the amount of polyK incorporated in the PLLA-chloroform solution. However, due to the distribution of the polyK throughout the polymer volume in the solid phase, some of the characteristics of the material, such as degradation and mechanical properties, could be altered, ultimately resulting in a potential limitation in the range of applications of the scaffold in tissue engineering, especially when mechanical strength is an important factor.

PolyK detection assays with periodate-HRP corroborated the availability of active polypeptide on the surface for further linkage of other molecules. The coupling of fluorescein-5-maleimide also supported these observations. By observing similar fluorescence intensities generated by the fluorescein-5-maleimide in different parts of the surface of the discs modified by acetone/DMSO soaking (technique c), we were able to infer that a competent level of homogeneity in the distribution of polyK on the disc surface had been achieved. The absorbance generated by the release of the group pyridine-2-thionee, when SPDP was deprotected with DTT, not only corroborated the availability of polyK on the surface of the disks but also demonstrated its reactivity and that of the SPDP linked to the polyK.

Once the optimal entrapment technique had been determined (technique c), we proceeded with the modification of 3-D PLLA porous foams, which posed a challenge in terms of achieving homogeneity throughout porous network. The existence of capillary forces, the intricacy of the porous network, and the presence of tortuous paths inside the scaffold give rise to limitations in the penetration of the solutions into deeper sections of the scaffold. This problem was overcome by the application of vacuum in the different incubation steps. A similar vacuum methodology has been used in other studies to infiltrate porous constructs prior to cell seeding [30,55,56].

SPDP can be used to deliver either an activated thiol reactive group or a free sulfhydryl moiety and thus acts as a linker to attach specific bioactive molecules to the polyK surface, expanding the repertoire of molecules that may be attached to prepare biomimetic surfaces. Controls in Figure 4.4 eliminate the possible hypothesis of labeling of the PLLA surface due to physical absorption of the different reagents (polyK, SPDP or fluorescein-5-maleimide). Fluorescein-5-maleimide is only attached to the SPDP-linked polyK since no fluorescence was observed in the absence of SPDP and presence of polyK. The attachment of the periodate-activated HRP and SPDP to the surface demonstrates that the reactivity of the polyK is not dramatically changed by the physical interactions with the polymer. At this point, we had established a clear and easy protocol for the modification of 3-D porous PLLA scaffolds. It was then important to evaluate whether the entrapment could be perform in a controllable fashion.

A change in the polyK incubation concentration when modifying 3-D foams resulted in different amounts of entrapment, as observed in Figure 4.5, where lower

polyK incubation concentrations yielded decreased fluorescence signals. Nevertheless, the surface is saturated at higher polyK concentrations (above $1x10^{-4}$ mg/ml). Furthermore, it was demonstrated that at lower polyK incubation concentrations (as low as $1x10^{-8}$ mg/ml) there was measurable entrapment.

One of the concerns when the surface was prepared was the retainment of the polypeptide molecules in the surface; even more important was the preservation of its activity for a certain period of time after modification. The results indicate that the level of polyK was maintained, and, at the same time, that the reactivity of the polyK was not changed during the 10 days of incubation. The time of soaking in PBS was chosen based on the account that, by 10 days, cell population and the deposition of a collagenous matrix by the cells would have started to dominate cell adhesion properties.

After showing that the polyK-derivatized surface was stable, we examined the effects of the acetone treatment on the scaffold architecture. The scaffold morphology is a key component in tissue engineering approaches because it affects the way cells attach to the scaffold and migrate along its surface. Pore structure and interconnectivity influence the transportation of nutrients, tissue regeneration and the formation of a vascular network when the construct is implanted [4,5,10,11,57]. Micro computed tomography analysis performed after acetone/DMSO soaking demonstrated that scaffold porosity was preserved; moreover, a porous network with high levels of pore interconnectivity was found after the treatment, making the modified scaffold morphologically suitable for tissue engineering.

After being characterized, the surface was further modified to improve cell adhesion and thereby illustrate the functional capabilities that will allow it to be biomimetic. RGDC peptides were linked to the entrapped polyK by forming a disulfide bond with the SPDP. XPS analysis, detection of the release of pyridine-2-thionee and cell attachment assays demonstrated the presence of RGDC peptides on the polymer surface and their linkage to the polyK/SPDP-modified scaffolds. The amount of SPDP estimated when reacted with the RGDC was similar to the value estimated when unmasked with DTT.

RGD peptides have been demonstrated to enhance cell adhesion and deposition of a bone-like matrix on different substrates through the interactions with integrin receptors [58-62]. Rezania et al. reported that the presence of RGD peptides on two dimensional quartz surfaces affected osteoblastic differentiation of mesenchymal stem cells by boosting alkaline phosphatase activity and improving the deposition of calcium. At the same time a higher surface peptide concentration resulted in an increment in these parameters [40]. Thus, the incorporation of this peptide into the surface is a valuable asset due to its multi-functionality.

In the presence of RGDC peptides cells appeared more stretched, which is a sign of a stronger attachment. The rounded appearance of the cells in the unmodified discs and at lower extents of modification translates into weaker attachment. Higher surface concentrations of RGDC caused larger stretching of the cells seeded on two dimensional surfaces, and lower concentrations also seemed to have a significant effect when compared to plain surfaces, polyK-modified and polyK-RGDC modified surfaces.

These results demonstrate that the greatest effect on cell stretching was exerted by the whole modification, polyK-SPDP-RGDC, and not by possible adsorption of RGDC on the surface of the material or the charges presented by the polyK. Incubation of the plain disc in a solution of RGDC seemed to have no enhancing effect when compared to the plain polymer, implying minimal adsorption of RGDC on the PLLA surface or that the adsorbed RGDC was inactive. The improvement on the 3-D scaffold initial cellularity after incorporating small amounts of the adhesion peptide on the surface imply that cell-matrix interactions were greatly improved, but a higher RGDC surface concentration, represented by a higher amount of entrapped polyK, did not further increase scaffold cellularity. Although no significant difference was observed on scaffold cellularity when high and low RGDC surface concentrations were used, our results from the 2-D studies imply that the strength of cell attachment may have increased at higher levels of surface modification. The effect of the presence of the peptide on cell attachment observed in this study complies with the findings of other researchers in different studies [12,24,34,40,63-69]. Furthermore, the results from the extended cell culture, which show cell growth after 48 h, demonstrate that the modified scaffolds are able to support cell proliferation and do not have any appreciable cytotoxic effects.

4.5. Conclusions

Poly (L-lactic acid), three-dimensional, tissue engineering scaffolds were modified by physically entrapping poly (L-lysine) in their surface in order to create a functionally flexible construct that can be utilized for different applications. PolyK, a source of amino groups, was homogenously entrapped throughout the surface of 3-D foams and in a controllable fashion. The modified surface was stable and the modification technique was non-destructive. Further functionalization of the scaffold was demonstrated by the incorporation of sulfhydryl compounds and RGDC peptides. Cell stretching was greatly affected by the RGDC surface concentration on two dimensional disks but did not affect the cellularity of three dimensional scaffolds.

4.6. References

1. Boyan, B.D., Hummert, T.W., Dean, D.D., and Schwartz, Z. Role of material surfaces in regulating bone and cartilage cell response. Biomaterials 17, 137, 1996.
2. Liu, X., and Ma, P.X. Polymeric scaffolds for bone tissue engineering. Ann Biomed Eng 32, 477, 2004.
3. Anselme, K. Osteoblast adhesion on biomaterials. Biomaterials 21, 667, 2000.
4. Saltzman, M.W. Cell Interactions with Polymers. In: Lanza R, Langer R, Vacanti J, eds. Principles of Tissue Engineering. 2 ed. San Diego: Academic Press, pp. 221, 2000.
5. Vacanti, J.P., Langer, R., Upton, J., and Marler, J.J. Transplantation of cells in matrices for tissue regeneration. Adv Drug Deliv Rev 33, 165, 1998.
6. Bonassar, L.J., and Vacanti, C.A. Tissue engineering: the first decade and beyond. J Cell Biochem Suppl 30-31, 297, 1998.
7. Moroni, L., de Wijn, J.R., and van Blitterswijk, C.A. 3D fiber-deposited scaffolds for tissue engineering: influence of pores geometry and architecture on dynamic mechanical properties. Biomaterials 27, 974, 2006.
8. Temenoff, J.S., Lu, L., and Mikos, A.G. Bone Tissue Engineering Using Synthetic Biodegradable Polymer Scaffolds. In: Davies JE, ed. Bone Engineering. Toronto: University of Toronto, pp. 454, 2000.
9. Wang, Y., Kim, U.J., Blasioli, D.J., Kim, H.J., and Kaplan, D.L. *In vitro* cartilage tissue engineering with 3D porous aqueous-derived silk scaffolds and mesenchymal stem cells. Biomaterials 26, 7082, 2005.

10. Bostrom, R.D., and Mikos, A.G. Tissue Engineering of Bone. In: Atala A, Mooney DJ, eds. Synthetic biodegradable polymer scaffolds. Boston: Birkhäuser, pp. 215, 1997.

11. Holy, C.E., Shoichet, M.S., and Davies, J.E. Engineering three-dimensional bone tissue *in vitro* using biodegradable scaffolds: investigating initial cell-seeding density and culture period. J Biomed Mater Res 51, 376, 2000.

12. Yang, X.B., Roach, H.I., Clarke, N.M., Howdle, S.M., Quirk, R., Shakesheff, K.M., and Oreffo, R.O. Human osteoprogenitor growth and differentiation on synthetic biodegradable structures after surface modification. Bone 29, 523, 2001.

13. Altman, G.H., Diaz, F., Jakuba, C., Calabro, T., Horan, R.L., Chen, J., Lu, H., Richmond, J., and Kaplan, D.L. Silk-based biomaterials. Biomaterials 24, 401, 2003.

14. Lutolf, M.P., and Hubbell, J.A. Synthetic biomaterials as instructive extracellular microenvironments for morphogenesis in tissue engineering. Nat Biotechnol 23, 47, 2005.

15. Mapili, G., Lu, Y., Chen, S., and Roy, K. Laser-layered microfabrication of spatially patterned functionalized tissue-engineering scaffolds. J Biomed Mater Res B Appl Biomater 75, 414, 2005.

16. Mikos, A.G., Bao, Y., Cima, L.G., Ingber, D.E., Vacanti, J.P., and Langer, R. Preparation of poly(glycolic acid) bonded fiber structures for cell attachment and transplantation. J Biomed Mater Res 27, 189, 1993.

17. Nam, Y.S., Yoon, J.J., and Park, T.G. A novel fabrication method of macroporous biodegradable polymer scaffolds using gas foaming salt as a porogen additive. J Biomed Mater Res 53, 1, 2000.

18. Pattison, M.A., Wurster, S., Webster, T.J., and Haberstroh, K.M. Three-dimensional, nano-structured PLGA scaffolds for bladder tissue replacement applications. Biomaterials 26, 2491, 2005.

19. Ratner, B.D., and Bryant, S.J. Biomaterials: where we have been and where we are going. Annu Rev Biomed Eng 6, 41, 2004.

20. Riddle, K.W., and Mooney, D.J. Role of poly(lactide-co-glycolide) particle size on gas-foamed scaffolds. J Biomater Sci Polym Ed 15, 1561, 2004.

21. Thomson, R.C., Yaszemski, M.J., Powers, J.M., and Mikos, A.G. Fabrication of biodegradable polymer scaffolds to engineer trabecular bone. J Biomater Sci Polym Ed 7, 23, 1995.

22. Watanabe, J., Eriguchi, T., and Ishihara, K. Cell adhesion and morphology in porous scaffold based on enantiomeric poly(lactic acid) graft-type phospholipid polymers. Biomacromolecules 3, 1375, 2002.

23. Domaschke, H., Gelinsky, M., Burmeister, B., Fleig, R., Hanke, T., Reinstorf, A., Pompe, W., and Rosen-Wolff, A. *In vitro* ossification and remodeling of mineralized collagen I scaffolds. Tissue Eng 12, 949-958, 2006.

24. Hwang, N.S., Kim, M.S., Sampattavanich, S., Baek, J.H., Zhang, Z., and Elisseeff, J. Effects of three-dimensional culture and growth factors on the chondrogenic differentiation of murine embryonic stem cells. Stem Cells 24, 284-291, 2006.

25. Ruhe, P.Q., Hedberg-Dirk, E.L., Padron, N.T., Spauwen, P.H., Jansen, J.A., and Mikos, A.G. Porous poly(DL-lactic-co-glycolic acid)/calcium phosphate cement composite for reconstruction of bone defects. Tissue Eng 12, 789-800, 2006.

26. Wu, L., Zhang, H., Zhang, J., and Ding, J. Fabrication of three-dimensional porous scaffolds of complicated shape for tissue engineering. I. Compression molding based on flexible-rigid combined mold. Tissue Eng 11, 1105-1114, 2005.

27. Pham, Q.P., Sharma, U., and Mikos, A.G. Electrospinning of polymeric nanofibers for tissue engineering applications: a review. Tissue Eng 12, 1197-1211, 2006.

28. Hollinger, J.O., and Battistone, G.C. Biodegradable bone repair materials. Synthetic polymers and ceramics. Clin Orthop Relat Res, 290, 1986.

29. Hubbell, J.A. Bioactive biomaterials. Curr Opin Biotechnol 10, 123, 1999.

30. Ishaug, S.L., Crane, G.M., Miller, M.J., Yasko, A.W., Yaszemski, M.J., and Mikos, A.G. Bone formation by three-dimensional stromal osteoblast culture in biodegradable polymer scaffolds. J Biomed Mater Res 36, 17, 1997.

31. Trivedi, N., Steil, G.M., Colton, C.K., Bonner-Weir, S., and Weir, G.C. Improved vascularization of planar membrane diffusion devices following continuous infusion of vascular endothelial growth factor. Cell Transplant 9, 115, 2000.

32. Shin, H., Jo, S., and Mikos, A.G. Biomimetic materials for tissue engineering. Biomaterials 24, 4353, 2003.

33. Rowley, J.A., Madlambayan, G., and Mooney, D.J. Alginate hydrogels as synthetic extracellular matrix materials. Biomaterials 20, 45, 1999.

34. Cook, A.D., Hrkach, J.S., Gao, N.N., Johnson, I.M., Pajvani, U.B., Cannizzaro, S.M., and Langer, R. Characterization and development of RGD-peptide-modified poly(lactic acid-co-lysine) as an interactive, resorbable biomaterial. J Biomed Mater Res 35, 513, 1997.

35. Elbert, D.L., and Hubbell, J.A. Conjugate addition reactions combined with free-radical cross-linking for the design of materials for tissue engineering. Biomacromolecules 2, 430, 2001.

36. Hsu, S.H., Tsai, C.L., and Tang, C.M. Evaluation of cellular affinity and compatibility to biodegradable polyesters and Type-II collagen-modified scaffolds using immortalized rat chondrocytes. Artif Organs 26, 647, 2002.

37. Stile, R.A., and Healy, K.E. Thermo-responsive peptide-modified hydrogels for tissue regeneration. Biomacromolecules 2, 185, 2001.

38. Yuan, X., Mak, A.F., and Li, J. Formation of bone-like apatite on poly(L-lactic acid) fibers by a biomimetic process. J Biomed Mater Res 57, 140, 2001.

39. Tessmar, J., Kellner, K., Schulz, M.B., Blunk, T., and Gopferich, A. Toward the development of biomimetic polymers by protein immobilization: PEGylation of insulin as a model reaction. Tissue Eng 10, 441-453, 2004.

40. Rezania, A., and Healy, K.E. The effect of peptide surface density on mineralization of a matrix deposited by osteogenic cells. J Biomed Mater Res 52, 595, 2000.

41. Vunjak-Novakovic, G., Obradovic, B., Martin, I., Bursac, P.M., Langer, R., and Freed, L.E. Dynamic cell seeding of polymer scaffolds for cartilage tissue engineering. Biotechnol Prog 14, 193, 1998.

42. Croll, T.I., O'Connor, A.J., Stevens, G.W., and Cooper-White, J.J. Controllable surface modification of poly(lactic-co-glycolic acid) (PLGA) by hydrolysis or aminolysis I: physical, chemical, and theoretical aspects. Biomacromolecules 5, 463, 2004.

43. Cui, Y.L., Hou, X., Qi, A.D., Wang, X.H., Wang, H., Cai, K.Y., Ji Yin, Y., and De Yao, K. Biomimetic surface modification of poly (L-lactic acid) with gelatin and its effects on articular chondrocytes *in vitro*. J Biomed Mater Res 66A, 770, 2003.

44. Hagerman, E.M., Chao, S.H.H., Dunn, J.C.Y., and Wu, B.M. Surface modification and initial adhesion events for intestinal epithelial cells. J Biomed Mater Res 76A, 272, 2005.

45. Hu, Y., Winn, S.R., Krajbich, I., and Hollinger, J.O. Porous polymer scaffolds surface-modified with arginine-glycine-aspartic acid enhance bone cell attachment and differentiation *in vitro*. J Biomed Mater Res 64A, 583, 2003.

46. Mingyu, C., Kai, G., Jiamou, L., Yandao, G., Nanming, Z., and Xiufang, Z. Surface modification and characterization of chitosan film blended with poly-L-lysine. J Biomater Appl. 19, 59, 2004.

47. Quirk, R.A., Chan, W.C., Davies, M.C., Tendler, S.J., and Shakesheff, K.M. Poly(L-lysine)-GRGDS as a biomimetic surface modifier for poly(lactic acid). Biomaterials 22, 865, 2001.

48. Takai, E., Landesberg, R., Katz, R.W., Hung, C.T., and Guo, X.E. Substrate modulation of osteoblast adhesion strength, focal adhesion kinase activation, and responsiveness to mechanical stimuli. Mol Cell Biomech. 3, 1, 2006.

49. Tryoen-Toth, P., Vautier, D., Haikel, Y., Voegel, J.-C., Schaaf, P., Chluba, J., and Ogier, J. Viability, adhesion, and bone phenotype of osteoblast-like cells on polyelectrolyte multilayer films. J Biomed Mater Res 60, 657, 2002.

50. Hategan, A., Sengupta, K., Kahn, S., Sackmann, E., and Discher, D.E. Topographical pattern dynamics in passive adhesion of cell membranes. Biophysical journal. 87, 3547-3560, 2004.

51. Huang, W.M., Gibson, S.J., Facer, P., Gu, J., and Polak, J.M. Improved section adhesion for immunocytochemistry using high molecular weight polymers of L-lysine as a slide coating. Histochemistry. 77, 275-279, 1983.

52. Mikos, A.G., Lyman, M.D., Freed, L.E., and Langer, R. Wetting of poly(L-lactic acid) and poly(DL-lactic-co-glycolic acid) foams for tissue culture. Biomaterials 15, 55, 1994.

53. Mikos, A.G., Thorsen, A.J., Czerwonka, L.A., Bao, Y., Langer, R., Winslow, D.N., and Vacanti, J.P. Preparation and characterization of poly(L-lactic acid) foams. Polymer 35, 1068, 1994.

54. Ketcham, R.A. Computational methods for quantitative analysis of three-dimensional features in geological specimens. Geosphere 1, 32, 2005.

55. Bancroft, G.N., Sikavitsas, V.I., van den Dolder, J., Sheffield, T.L., Ambrose, C.G., Jansen, J.A., and Mikos, A.G. Fluid flow increases mineralized matrix deposition in 3D perfusion culture of marrow stromal osteoblasts in a dose-dependent manner. Proc Natl Acad Sci U S A 99, 12600, 2002.

56. Sikavitsas, V.I., Bancroft, G.N., Holtorf, H.L., Jansen, J.A., and Mikos, A.G. Mineralized matrix deposition by marrow stromal osteoblasts in 3D perfusion culture increases with increasing fluid shear forces. Proc Natl Acad Sci U S A 100, 14683, 2003.

57. Ma, P.X., and Zhang, R. Synthetic nano-scale fibrous extracellular matrix. J Biomed Mater Res 46, 60, 1999.

58. Behravesh, E., Zygourakis, K., and Mikos, A.G. Adhesion and migration of marrow-derived osteoblasts on injectable *in situ* crosslinkable poly(propylene

fumarate-co-ethylene glycol)-based hydrogels with a covalently linked RGDS peptide. J Biomed Mater Res 65A, 260, 2003.

59. Ferris, D.M., Moodie, G.D., Dimond, P.M., Gioranni, C.W., Ehrlich, M.G., and Valentini, R.F. RGD-coated titanium implants stimulate increased bone formation *in vivo*. Biomaterials 20, 2323, 1999.

60. LeBaron, R.G., and Athanasiou, K.A. Extracellular matrix cell adhesion peptides: functional applications in orthopedic materials. Tissue Eng 6, 85, 2000.

61. Puleo, D.A., and Bizios, R. RGDS tetrapeptide binds to osteoblasts and inhibits fibronectin-mediated adhesion. Bone 12, 271, 1991.

62. Sofia, S., McCarthy, M.B., Gronowicz, G., and Kaplan, D.L. Functionalized silk-based biomaterials for bone formation. J Biomed Mater Res 54, 139, 2001.

63. Alsberg, E., Kong, H.J., Hirano, Y., Smith, M.K., Albeiruti, A., and Mooney, D.J. Regulating bone formation via controlled scaffold degradation. J Dent Res 82, 903, 2003.

64. Elmengaard, B., Bechtold, J.E., and Soballe, K. *In vivo* effects of RGD-coated titanium implants inserted in two bone-gap models. J Biomed Mater Res A 75, 249, 2005.

65. Kurihara, H., and Nagamune, T. Cell adhesion ability of artificial extracellular matrix proteins containing a long repetitive Arg-Gly-Asp sequence. J Biosci Bioeng 100, 82, 2005.

66. Sawyer, A.A., Weeks, D.M., Kelpke, S.S., McCracken, M.S., and Bellis, S.L. The effect of the addition of a polyglutamate motif to RGD on peptide

tethering to hydroxyapatite and the promotion of mesenchymal stem cell adhesion. Biomaterials 26, 7046, 2005.

67. Yang, F., Williams, C.G., Wang, D.A., Lee, H., Manson, P.N., and Elisseeff, J. The effect of incorporating RGD adhesive peptide in polyethylene glycol diacrylate hydrogel on osteogenesis of bone marrow stromal cells. Biomaterials 26, 5991, 2005.

68. Kim, T.G., and Park, T.G. Biomimicking extracellular matrix: cell adhesive RGD peptide modified electrospun poly(D,L-lactic-co-glycolic acid) nanofiber mesh. Tissue Eng 12, 221-233, 2006.

69. Markusen, J.F., Mason, C., Hull, D.A., Town, M.A., Tabor, A.B., Clements, M., Boshoff, C.H., and Dunnill, P. Behavior of adult human mesenchymal stem cells entrapped in alginate-GRGDY beads. Tissue Eng 12, 821-830, 2006.

Chapter 5

Improved Mesenchymal Stem Cell Seeding on RGD-Modified Poly (L-lactic acid) Scaffolds using Flow Perfusion

Chapter Abstract

Arg-Gly-Asp (RGD) has been widely utilized to increase cell adhesion on three dimensional scaffolds for tissue engineering. However, cell seeding on these scaffolds has only been carried out statically, yielding low cell seeding efficiencies. We have characterized, for the first time, the seeding of rat mesenchymal stem cells on RGD-modified poly (L-lactic acid) (PLLA) foams using oscillatory flow perfusion. Incorporation of RGD on the PLLA foams improved scaffold cellularity in a dose dependent manner under oscillatory flow perfusion seeding. When compared to static seeding, oscillatory flow perfusion was the most efficient seeding technique. Cell detachment studies showed that cell adhesion depended on the applied flow rate, and that cell attachment strengthened at higher levels of RGD modification.

5.1 Introduction

Tissue engineering seeks to replace lost or damaged tissue through the use of different bioactive factors that can induce regeneration. Common tissue engineering strategies involve the culture of a specific type of cells in a three dimensional scaffold that has been appropriately chosen for the desired application. The cell-seeded scaffold is then implanted in the affected area for a complete *in vivo* regeneration and formation of new tissue [1-3].

The scaffold must support cell adhesion, migration and proliferation, as well as allow the transport of nutrients to its interior by having sufficient porosity, an optimum pore size, and pore interconnectivity. Ideally, the scaffold should be biodegradable and permit progressive tissue formation without compromising the mechanical needs at the site of implantation [4-10]. A wide variety of techniques and materials, both synthetic and natural, have been used to make scaffolds [11-17]. Poly(α-hydroxy esters) are biodegradable polymers that have been frequently used in tissue engineering applications, particularly poly(lactic acid), poly(glycolic acid) and their copolymers. Nevertheless, these polymers can only support cell adhesion and growth to a certain extent since they lack functional groups that the cells could interact with [18]. The creation of a scaffold that enhances cell-matrix interactions is thus necessary in the creation of efficient tissue engineering constructs [17,19].

The development of functionalized scaffolds involves the bulk or surface modification of a base biomaterial with growth and differentiation factors [19,20]. Common modification techniques include chemical modification such as cross-

linking polymer chains with a bioactive molecule and surface activation through hydrolysis, aminolysis or plasma treatment [19,21-27]. Physical modification can also be carried out by physisorption of the molecule onto the surface, or by entrapment [27-29]. Cui et al. entrapped gelatin in the surface of poly(L-lactic acid) (PLLA) films and enhanced the attachment of chondrocytes [30]. In this technique, the material is incubated in a partial solvent in order to swell the surface and later placed in a solution of the modifying agent that can stop the partial dissolution of the base material, namely PLLA, so that some of the molecules of the modifying agent are entrapped in the surface. A similar modification methodology has been recently proposed involving the creation of an amine-functionalized, three-dimensional scaffold by entrapping poly (L-lysine) [31].

In this study, we have linked Arg-Gly-Asp (RGD) peptides to the amine functionalized scaffold in order to improve cell seeding efficiency on three dimensional PLLA foams. Different two-dimensional surfaces have been modified with the adhesion sequence by physical and chemical means, displaying an improvement on cells attachment and morphology [32-40]. In three dimensional scaffolds, RGD peptides have been incorporated mainly by chemically cross-linking them with other molecules and materials that demonstrate poor cell adhesion characteristics [10,41-49]. Some of these studies have shown that the presence of RGD on these materials not only improves cell adhesion, but it also supports MSC osteoblastic differentiation in a dose dependent manner [41,46,48]. However, the effect of RGD on cell adhesion has been only studied using static seeding techniques in which a cell suspension is added on top of the scaffold in a drop-wise manner.

Static seeding has been shown to yield low seeding efficiencies and poor cell distributions. Most of the cells stay close to the upper surface of the scaffold, on which the suspension was placed [5,50]. One way to overcome these limitations is by utilizing flow perfusion during the seeding phase [50-54]. In flow perfusion systems, the construct is press fitted into a chamber, and the cell suspension is perfused through it, being forced to flow throughout the scaffold's porous network. Different systems that operate based on the concept of flow perfusion have been utilized to seed polymeric scaffolds and shown increases in seeding efficiency and yielded more homogeneous cell distributions throughout the scaffolds, compared with static and other dynamic systems such as spinner flasks and rotating wall vessels that can only provide convective forces on the exterior area of the scaffold [54-57].

In this study, we have characterized, for the first time, the seeding of MSC on RGD-modified PLLA foams using oscillatory flow perfusion. Flow perfusion was chosen as the seeding technique since it enhances cell penetration into the scaffold, and yields high efficiencies and homogeneous cell distributions [55]. Different levels of RGD modification were used to evaluate its effect on the number of cells attached to the scaffold (scaffold cellularity) at different cell suspension numbers. Static seeding and static seeding followed by the application of unidirectional flow perfusion were used as seeding controls. The different seeding techniques were compared based on seeding efficiency, and cell morphology. Furthermore, the strength of cell attachment after the completion of the seeding phase was evaluated by applying unidirectional flow at rates larger than the ones used during the seeding phase.

5.2 Materials and Methods

5.2.1. Scaffold Preparation

Poly (L-lactic acid) (Birmingham Polymers, average MW 100,000) foams were prepared by particulate leaching, using sodium chloride (NaCl) as the porogen [20,58]. The grain size of the NaCl was between 300-450μm. Briefly, PLLA was dissolved in chloroform at a concentration of 5% w/v. The solution was then poured on a sodium chloride bed, and the solvent was allowed to evaporate for 24 h. The solid salt-polymer composite, which was 95 wt% NaCl, was pressed in a cylindrical mold with an inner diameter of 8 mm at 500 psig, using a hydraulic press, with simultaneous heating at 130^{o}C for 30 min. The resulting pellet was cut into discs of 3 mm in thickness using a low speed diamond wheel saw (Model 650, South Bay Technology, Inc). Salt leaching was carried out using deionized water for 3 days, and the water was changed at least twice a day. The scaffolds had a porosity of 90% determined as the percentage ratio of the weight of the scaffold to the weight of a solid PLLA disc with the same dimensions.

5.2.2. Surface Modification

A technique has been developed and characterized for the surface modification of PLLA three-dimensional scaffolds [31]. Briefly, this technique consists on the physical entrapment of poly (L-lysine) (PolyK, 4000 MW, Pierce) on the surface of the polymer, and generates a homogeneous distribution of the polyK throughout the entire scaffold surface. The polyK entrapment can be done in a controllable fashion [31]. The surface can then be further functionalized by linking bioactive molecules of interest to the entrapped polyK using amine coupling chemistries. In this study,

RGDC peptides were linked to the polyK by creating a disulfide bond using N-Succinimidyl 3-(2-pyridyldithio) propionate (SPDP). Briefly, foams were soaked in a 1:3 acetone-water mixture for 1 h. Then, they were placed in 1 ml of a solution of PolyK in dimethyl sulfoxide (DMSO) at 0.1, $1x10^{-4}$, or $1x10^{-7}$ mg/ml for 12 h. Rinsing was carried out after that with 0.1% Triton X-100, followed by three washes with deionized water. PolyK-modified surfaces were incubated in 600µl of 1mM SPDP in HEPES buffer (pH 8.3) for 30 min. One cycle of rinsing with 0.1% Triton X-100 and three cycles with phosphate buffered saline (PBS) were performed succeeding the reaction. Surfaces were incubated in 100µM RGDC for one hour and rinsed. All the modification stages were carried out under vacuum and vigorous shaking. Controls in this study included scaffolds modified with polyK only and plain scaffolds incubated in the RGDC solution. All control scaffolds were rinsed with 0.1% Triton X-100, followed by three washes with PBS.

5.2.3. Cell Culture

Adult mesenchymal stem cells (MSC) were isolated from the bone marrow of eight-week-old male Wistar® rats (Harland Laboratories) using well established methods [59,60]. Briefly, rats were euthanized, and the tibiae and femura were extracted. The epiphyses were cut off, and the bone marrow was flushed and suspended in α-modified essential media (α-MEM, Atltanta Biological) supplemented with 10% fetal bovine serum (Atlanta Biological). The suspension was then distributed in polystyrene culture flasks (75 cm^2). Cells were cultured at 37°C and 5% CO_2. Non-adherent cells were discarded after two days of culture. At 70% confluency, MSC were detached using trypsin (Invitrogen), centrifuged at 400*g* for 5 min, re-suspended in α-MEM and re-plated until the 3rd passage. Cells from the 3rd passage were

detached and resuspended in fresh α-MEM. Seeding densities were $5x10^5$ and $1x10^6$ cells in 250μl of α-MEM.

5.2.4. Scaffold Seeding

An oscillatory flow perfusion seeding technique that improves seeding efficiency, cell spatial distribution and strength of cell adhesion was developed and characterized in our laboratory [55]. This flow perfusion system was also utilized in long term culture studies of MSC seeded in three dimensional scaffolds [51,61,62]. Briefly, scaffolds were confined in cassettes so as to force the flow throughout the porous network and restrict it from going around the scaffold. The cassettes were placed into the perfusion chambers of the main body of the bioreactor, which consists of a total of six chambers. Culture media was pumped to the top of the chambers using a peristaltic pump (Cole-Parmer) from a media reservoir and returned to a second reservoir, allowing recirculation.

Prior to seeding, the flow system was cured with α-MEM for 2 h. Scaffolds were press-fitted into cassettes and placed in the flow perfusion chambers of the bioreactor. Cell suspensions were poured on top of the scaffolds, and the chambers were filled up with fresh media to avoid the presence of air bubbles. Oscillating flow was then applied for 2 h at 0.15 ml/min by manually changing the direction of the pump every 5 min. This cycle time was previously demonstrated to be sufficient for all the cells to go through the scaffold before changing the direction of the flow [55]. Cell conditioning, without flow, was allowed for an additional period of 2h, after which unidirectional flow was incorporated at 0.15 ml/min for 8h. Static seeding was used as a seeding control. In this technique, the scaffolds are placed in cassettes

similar to those of the bioreactor system, and the cell suspension is added drop-wise on top of the scaffold. Cells were allowed to attach for 12h. In most flow perfusion studies, the scaffolds are seeded statically and then placed in the perfusion system for application of unidirectional flow [51,53,55,61-63]. Thus, a combination of dynamic and static seeding that emulates the initial stages of previous flow perfusion studies was also carried out by drop-wise adding the suspension on top of the scaffolds, allowing the cells to attach for 4h in the absence of flow, and then applying unidirectional flow in the flow perfusion system at 0.15 ml/min for 8h to mimic the last phase of the oscillatory seeding and measure any potential cell detachment from the statically seeded scaffolds due the presence of unidirectional flow.

5.2.5. Detachment Studies

All RGD-modified scaffolds were seeded dynamically as previously explained by applying oscillatory flow for 2h, letting the cells condition for 2 h without flow, and finally applying unidirectional flow perfusion for 8h at 0.15, 0.5 and 1 ml/min. The shear stress (dyn/cm^2) experienced by the cells under the different rates of flow perfusion can be estimated by using a model for parabolic flow through cylindrical pores:

$$\tau = \frac{32\,\mu\,Q}{\phi\pi d D^2} \qquad (5.1)$$

Where μ is the medium viscosity (0.01 g/cm.s), ϕ is the scaffold porosity, d is the pore diameter, and D is the scaffold diameter [53].

4.2.6. Evaluation of cell morphology on RGD-modified scaffolds

RGD-modified scaffolds at polyK concentrations of $1x10^{-7}$ and 0.1 mg/ml seeded statically or dynamically were fixed in 3.7% buffered formalin for 10 min. They were then rinsed with 0.1% Triton-X-100 and PBS. Cells were labeled with 2 units of BODIPY® FL phalloidin (Invitrogen), a high affinity probe for F-actin, for 20 min. After rinsing, fluorescence microscopy was performed using a Nikon Epifluorescence microscope, and image analysis was carried out with MetaMorph 6.2 (Universal Imaging Corporation). The excitation and emission wavelengths were 558nm and 569 nm, respectively. Images were captured at the top surface on which the cell suspension was placed and at the bottom surface.

5.3.7. Determination of the number of cells attached to the scaffolds (Scaffold Cellularity)

After seeding, scaffolds were quickly rinsed in PBS, suspended in 3 ml of deionized water, and broken down into small pieces. Samples were later submitted to three cycles of freeze/thaw to lyse the cells. A picogreen® DNA quantification assay (Invitrogen) was performed to obtain the number of cells attached to the scaffolds. A standard curve was made using known-concentration solutions of λDNA. Sample and standard aliquots of 43 µl were accommodated in a 96-well plate, along with 107 µl of reaction buffer (20mM Tris-HCl, 1 mM EDTA, pH 7.5) and 150 µl of the Picogreen® dye. Fluorescence was measured (490 nm excitation and 520 nm emission) using a Synergy HT plate reader (Biotek). The number of cells was calculated using the total amount of DNA determined in the sample divided by the amount of DNA contained in one cell. Based on the number of cells attached to the scaffold, we were able to determine the seeding efficiency, which is defined as the

percentage ratio of the number of cells attached to the scaffold to the initial number of cells in suspension.

5.2.8. Statistical analysis

For all the experiments, three to five samples were used (n = 3-5), unless otherwise specified. Values were reported as the average of all the samples, and the error was reported as the standard error of the mean. The data were analyzed by using ANOVA, and multiple pair-wise comparisons were carried out using the Tukey-HSD method at a confidence level of 95%.

5.3 Results

5.3.1. Effect of RGD modification on scaffold cellularity after oscillatory flow perfusion seeding

Scaffold cellularity for all RGD-modified scaffolds seeded under oscillatory flow perfusion is shown in Figure 5.1. The level of RGD modification is reported as the concentration of polyK in the incubation stage of the modification procedure before linking the SDPD and RGDC. Higher polyK concentration translates into a larger amount of RGDC present on the surface. Under oscillatory flow perfusion seeding, the lowest level of RGD modification (polyK-SPDP-RGDC), represented by a polyK incubation concentration of $1x10^{-7}$ mg/ml, yielded a scaffold cellularity significantly higher than those yielded by the controls (plain scaffold, polyK-modified scaffold without RGDC, and plain scaffold incubated in an RGDC solution). Further increases in the polyK incubation concentration resulted in significantly higher scaffold cellularities.

Figure 5.2 shows the dependence of scaffold cellularity with the initial number of cells in suspension for all levels of modification. It can be seen that the scaffold cellularity increased with the initial number of cells in suspension for all RGD modification levels. A cell suspension number of $1x10^{6}$ nearly doubled scaffold cellularity at all polyK incubation concentrations. At any cell suspension number scaffold cellularity significantly increased along with the RGD modification level.

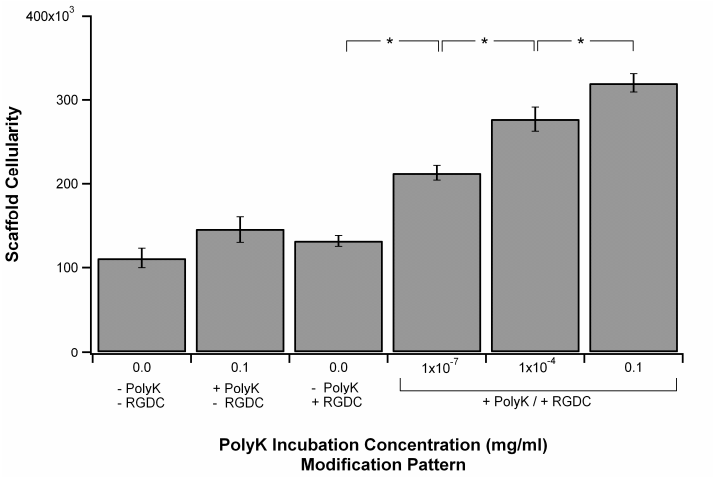


Figure 5.1. Scaffold cellularity at different levels of RGD modification after oscillatory flow perfusion seeding at 0.15 ml/min. Number of cells in suspension was $5x10^5$. The x-axis shows the levels of RGD modification represented by polyK incubation concentrations during the polyK entrapment phase, with the pattern of modification used (±polyK/±RGDC). Controls for this set of experiments included plain scaffold, scaffolds modified with polyK only at 0.1 mg/ml (no RGDC), and plain scaffolds incubated in an RGDC solution. (* $p< 0.05$).

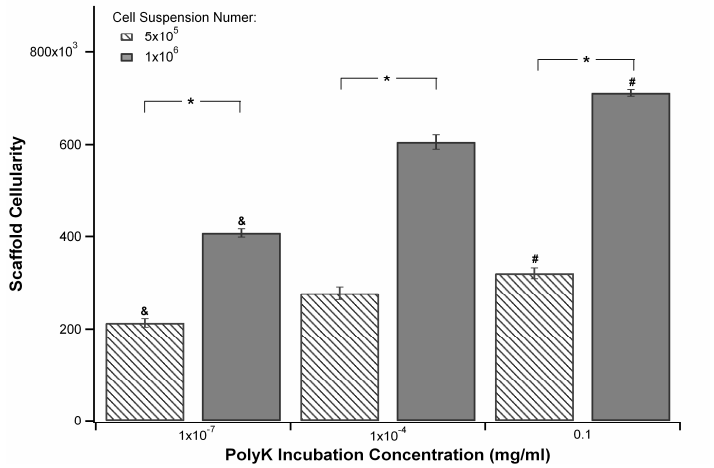


Figure 5.2. Dependence of scaffold cellularity on the cell suspension number at different levels of modification. Scaffolds were seeded under oscillatory flow perfusion at 0.15 ml/min. (#) and (&) represent respectively the highest and the lowest scaffold cellularity at a given cell suspension number. (* $p< 0.05$).

5.3.2. Effect of oscillatory flow perfusion on seeding efficiency of RGD-modified scaffolds

In Figure 5.3, oscillatory flow perfusion seeding of RGD-modified scaffolds is compared to static seeding, and static seeding followed by unidirectional flow perfusion. The comparison is made in terms of seeding efficiency. For plain scaffolds and at a polyK incubation concentration of 0.1 mg/ml, oscillatory flow perfusion seeding yielded the highest seeding efficiency when compared to static seeding, achieving values of (22±2%) and (64±2%), respectively. In all cases, the static seeding followed by unidirectional flow perfusion yielded the lowest efficiency, reaching values as low as (10±1%) for plain scaffolds and as high as (34±4%) at a polyK concentration of 0.1 mg/ml. A polyK incubation concentration of 0.1 mg/ml yielded the highest seeding efficiency for flow perfusion seeding and static seeding followed by unidirectional flow perfusion (34±4%), while plain scaffolds yielded the lowest efficiency when compared to the other modification levels at flow perfusion seeding, static seeding (17±2%), and static followed by unidirectional flow perfusion (10±1%). Under static seeding, there were no statistical differences on seeding efficiency between the different levels of modification.

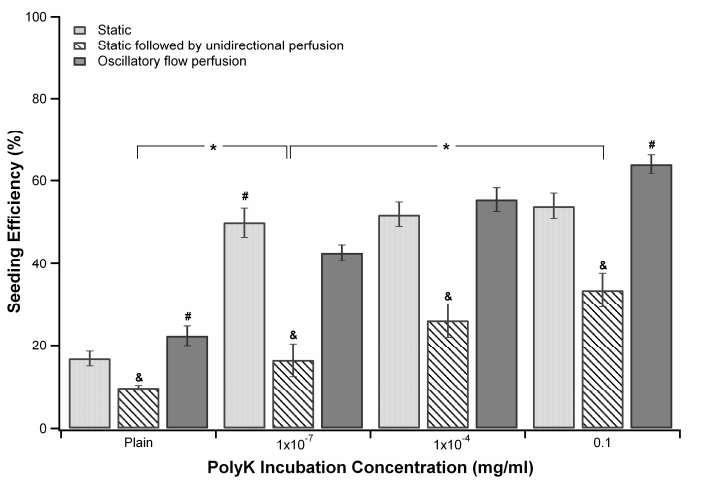


Figure 5.3. Dependence of seeding efficiency on the different techniques used to seed RGD-modified scaffolds at different modification levels. Flow rate applied in the flow perfusion system was 0.15 ml/min. Number of cells in suspension was $5x10^5$. (&) and (#) represent the seeding technique that yielded the highest and the lowest cellularity at a given polyK incubation concentration. ($* p< 0.05$).

Figure 5.4 shows the effect of seeding technique on cell morphology on RGD-modified scaffolds at polyK incubation concentrations of $1x10^{-7}$ and 0.1 mg/ml. On scaffolds seeded statically, cells appeared rounded in shape and were mostly clustered at the top surface, where the cell suspension was placed (Figure 5.4 c and g). Some of these clusters seemed to be attached to the pore walls only through a single cell. Cell density was higher at the edges of the scaffolds. These observations were found at both the lowest and highest RGD-modification levels. There were no cells found at the bottom surface on statically seeded scaffolds (Figure 5.4 d and h). On scaffolds seeded under oscillatory flow perfusion, a lower cell density was found at the top (Figure 5.4 a and e) compared to statically seeded foams, but a significant number of cells was found on the bottom surface of the scaffold (Figure 5.4 b and f).Fewer and smaller cell clusters were found at the top, specially at the lower modification lever, where cells still looked rounded with only some of them showing significant stretching (Figure 5.4e). At the highest modification level, cells looked clearly

stretched along the edges of the pore, and virtually no clusters were visible (Figure 5.4a). A uniform cell density was observed throughout the upper and lower surfaces.

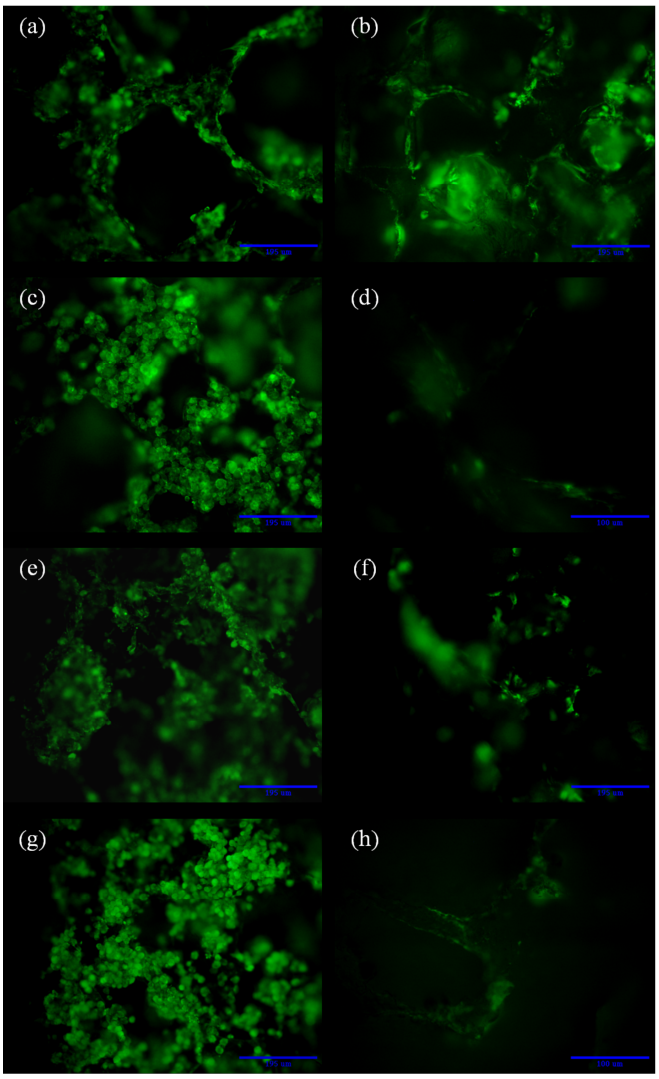


Figure 5.4. Fluorescence microscopy of the top and bottom surfaces of RGD-modified scaffolds seeded statically or under flow perfusion. The top surface is where the initial cell suspension was placed. Number of cells in suspension was $5x10^5$. Images of scaffolds modified at a polyK incubation concentration of 0.1 mg/ml: (a) oscillatory flow perfusion, top (b) oscillatory flow perfusion, bottom (C) static, top (d) static, bottom. Images of scaffolds modified at a polyK incubation concentration of $1x10^{-7}$ mg/ml: (e) oscillatory flow perfusion, top (f) oscillatory flow perfusion, bottom (g) static, top (h) static, bottom. Calibration bar: 195 μm.

5.3.3. Cell detachment on dynamically seeded RGD-modified scaffolds

The percentage of cells seeded statically that detached when submitted to unidirectional flow perfusion decreased at higher levels of RGD modification. At polyK incubation concentrations of $1x10^{-4}$ and $1x10^{-7}$ mg/ml the percent of detachment was 50% and 67% respectively. While only 38% of the cells seeded

statically were detached when flow was applied to scaffolds modified with a polyK incubation concentration of 0.1 mg/ml.

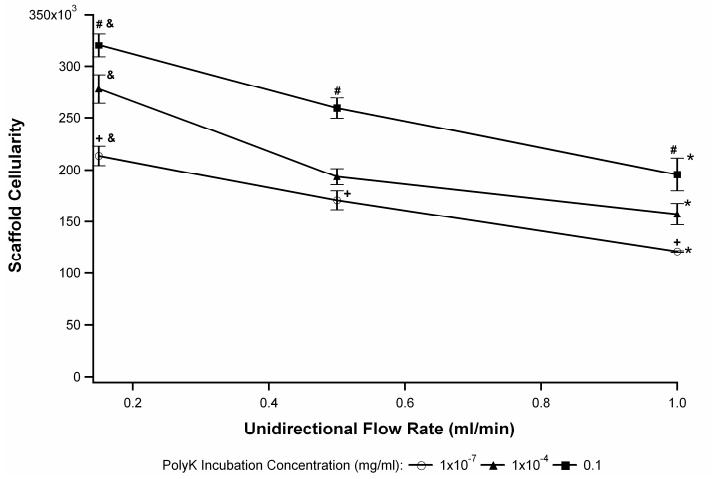


Figure 5.5. Detachment profile of cells seeded under oscillatory flow perfusion on RGD-modified scaffolds. Unidirectional flow rate refers to the phase of flow shearing applied after the 2 h of oscillatory flow and 2 h of cell conditioning without flow. Number of cells in suspension was $5x10^5$. (&) represents the flow rate that yielded the highest scaffold cellularity at a given polyK incubation concentration. (*) represents the flow rate that yielded the lowest scaffold cellularity at a given polyK incubation concentration. (#) represents the level of modification that yielded the highest cellularity at a given flow rate. (+) represents the level of modification that yielded the lowest cellularity at a given flow rate.

Results for the cell detachment studies on scaffolds seeded under oscillatory flow perfusion are shown in Figure 5.5. In these studies, we varied the flow rate at the unidirectional flow perfusion phase of the dynamic seeding in order to evaluate how well the cells attached to the scaffold. The shear stress experienced by the cells under the conditions of detachment was estimated, through equation 5.1, to be in the range of 0.02 to 0.15 dyn/cm^2. These values of shear stress are lower than that experienced by osteocytes under physiological interstitial shear (8-30 dyn/cm^2) or by endothelial cells in a superficial femoral artery (2.7 dyn/cm^2) (refs). Cellularity of RGD-modified scaffolds decreased at higher flow rates for all modification levels. At all flow rates,

scaffold cellularity was directly dependant on the RGD modification level. However, detachment was more pronounced at lower RGD modification levels. At polyK incubation concentrations of $1x10^{-7}$ and $1x10^{-4}$ mg/ml, 43% of the cells that adhered originally were detached after applying a flow rate of 1.0 ml/min, while at 0.1 mg /ml the percentage of detachment significantly decreased to 39%.

5.4. Discussion

The objective of this study was to evaluate the effect of the presence of RGD, at different modification levels, on cell adhesion when seeding MSC on PLLA scaffolds under oscillatory flow perfusion conditions. Specifically: a) we assessed the effect of the RGD modification level on the cellularity of PLLA foams seeded under static or oscillatory flow perfusion conditions, b) we compared the oscillatory flow perfusion with static seeding in terms of cell seeding efficiency and cell morphology on RGD-modified PLLA scaffolds, and c) we examined the levels of cell detachment in statically and oscillatory flow perfusion seeded RGD-modified scaffolds after their exposure for 8 h to different unidirectional fluid flow perfusion rates.

5.4.1. Effect of RGD modification on scaffold cellularity after oscillatory flow perfusion and static seeding

Cell adhesion on modified PLLA foams under oscillatory flow perfusion seeding was enhanced by the presence of RGDC in a dose dependent manner. MSC adhesion was improved mostly due to the presence of the RGDC linked to entrapped polyK. Scaffolds modified with polyK only (no RGDC) or plain scaffolds incubated in RGDC (no polyK) displayed small improvement on scaffold cellularity when compared to all the levels of RGD modification (polyK-SPDP-RGDC) (Figure 5.1). This is corroborated by the increased cellularity at increased modification levels. This pattern persisted when different cell suspension densities were used (Figure 5.2). Previous studies have also shown that cell attachment is dose dependent on RGD modification levels. However, these studies have only used static seeding [46,48,59]. In this study, RGD modification improved cell seeding efficiency under any seeding

technique. Unlike the dose dependent behavior of cell seeding efficiency under oscillatory flow perfusion, static seeding conditions resulted in comparable scaffold cellularities at every level of RGD modification. However, the pattern of increased cellularity at increased RGD modification levels reappears after submitting statically seeded scaffolds to unidirectional flow perfusion at the lowest flow rate utilized in our experiments (Figure 5.3). A potential reason for this behavior could be that weakly adherent cell clusters that appear predominantly on statically seeded scaffolds (Figure 5.4) are detached easier from scaffolds containing low RGD modification levels in the presence of fluid flow. Among all the seeding techniques, oscillatory flow perfusion not only demonstrated the strongest influence of RGD modification level on scaffold cellularity, but it also significantly improved cell seeding for the same level of RGD modification when compared to the traditional static seeding technique.

It is important to note that after using that after increasing the polyK incubation concentration by six orders of magnitude, scaffold cellularity increased in only about 80-90%. It was expected a larger increase in scaffold cellularity; however, a previous study carried out in our group made estimations on the amount of entrapped polyK at different incubation concentrations. A merely three-fold increase in the amount of polyK entrapped, from about 23 to 64 pg, was observed when the incubation concentration was increased from $1x10^{-7}$ to 0.1 mg/ml (six orders of magnitude) [31].

5.4.2. Comparison of oscillatory flow perfusion and static seeding of RGD-modified scaffolds

Long term cultures performed in flow perfusion systems are often preceded by static seeding outside the bioreactor [51,53,60-65]. Nevertheless, static seeding is not an ideal method because it yields low seeding efficiencies and poor cell distribution throughout the scaffold's porous network [54,56,57]. Oscillatory flow perfusion, on the other hand, ensures flow throughout the porous network and thereby allows more cells to reach the interior of the scaffold. Thus, more of the surface area available for adhesion can be utilized by the cells. Oscillatory flow perfusion seeding inherently allows the cells to penetrate the scaffold multiple times from the top and the bottom, thus increasing the probabilities for cell attachment and consequently leading to increased seeding efficiency. Oscillatory flow perfusion seeding has been shown to improve cell seeding efficiency in unmodified polymeric scaffolds containing no adhesion molecules when compared to static seeding [55].This observation was supported by our findings where in plain scaffolds, oscillatory flow perfusion yielded the highest seeding efficiency (Figure 5.3).

Although oscillatory flow perfusion seeding was expected to improve cell seeding efficiency when compared to static techniques, the combined effect of this seeding technique with the presence of RGD peptides on the scaffold surface was not obvious. Even though static seeding in some cases yielded seeding efficiencies higher than (polyK, $1x10^{-7}$ mg/ml) or equal (polyK, $1x10^{-4}$ mg/ml) to those yielded by the oscillatory flow perfusion (contrary to the behavior observed in plain scaffolds), the significant decrease on scaffold cellularity when statically seeded scaffolds are submitted to unidirectional flow perfusion indicates that oscillatory flow perfusion is

preferable over static seeding. Performing the seeding in the flow perfusion system provides an additional advantage when long term culture under flow perfusion is attempted since scaffold handling would be minimized by performing the seeding in the same environment as the long term culture. Seeding scaffolds statically and transporting them into the bioreactor poses an increased risk of contamination due to excessive manipulation.

This conclusion is also supported by the microscopy results where it was found that under conditions of flow perfusion cells appeared to stretch along the pore edges of the top surface (Figure 5.4), demonstrating improved cell-matrix interactions when compared to the static seeding. Furthermore, microscopy also demonstrated a greater degree of penetration of the cells under dynamic seeding than under the static technique evident from the abundant presence of cells at the bottom surface of the scaffold (Figure 5.4), implying improved cell distribution.

5.4.3. Cell detachment on oscillatory flow perfusion seeded RGD-modified scaffolds

Cell detachment under different flow conditions has been studied on two-dimensional surfaces containing adhesion peptides. It has been reported that the extent of cell detachment increases with the shear forces caused by the flow rate applied on the surface [66-69]. Our studies demonstrate that this behavior extrapolates to cells seeded on a three dimensional porous network. Increased flow rates, which translate into higher shear forces, result in greater cells detachment from the scaffold at all RGD modification levels. However, the highest level of RGD modification resulted in the lowest cell detachment (reported as the ratio of the remaining cells on the scaffold

to the number of cells originally attached) after applying a flow rate of 1 ml/min. Thus, the highest level of RGD modification not only generates scaffolds with the highest cellularity after oscillatory flow perfusion seeding (compared to the lower RGD modification levels), but it also retains the largest portion of these cells in the presence of increased shear forces.

5.5. Conclusions

For the first time, the oscillatory flow perfusion seeding of rat MSC on RGD-modified PLLA foams has been characterized. Scaffold cellularity was improved by the incorporation of RGDC peptides in a dose-dependent manner. Furthermore, it was demonstrated that oscillatory flow perfusion was the most efficient seeding technique when compared to the more traditional static seeding. Cell detachment increased at higher unidirectional flow rates, and the extent of cell detachment was also dependent on the level of RGD modification. The use of oscillatory flow perfusion seeding of RGD-modified foams will allow the efficient preparation of uniformly seeded scaffolds with MSC or mature osteoblastic cells prior to implantation, and in addition the design of long term culture studies of MSCs seeded uniformly on three dimensional scaffolds in the absence of clustered cells that do not sense the signaling moieties attached to the scaffold's surface.

5.6. References

1. Alsberg, E., Kong, H.J., Hirano, Y., Smith, M.K., Albeiruti, A., and Mooney, D.J. Regulating bone formation via controlled scaffold degradation. J Dent Res 82, 903, 2003.
2. Bonassar, L.J., and Vacanti, C.A. Tissue engineering: the first decade and beyond. J Cell Biochem Suppl 30-31, 297, 1998.
3. Laurencin, C.T., Ambrosio, A.M., Borden, M.D., and Cooper, J.A.J. Tissue engineering: orthopedic applications. Annu Rev Biomed Eng 1, 19, 1999.
4. Bostrom, R.D., and Mikos, A.G. Tissue Engineering of Bone. In: Atala A, Mooney DJ, eds. Synthetic biodegradable polymer scaffolds. Boston: Birkhäuser, pp. 215, 1997.
5. Holy, C.E., Shoichet, M.S., and Davies, J.E. Engineering three-dimensional bone tissue *in vitro* using biodegradable scaffolds: investigating initial cell-seeding density and culture period. J Biomed Mater Res 51, 376, 2000.
6. Ma, P.X., and Zhang, R. Synthetic nano-scale fibrous extracellular matrix. J Biomed Mater Res 46, 60, 1999.
7. Staltzman, M.W. Cell Interactions with Polymers. In: Lanza R, Langer R, Vacanti J, eds. Principles of Tissue Engineering. 2 ed. San Diego: Academic Press, pp. 221, 2000.
8. Temenoff, J.S., Lu, L., and Mikos, A.G. Bone Tissue Engineering Using Synthetic Biodegradable Polymer Scaffolds. In: Davies JE, ed. Bone Engineering. Toronto: University of Toronto, pp. 454, 2000.
9. Vacanti, J.P., Langer, R., Upton, J., and Marler, J.J. Transplantation of cells in matrices for tissue regeneration. Adv Drug Deliv Rev 33, 165, 1998.

10. Yang, X.B., Roach, H.I., Clarke, N.M., Howdle, S.M., Quirk, R., Shakesheff, K.M., and Oreffo, R.O. Human osteoprogenitor growth and differentiation on synthetic biodegradable structures after surface modification. Bone 29, 523, 2001.

11. Altman, G.H., Diaz, F., Jakuba, C., Calabro, T., Horan, R.L., Chen, J., Lu, H., Richmond, J., and Kaplan, D.L. Silk-based biomaterials. Biomaterials 24, 401, 2003.

12. Lutolf, M.P., and Hubbell, J.A. Synthetic biomaterials as instructive extracellular microenvironments for morphogenesis in tissue engineering. Nat Biotechnol 23, 47, 2005.

13. Mikos, A.G., Bao, Y., Cima, L.G., Ingber, D.E., Vacanti, J.P., and Langer, R. Preparation of poly(glycolic acid) bonded fiber structures for cell attachment and transplantation. J Biomed Mater Res 27, 189, 1993.

14. Nam, Y.S., Yoon, J.J., and Park, T.G. A novel fabrication method of macroporous biodegradable polymer scaffolds using gas foaming salt as a porogen additive. J Biomed Mater Res 53, 1, 2000.

15. Ratner, B.D., and Bryant, S.J. Biomaterials: where we have been and where we are going. Annu Rev Biomed Eng 6, 41, 2004.

16. Hollinger, J.O., and Battistone, G.C. Biodegradable bone repair materials. Synthetic polymers and ceramics. Clin Orthop Relat Res, 290, 1986.

17. Hubbell, J.A. Bioactive biomaterials. Curr Opin Biotechnol 10, 123, 1999.

18. Ishaug, S.L., Crane, G.M., Miller, M.J., Yasko, A.W., Yaszemski, M.J., and Mikos, A.G. Bone formation by three-dimensional stromal osteoblast culture in biodegradable polymer scaffolds. J Biomed Mater Res 36, 17, 1997.

19. Shin, H., Jo, S., and Mikos, A.G. Biomimetic materials for tissue engineering. Biomaterials 24, 4353, 2003.

20. Liu, X., and Ma, P.X. Polymeric scaffolds for bone tissue engineering. Ann Biomed Eng 32, 477, 2004.

21. Teraoka, F., Nakagawa, M., and Hara, M. Surface modification of poly (L-lactide) by atmospheric pressure plasma treatment and cell response. Dent Mater J 25, 560-565, 2006.

22. Cook, A.D., Hrkach, J.S., Gao, N.N., Johnson, I.M., Pajvani, U.B., Cannizzaro, S.M., and Langer, R. Characterization and development of RGD-peptide-modified poly(lactic acid-co-lysine) as an interactive, resorbable biomaterial. J Biomed Mater Res 35, 513, 1997.

23. Elbert, D.L., and Hubbell, J.A. Conjugate addition reactions combined with free-radical cross-linking for the design of materials for tissue engineering. Biomacromolecules 2, 430, 2001.

24. Hsu, S.H., Tsai, C.L., and Tang, C.M. Evaluation of cellular affinity and compatibility to biodegradable polyesters and Type-II collagen-modified scaffolds using immortalized rat chondrocytes. Artif Organs 26, 647, 2002.

25. Rowley, J.A., Madlambayan, G., and Mooney, D.J. Alginate hydrogels as synthetic extracellular matrix materials. Biomaterials 20, 45, 1999.

26. Stile, R.A., and Healy, K.E. Thermo-responsive peptide-modified hydrogels for tissue regeneration. Biomacromolecules 2, 185, 2001.

27. Yuan, X., Mak, A.F., and Li, J. Formation of bone-like apatite on poly(L-lactic acid) fibers by a biomimetic process. J Biomed Mater Res 57, 140, 2001.

28. Rezania, A., and Healy, K.E. The effect of peptide surface density on mineralization of a matrix deposited by osteogenic cells. J Biomed Mater Res 52, 595, 2000.

29. Vunjak-Novakovic, G., Obradovic, B., Martin, I., Bursac, P.M., Langer, R., and Freed, L.E. Dynamic cell seeding of polymer scaffolds for cartilage tissue engineering. Biotechnol Prog 14, 193, 1998.

30. Cui, Y.L., Hou, X., Qi, A.D., Wang, X.H., Wang, H., Cai, K.Y., Ji Yin, Y., and De Yao, K. Biomimetic surface modification of poly (L-lactic acid) with gelatin and its effects on articular chondrocytes *in vitro*. J Biomed Mater Res 66A, 770, 2003.

31. Alvarez-Barreto, J.F., Shreve, M.C., DeAngelis, P.L., and Sikavitsas, V.I. Preparation of a functionally flexible, three-dimensional, biomimetic scaffold for different tissue engineering applications. Tissue Eng (in press), 2007.

32. Deng, C., Tian, H., Zhang, P., Sun, J., Chen, X., and Jing, X. Synthesis and characterization of RGD peptide grafted poly(ethylene glycol)-b-poly(L-lactide)-b-poly(L-glutamic acid) triblock copolymer. Biomacromolecules 7, 590, 2006.

33. Fussell, G.W., and Cooper, S.L. Endothelial cell adhesion on RGD-containing methacrylate terpolymers. J Biomed Mater Res A 70, 265, 2004.

34. Garcia, A.J., Ducheyne, P., and Boettiger, D. Effect of surface reaction stage on fibronectin-mediated adhesion of osteoblast-like cells to bioactive glass. J Biomed Mater Res 40, 48, 1998.

35. Gilbert, M., Shaw, W.J., Long, J.R., Nelson, K., Drobny, G.P., Giachelli, C.M., and Stayton, P.S. Chimeric peptides of statherin and osteopontin that

bind hydroxyapatite and mediate cell adhesion. J Biol Chem 275, 16213, 2000.

36. Kang, C.E., Gemeinhart, E.J., and Gemeinhart, R.A. Cellular alignment by grafted adhesion peptide surface density gradients. J Biomed Mater Res A 71, 403, 2004.

37. Kurihara, H., and Nagamune, T. Cell adhesion ability of artificial extracellular matrix proteins containing a long repetitive Arg-Gly-Asp sequence. J Biosci Bioeng 100, 82, 2005.

38. Lee, M.H., Adams, C.S., Boettiger, D., Degrado, W.F., Shapiro, I.M., Composto, R.J., and Ducheyne, P. Adhesion of MC3T3-E1 cells to RGD peptides of different flanking residues: Detachment strength and correlation with long-term cellular function. J Biomed Mater Res A, 2006.

39. Santiago, L.Y., Nowak, R.W., Peter Rubin, J., and Marra, K.G. Peptide-surface modification of poly(caprolactone) with laminin-derived sequences for adipose-derived stem cell applications. Biomaterials 27, 2962, 2006.

40. Sawyer, A.A., Hennessy, K.M., and Bellis, S.L. Regulation of mesenchymal stem cell attachment and spreading on hydroxyapatite by RGD peptides and adsorbed serum proteins. Biomaterials 26, 1467, 2005.

41. Meinel, L., Karageorgiou, V., Hofmann, S., et al. Engineering bone-like tissue *in vitro* using human bone marrow stem cells and silk scaffolds. J Biomed Mater Res A 71, 25, 2004.

42. Chen, J., Altman, G.H., Karageorgiou, V., Horan, R., Collette, A., Volloch, V., Colabro, T., and Kaplan, D.L. Human bone marrow stromal cell and ligament fibroblast responses on RGD-modified silk fibers. J Biomed Mater Res A 67, 559, 2003.

43. Ho, M.H., Wang, D.M., Hsieh, H.J., Liu, H.C., Hsien, T.Y., Lai, J.Y., and Hou, L.T. Preparation and characterization of RGD-immobilized chitosan scaffolds. Biomaterials 26, 3197, 2005.

44. Hsu, S.H., Chang, S.H., Yen, H.J., Whu, S.W., Tsai, C.L., and Chen, D.C. Evaluation of biodegradable polyesters modified by type II collagen and Arg-Gly-Asp as tissue engineering scaffolding materials for cartilage regeneration. Artif Organs 30, 42, 2006.

45. Hsu, S.H., Whu, S.W., Hsieh, S.C., Tsai, C.L., Chen, D.C., and Tan, T.S. Evaluation of chitosan-alginate-hyaluronate complexes modified by an RGD-containing protein as tissue-engineering scaffolds for cartilage regeneration. Artif Organs 28, 693, 2004.

46. Shin, H., Temenoff, J.S., Bowden, G.C., Zygourakis, K., Farach-Carson, M.C., Yaszemski, M.J., and Mikos, A.G. Osteogenic differentiation of rat bone marrow stromal cells cultured on Arg-Gly-Asp modified hydrogels without dexamethasone and beta-glycerol phosphate. Biomaterials 26, 3645, 2005.

47. Smith, E., Yang, J., McGann, L., Sebald, W., and Uludag, H. RGD-grafted thermoreversible polymers to facilitate attachment of BMP-2 responsive C2C12 cells. Biomaterials 26, 7329, 2005.

48. Yang, F., Williams, C.G., Wang, D.A., Lee, H., Manson, P.N., and Elisseeff, J. The effect of incorporating RGD adhesive peptide in polyethylene glycol diacrylate hydrogel on osteogenesis of bone marrow stromal cells. Biomaterials 26, 5991, 2005.

49. Zhang, L., Hum, M., Wang, M., Li, Y., Chen, H., Chu, C., and Jiang, H. Evaluation of modifying collagen matrix with RGD peptide through periodate oxidation. J Biomed Mater Res A 73, 468, 2005.

50. Burg, K.J., Holder, W.D.J., Culberson, C.R., et al. Comparative study of seeding methods for three-dimensional polymeric scaffolds. J Biomed Mater Res 52, 576, 2000.

51. Bancroft, G.N., Sikavitsas, V.I., and Mikos, A.G. Design of a flow perfusion bioreactor system for bone tissue-engineering applications. Tissue Eng 9, 549, 2003.

52. Cartmell, S.H., Porter, B.D., Garcia, A.J., and Guldberg, R.E. Effects of medium perfusion rate on cell-seeded three-dimensional bone constructs *in vitro*. Tissue Eng 9, 1197, 2003.

53. Goldstein, A.S., Juarez, T.M., Helmke, C.D., Gustin, M.C., and Mikos, A.G. Effect of convection on osteoblastic cell growth and function in biodegradable polymer foam scaffolds. Biomaterials 22, 1279, 2001.

54. Wendt, D., Marsano, A., Jakob, M., Heberer, M., and Martin, I. Oscillating perfusion of cell suspensions through three-dimensional scaffolds enhances cell seeding efficiency and uniformity. Biotechnol Bioeng 84, 205, 2003.

55. Alvarez-Barreto, J.F., Linehan, S.M., Shambaugh, R.L., and Sikavitsas, V.I. Flow Perfusion Improves Seeding of Tissue Engineering Scaffolds with Different Architectures. Ann Biomed Eng, 2007.

56. Li, Y., Ma, T., Kniss, D.A., Lasky, L.C., and Yang, S.T. Effects of filtration seeding on cell density, spatial distribution, and proliferation in nonwoven fibrous matrices. Biotechnol Prog 17, 935, 2001.

57. Zhao, F., and Ma, T. Perfusion bioreactor system for human mesenchymal stem cell tissue engineering: dynamic cell seeding and construct development. Biotechnol Bioeng 91, 482, 2005.

58. Mikos, A.G., Lyman, M.D., Freed, L.E., and Langer, R. Wetting of poly(L-lactic acid) and poly(DL-lactic-co-glycolic acid) foams for tissue culture. Biomaterials 15, 55, 1994.

59. Holtorf, H.L., Jansen, J.A., and Mikos, A.G. Ectopic bone formation in rat marrow stromal cell/titanium fiber mesh scaffold constructs: effect of initial cell phenotype. Biomaterials 26, 6208, 2005.

60. Datta, N., Holtorf, H.L., Sikavitsas, V.I., Jansen, J.A., and Mikos, A.G. Effect of bone extracellular matrix synthesized *in vitro* on the osteoblastic differentiation of marrow stromal cells. Biomaterials 26, 971, 2005.

61. Bancroft, G.N., Sikavitsas, V.I., van den Dolder, J., Sheffield, T.L., Ambrose, C.G., Jansen, J.A., and Mikos, A.G. Fluid flow increases mineralized matrix deposition in 3D perfusion culture of marrow stromal osteoblasts in a dose-dependent manner. Proc Natl Acad Sci U S A 99, 12600, 2002.

62. Sikavitsas, V.I., Bancroft, G.N., Holtorf, H.L., Jansen, J.A., and Mikos, A.G. Mineralized matrix deposition by marrow stromal osteoblasts in 3D perfusion culture increases with increasing fluid shear forces. Proc Natl Acad Sci U S A 100, 14683-14688, 2003.

63. Gomes, M.E., Bossano, C.M., Johnston, C.M., Reis, R.L., and Mikos, A.G. *In vitro* localization of bone growth factors in constructs of biodegradable scaffolds seeded with marrow stromal cells and cultured in a flow perfusion bioreactor. Tissue Eng 12, 177, 2006.

64. Hosseinkhani, H., Inatsugu, Y., Hiraoka, Y., Inoue, S., and Tabata, Y. Perfusion culture enhances osteogenic differentiation of rat mesenchymal stem cells in collagen sponge reinforced with poly(glycolic Acid) fiber. Tissue Eng 11, 1476, 2005.

65. Kreke, M.R., Badami, A.S., Brady, J.B., Akers, R.M., and Goldstein, A.S. Modulation of protein adsorption and cell adhesion by poly(allylamine hydrochloride) heparin films. Biomaterials 26, 2975, 2005.

66. Chan, B.P., Reichert, W.M., and Truskey, G.A. Effect of streptavidin RGD mutant on the adhesion of endothelial cells. Biotechnol Prog 20, 566, 2004.

67. Knerr, R., Weiser, B., Drotleff, S., Steinem, C., and Gopferich, A. Measuring cell adhesion on RGD-modified, self-assembled PEG monolayers using the quartz crystal microbalance technique. Macromol Biosci 6, 827, 2006.

68. Koo, L.Y., Irvine, D.J., Mayes, A.M., Lauffenburger, D.A., and Griffith, L.G. Co-regulation of cell adhesion by nanoscale RGD organization and mechanical stimulus. J Cell Sci 115, 1423, 2002.

69. Rezania, A., Thomas, C.H., Branger, A.B., Waters, C.M., and Healy, K.E. The detachment strength and morphology of bone cells contacting materials modified with a peptide sequence found within bone sialoprotein. J Biomed Mater Res 37, 9, 1997.

Chapter 6

RGD Peptides Affect the Osteoblastic Differentiation of Rat Mesenchymal Stem Cells under Flow Perfusion in a Dose Dependent Manner

Chapter Abstract

Arg-Gly-Asp (RGD) peptides incorporated into different biomaterials have been shown to up-regulate the osteoblastic differentiation of mesenchymal stem cells (MSC). However, the effect of RGD on MSC osteoblastic differentiation has been carried out mostly statically. It has been reported that flow perfusion also has an enhancing effect on MSC osteoblastic differentiation. Nonetheless, there is a lack of studies that combine RGD surface modification of biomaterials with the mechanical stimulation of MSCs due to flow perfusion. In the present study, the effect of the RGD modification level of poly(L-lactic acid) scaffolds on osteoblastic differentiation under conditions of flow perfusion was evaluated for the first time. It was found that there is an enhanced effect on the combination of flow perfusion and the presence of RGD on the surface of PLLA foams when compared to their individual effects. Furthermore, under conditions of flow perfusion, there exists a critical RGD surface concentration that is flow rate dependant.

6.1 Introduction

Bioreactors have been widely used in emerging tissue engineering approaches to impart certain forces that imitate different mechanical stimuli occurring in the body [1,2]. These stimuli enhance the proper formation of *in vitro* generated extracellular matrix (ECM) that, to a certain extent, mimic the physiological morphology of the desired tissue [3-5]. However, these devices are not limited to the sole application of mechanical stimuli; they must meet other requirements in order to create grafts that, when implanted, will lead to the regeneration of damaged organs. A bioreactor must efficiently transport nutrients and oxygen to the construct, maintaining an appropriate concentration in solution [6]. In most tissue engineering applications, a scaffold is seeded with cells and supports the formation of ECM [7]. Consequently, the bioreactor has to induce a homogeneous cell distribution throughout these structures in order to generate a uniformly distributed ECM [2].

The scaffolding material must support cell adhesion, migration and proliferation. It must also allow the transport of nutrients to its interior by having sufficient porosity, an optimum pore size, and pore interconnectivity. These parameters not only affect the nutrient transport into the scaffold but also the formation of new tissue and the establishment of a vascular network that will guarantee the survival of the *de novo* tissue. Ideally, the scaffold should be biodegradable and permit progressive tissue formation without compromising the fulfillment of the mechanical requirements at the site of implantation [8-14].

Different materials, both natural and synthetic, have been used to create a wide array of scaffolds for different tissue engineering applications using numerous techniques[15-21]. Poly(α-hydroxy esters), which include poly(lactic acid), poly(glycolic acid) and their copolymers, are biodegradable polymers that have been widely used in tissue engineering applications. Nevertheless, these polymers can only support cell adhesion and growth to a certain extent since they lack functional groups that the cells could interact with [22]. The creation of a scaffold that enhances cell-matrix interactions is thus imperative in the creation of efficient tissue engineering constructs [21,23].

The development of functionalized, biomimetic scaffolds involves the bulk or surface modification of a base biomaterial using growth and differentiation factors [23,24]. Common modification techniques include chemical modification such as cross-linking polymer chains with a bioactive molecule and surface activation through hydrolysis, aminolysis or plasma treatment [23,25-31]. Physical modification can also be carried out by physisorption of the molecule onto the surface, or by entrapment [31-33]. Cui et al. entrapped gelatin in the surface of poly(L-lactic acid) (PLLA) films and enhanced the attachment of chondrocytes [34]. A similar modification methodology has been recently proposed involving the creation of an amine-functionalized, three-dimensional scaffold by entrapping poly (L-lysine) [35]. Different bioactive molecules appropriate for specific tissue engineering applications can be further linked to the amine groups present on the surface.

In this study, we have linked Arg-Gly-Asp (RGD) peptides to the amine functionalized scaffold in order to improve cell seeding efficiency on three

dimensional PLLA foams and assess its effect on the osteoblastic differentiation of MSCs. This amino acid sequence has been demonstrated to improve cell adhesion to different materials [26,32,36-40]. The RGD sequence is encountered in different extracellular matrix components such as fibronectin, osteopontin and bone sialoprotein, and cells interact with this sequence through integrin receptors [41]. Improvement on the adhesion of different types of cells via RGD incorporation has been carried out on 2D and 3D surfaces [6,38-60]. Ceramic, glass, hydroxyapatite and polymeric two-dimensional surfaces have been modified with the adhesion sequence by physical and chemical means, displaying an improvement on cells attachment and morphology [38,39,41,45-48,51,57].

In three dimensional scaffolds, RGD peptides have been incorporated mainly by chemically cross-linking them with other molecules such as collagen, chitosan and poly(ethylene glycol) and materials that demonstrate poor cell adhesion characteristics [6,14,40,43,49,50,58-61]. Some of these studies have shown that the presence of RGD on these materials not only improves cell adhesion, but it also supports MSC osteoblastic differentiation in a dose dependent manner [6,40,58]. However, the effect of RGD on the osteoblastic differentiation of MSCs in three dimensional environments has been mostly studied statically.

Static culture of cells in three dimensional scaffolds posses limitations on the transport of nutrients to the interior of the scaffolds, and thereby cell and matrix distributions throughout the scaffold's surface lack a sufficient level of homogeneity. One way to overcome these limitations is by utilizing flow perfusion during the seeding phase [62-66]. In flow perfusion systems, the construct is press fitted into a

chamber, and the culture medium is perfused through it, being forced to flow throughout the scaffold's porous network. Different systems that operate based on the concept of flow perfusion have been utilized to culture cell-seeded polymeric scaffolds, not only showing more homogeneous cell and matrix spatial distribution when compared to the static cultures but also improved osteogenic MSC differentiation by yielding higher levels of secreted calcium, alkaline phosphatase activity and other osteogenic markers. These improvements have been found with respect to static cultures and other dynamic systems such as spinner flasks and rotating wall vessels that can only provide convective forces on the exterior area of the scaffold [66-69]. A previous study have shown that the incorporation of RGD, through physisorption, improves MSC adhesion and their osteoblastic differentiation under conditions of flow perfusion [70].

In the present study, we evaluate the effect of different extents of RGD incorporation into PLLA foams on the osteogenic differentiation of MSCs under conditions of flow perfusion at different flow rates. Static culture controls without flow but seeded the same way have been used as controls. Additionally, we have utilized an oscillatory flow perfusion seeding technique which has been shown to yield higher seeding efficiencies and more homogeneous cell distributions when compared to static seeding.

6.2. Materials and Methods

6.2.1. Scaffold Preparation

Poly (L-lactic acid) (Birmingham Polymers, average MW 100,000) foams were prepared by particulate leaching, using sodium chloride (NaCl) as the porogen [24,71]. The grain size of the NaCl was between 200-350μm. Briefly, PLLA was dissolved in chloroform at a concentration of 5% w/v. The solution was then poured on a sodium chloride bed, and the solvent was allowed to evaporate for 24 h. The solid salt-polymer composite, which was 95 wt% NaCl, was pressed in a cylindrical mold with an inner diameter of 8 mm at 500 psig, using a hydraulic press, with simultaneous heating at 130^{o}C for 30 min. The resulting pellet was cut into discs of 3 mm in thickness using a low speed diamond wheel saw (Model 650, South Bay Technology, Inc). Salt leaching was carried out using deionized water for 3 days, and the water was changed at least twice a day. The scaffolds had a porosity of 90% determined as the percentage ratio of the weight of the scaffold to the weight of a solid PLLA disc with the same dimensions.

6.2.2. Surface Modification

A technique has been developed and characterized for the surface modification of PLLA three-dimensional scaffolds [35]. Briefly, this technique consists on the physical entrapment of poly (L-lysine) (PolyK, 4000 MW, Pierce) on the surface of the polymer, and generates a homogeneous distribution of the polyK throughout the entire scaffold surface. The polyK entrapment can be done in a controllable fashion [35]. The surface can then be further functionalized by linking bioactive molecules of interest to the entrapped polyK using amine coupling chemistries. In this study,

RGDC peptides were linked to the polyK by creating a disulfide bond using N-Succinimidyl 3-(2-pyridyldithio) propionate (SPDP). Briefly, foams were soaked in a 1:3 acetone-water mixture for 1 h. Then, they were placed in 1 ml of a solution of PolyK in dimethyl sulfoxide (DMSO) at 0.1, $1x10^{-4}$, or $1x10^{-7}$ mg/ml for 12 h. Rinsing was carried out after that with 0.1% Triton X-100, followed by three washes with deionized water. PolyK-modified surfaces were incubated in 600µl of 1mM SPDP in HEPES buffer (pH 8.3) for 30 min. One cycle of rinsing with 0.1% Triton X-100 and three cycles with phosphate buffered saline (PBS) were performed succeeding the reaction. Surfaces were incubated in 100µM RGDC for one hour and rinsed. All the modification stages were carried out under vacuum and vigorous shaking. Controls in this study included scaffolds modified with polyK only and plain scaffolds incubated in the RGDC solution. All control scaffolds were rinsed with 0.1% Triton X-100, followed by three washes with PBS.

.

6.2.3. Cell Culture

Adult mesenchymal stem cells (MSC) were isolated from the bone marrow of eight-week-old male Wistar® rats (Harland Laboratories) using well established methods [70,72]. Briefly, rats were euthanized, and the tibiae and femura were extracted. The epiphyses were cut off, and the bone marrow was flushed and suspended in α-modified essential media (α-MEM, Atltanta Biological) supplemented with 10% fetal bovine serum (Atlanta Biological). The suspension was then distributed in polystyrene culture flasks (75 cm^2). Cells were cultured at 37°C and 5% CO_2. Non-adherent cells were discarded after two days of culture. At 70% confluency, MSC were detached using trypsin (Invitrogen), centrifuged at 400*g* for 5 min, re-suspended in α-MEM and re-plated until the 3rd passage. Cells from the 3rd passage were

detached and resuspended in fresh α-MEM. Seeding densities were $5x10^5$ and $1x10^6$ cells in 250μl of α-MEM.

6.2.4. Scaffold Seeding

An oscillatory flow perfusion seeding technique that improves seeding efficiency, cell spatial distribution and strength of cell adhesion was developed and characterized in our laboratory [67]. This flow perfusion system was also utilized in long term culture studies of MSC seeded in three dimensional scaffolds [62,73,74]. Briefly, scaffolds were confined in cassettes so as to force the flow throughout the porous network and restrict it from going around the scaffold. The cassettes were placed into the perfusion chambers of the main body of the bioreactor, which consists of a total of six chambers. Culture media was pumped to the top of the chambers using a peristaltic pump (Cole-Parmer) from a media reservoir and returned to a second reservoir, allowing recirculation.

Prior to seeding, the flow system was cured with α-MEM for 2 h. Scaffolds were press-fitted into cassettes and placed in the flow perfusion chambers of the bioreactor. Cell suspensions were poured on top of the scaffolds, and the chambers were filled up with fresh media to avoid the presence of air bubbles. Oscillating flow was then applied for 2 h at 0.15 ml/min by manually changing the direction of the pump every 5 min. This cycle time was previously demonstrated to be sufficient for all the cells to go through the scaffold before changing the direction of the flow [67]. Cell conditioning, without flow, was allowed for an additional period of 2h, after which unidirectional flow was incorporated at 0.15 ml/min for 8h.

6.2.5. Long term cultures

After oscillatory perfusion seeding, the scaffolds were cultured statically or in the bioreactor. In the static culture, the seeded scaffolds were placed in 6-well Petri dishes. The wells were filled with fresh a-MEM, and the cultures were carried out for 4, 8 and 16 days. Culture medium was changed every three days. In the flow perfusion culture (also called dynamic culture), after scaffold seeding, unidirectional flow perfusion was applied for 3, 8 and 16 days at flow rates of 0.1 and 1.0 ml/min. Total changes of medium in the flow perfusion system were carried out every three days.

6.2.6. Determination of the number of cells attached to the scaffolds (Scaffold Cellularity)

After every culture time point, scaffolds were quickly rinsed in PBS, suspended in 3 ml of deionized water, and broken down into small pieces. Samples were later submitted to three cycles of freeze/thaw to lyse the cells. A picogreen® DNA quantification assay (Invitrogen) was performed to obtain the number of cells attached to the scaffolds. A standard curve was made using known-concentration solutions of λDNA. Sample and standard aliquots of 43 μl were accommodated in a 96-well plate, along with 107 μl of reaction buffer (20mM Tris-HCl, 1 mM EDTA, pH 7.5) and 150 μl of the Picogreen® dye. Fluorescence was measured (490 nm excitation and 520 nm emission) using a Synergy HT plate reader (Biotek). The number of cells was calculated using the total amount of DNA determined in the sample divided by the amount of DNA contained in one cell. Based on the number of cells attached to the scaffold, we were able to determine the seeding efficiency, which

is defined as the percentage ratio of the number of cells attached to the scaffold to the initial number of cells in suspension.

6.2.7. Alkaline phosphatase (ALP) activity

Lysates obtained for the DNA quantification assay were used for the determination of ALP activity. This parameter was determined by using a fluorimetric assay using p-nitrophenol as standards. Samples and standards aliquots of 80ml were arranged in a transparent 96-well plate with 20 μl of a buffer solution (5 mM MgCl2, 0.5 M 2-amino-2methyl-1-propanol), and 100 μl of substrate solution (5 mM paranitrophenylphosphate). After 30 min, the reaction was stopped by adding 100 μl of 0.1M NaOH. Absorbance was read at 405 nm in a Synergy HT plate reader (Biotek).

6.2.8. Calcium deposition

Calcium deposition in each scaffold was determined by using the ortho-cresolphtalein method. Lysates were mixed with an equal volume of 1N acetic acid. The assay working solution was prepares by mixing equal volumes of the calcium binding reagent (0.024% ortho-cresolphtalein complexone and 0.25% 8-hydroxyquinoline) and buffer (500 mmol/l 2-amino-2-methyl-1,3 propanediol and other nonreactive stabilizers). Standards were prepared with $CaCl_2$. Sample and standard aliquots of 10ml were arranged in a transparent 96-well plate along with 200ml of the working solution, and absorbance was read at 575nm.

6.2.9. Statistical analysis

For all the experiments, six samples were used (n = 6). Values were reported as the average of all the samples, and the error was reported as the standard error of the mean. The data were analyzed by using ANOVA, and multiple pair-wise comparisons were carried out using the Tukey-HSD method at a confidence level of 95%.

6.3. Results and Discussion

6.3.1. Scaffold Cellularity

Scaffold cellularity is defined as the number of cells attached to the scaffold at a given time point. This parameter was determined through the use of the PicoGreen DNA quantification assay, and the results are shown in Figure 6.1 for static condition (1a) and under flow perfusion at 0.1 ml/min (1b) and 1.0 ml/min (1c). PolyK-modified scaffolds at an incubation concentration of $1x10^{-7}$ mg/ml were included, and a plain scaffold incubated in an RGDC solution was used as a control. In general, scaffold cellularity increased during the first days of culture, reaching a peak at day 8, after which the cellularity decreased considerably by day 16. At all culture conditions, scaffolds that were modified with the complete pattern (polyK-SPDP-RGDC) yielded higher cellularities than the controls. There was not a clear difference between the number of cells among the different culture conditions at days 4 and 16. Nevertheless, scaffold cellularity at day 8 significantly increased with the flow rate ($p<0.05$), with the static culture yielding the lowest value.

Under static conditions, the highest extent of modification (0.1mg polyK/ml) yielded the highest scaffold cellularity at every time point. Under flow perfusion the difference between the different extents of modification could only be observed at day 8. Scaffolds modified with a polyK incubation concentration of $1x10^{-4}$mg/ml presented the highest number of cells, both at 0.1 and 1.0 ml/min, $(5.74\pm0.38)x10^5$ cells and $(6.45\ 0.34)x10^5$ cells respectively. Cellularity of the scaffolds at the highest and the lowest modification extent did not present significant differences at any time point when cultured under flow perfusion at 0.1 ml/min. However, the higher flow rate (1.0 ml/min) made the differences among these extents of modification more

pronounced. At this flow rate, scaffolds at the lowest modification level ($1x10^{-7}$ mg polyK/ml) presented significantly higher number of cells than those at the highest level (0.1 mg polyK/ml) at days 4 and 8.

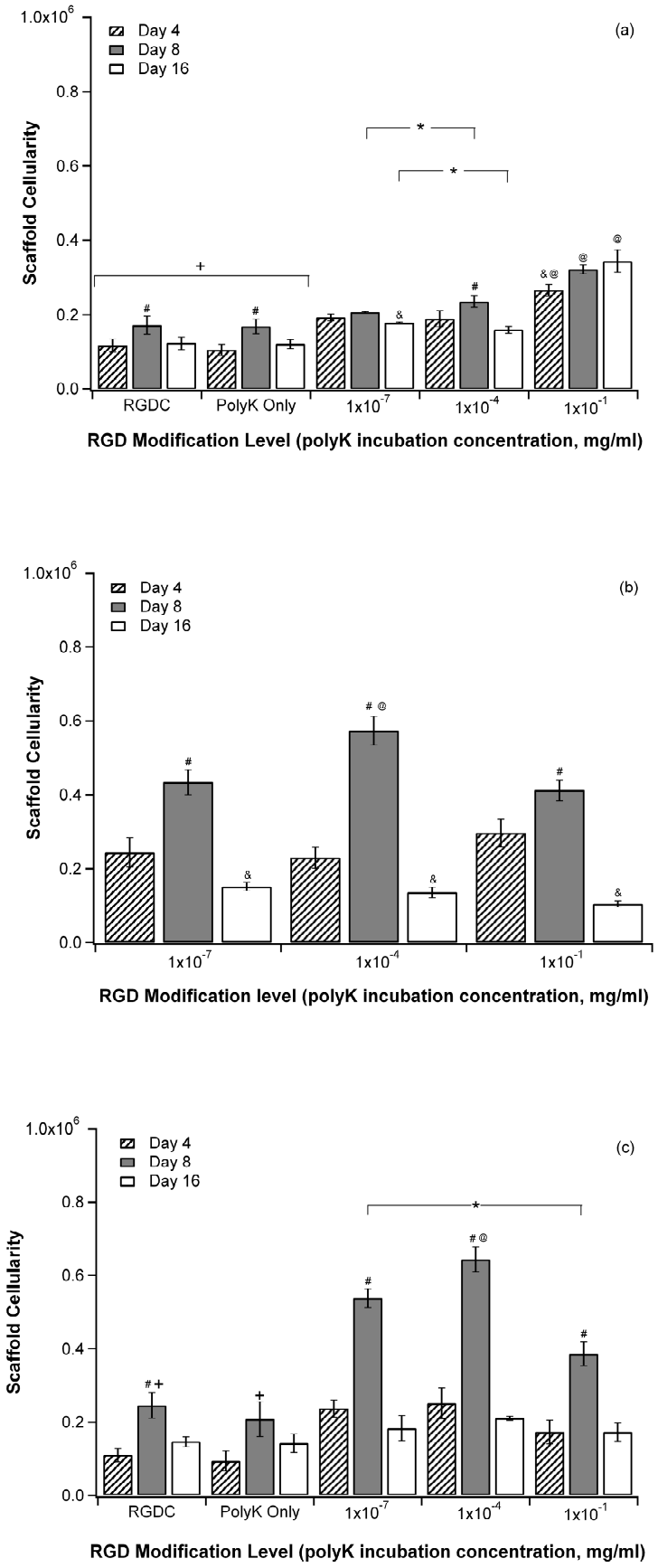
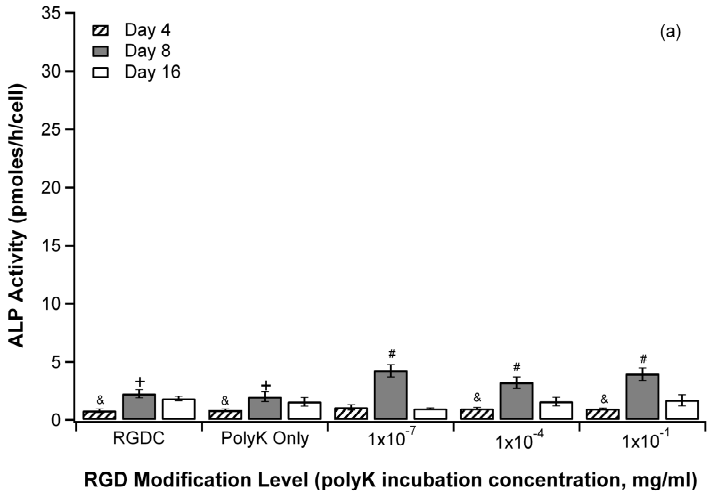
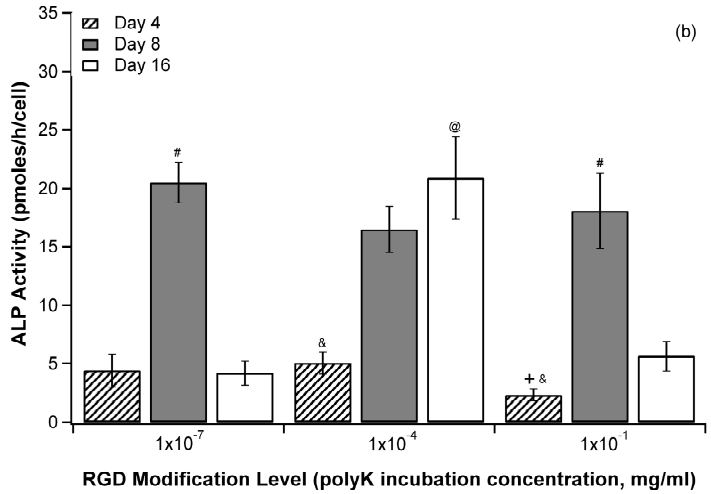


Figure 6.1. Effect of the RGD modification level (expressed as the concentration of polyK in the incubation phase of the modification) on the growth of cells cultured under (a) static conditions, and under flow perfusion at flow rates of (b) 0.1 ml/min and (c) 1.0 ml/min. Controls included a plain PLLA scaffold incubated in an RGDC solution (RGDC) and a scaffold modified with polyK only at an incubation concentration of $1x10^{-7}$ mg/min (polyK only). @ denotes the modification level that yields the highest cellularity at a specific day. + represents the controls having significant lower cellularity than the polyK-SPDP-RGDC modified scaffolds. # and & represent the days with the highest and lowest cellularity at a specific modification level. (*) signifies $p< 0.05$.

6.3.2.. Alkaline Phosphatase Activity

Alkaline phosphatase (ALP) activity was reported as pg of ALP per cell per hour, and it is depicted in Figure 6.2 for scaffolds at all levels of modification and controls cultured under static conditions (2a) and flow perfusion at 0.1 ml/min (2b) and 1.0 ml/min (2c). As observed with the scaffold cellularity, ALP activity presented a peak after eight days of culture under most culture conditions, and modification levels and patterns. Under static culture, the activity was statistically equal for all the polyK concentrations on polyK-SPDP-RGDC scaffolds; however, the controls presented a significantly lower activity at day 8. The values of ALP activity under static conditions reached values as high as (4.26±0.55) pmol/hr/cell. Under flow perfusion ALP activity was enhanced to values as high as (20.91±3.50) pmol/hr/cell after 16 days for a polyK incubation concentration of $1x10^{-4}$ mg/ml at a flow rate of 0.1 ml/min; and (22.28±2.18) pmol/hr/cell after 8 days for a polyK incubation concentration of $1x10^{-7}$ mg/ml at 1.0 ml/min. At the lowest flow rate, there were no significant differences between the different modification levels at days 4 and 8. However, ALP activity continued to grow after 16 days for the middle level of modification ($1x10^{-4}$ mg polyK/ml), while declining at the highest and lowest modification levels. At 1.0 ml/min on the other hand, cells cultured at the lowest modification level presented the highest ALP activity after 4, 8 and 16 days when compared to the other two levels, which did not present significant differences among them.





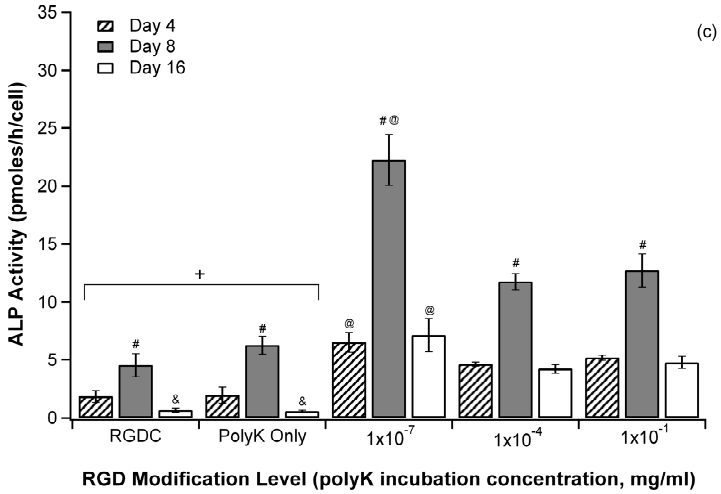
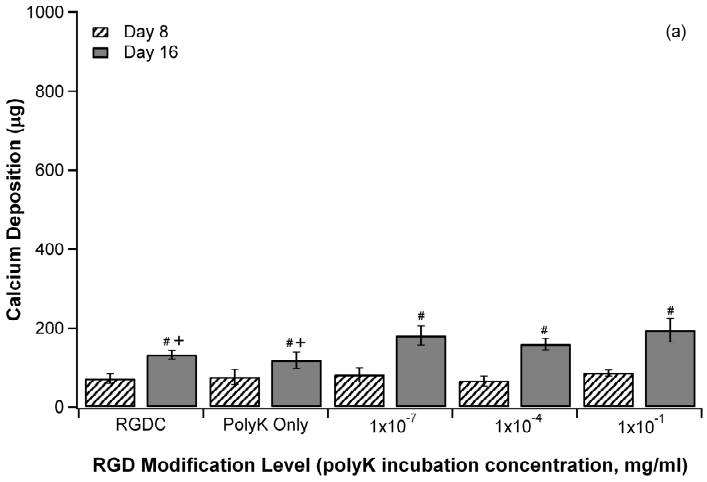
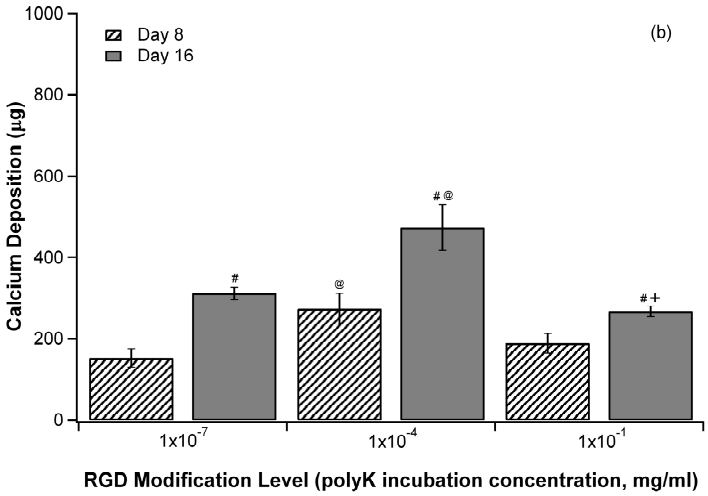


Figure 6.2. Effect of the RGD modification level (expressed as the concentration of polyK in the incubation phase of the modification) on Alkaline Phosphatase Activity of cells cultured under (a) static conditions, and under flow perfusion at flow rates of (b) 0.1 ml/min and (c) 1.0 ml/min. Controls included a plain PLLA scaffold incubated in an RGDC solution (RGDC) and a scaffold modified with polyK only at an incubation concentration of $1x10^{-7}$ mg/min (polyK only). @ denotes the modification level that yields the highest cellularity at a specific day. + represents the controls having significant lower cellularity than the polyK-SPDP-RGDC modified scaffolds. # and & represent the days with the highest and lowest cellularity at a specific modification level. (*) signifies $p< 0.05$.

6.3.3. Calcium Deposition

Mineralization of the scaffolds is reported as mg of calcium, and it is shown in Figure 6.3 for all culture conditions at every extent of modification. At all culturing conditions, the calcium deposition significantly increased with time, and the control scaffolds presented significantly lower calcium levels. Under static conditions, the control scaffolds presented significantly lower calcium deposition after 16 days, but there was no difference between the different modification levels. At day 8there were no difference between the controls and the modified scaffolds. The amount of deposited calcium reached values as high as (195±30mg). Under flow perfusion the calcium deposition was greatly improved when compared to that found under static conditions. At a flow rate of 0.1 ml/min, scaffolds modified at polyK incubation concentration of $1x10^{-4}$ mg/ml yielded the highest calcium levels at all time points, reaching a maximum of (473±55mg). At 1.0 ml/min, the highest calcium deposition was encountered at the lowest RGDC level ($1x10^{-7}$ mg polyK/ml) at all time points, reaching a maximum of (786±120mg). There are no significant differences between the other modification levels at this flow rate.





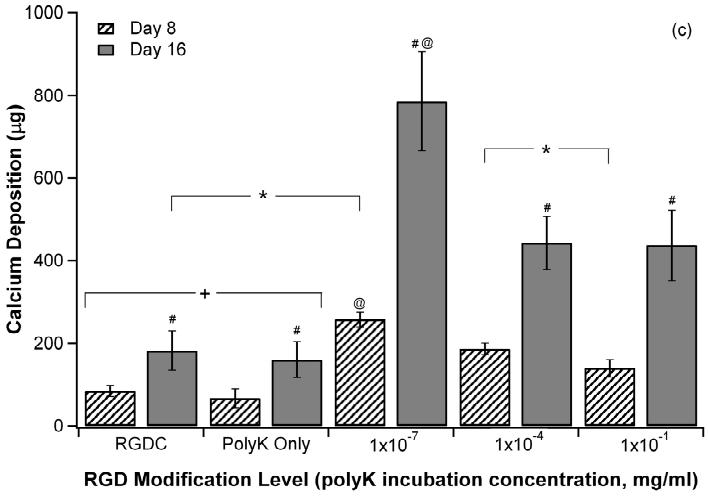


Figure 6.3. Effect of the RGD modification level (expressed as the concentration of polyK in the incubation phase of the modification) on the deposition of calcium by cells cultured under (a) static conditions, and under flow perfusion at flow rates of (b) 0.1 ml/min and (c) 1.0 ml/min. Controls included a plain PLLA scaffold incubated in an RGDC solution (RGDC) and a scaffold modified with polyK only at an incubation concentration of $1x10^{-7}$ mg/min (polyK only). @ denotes the modification level that yields the highest cellularity at a specific day. + represents the controls having significant lower cellularity than the polyK-SPDP-RGDC modified scaffolds. # and & represent the days with the highest and lowest cellularity at a specific modification evel. (*) signifies $p< 0.05$.

6.4. Discussion

The objective of the present study was to evaluate the effect of the extent of RGD-modification of PLLA foams on the osteoblastic differentiation of rat mesenchymal stem cells under conditions of flow perfusion. Thus, we aimed to study the effect of mechanical stimulation (represented by flow perfusion) and chemical stimulation (represented by the incorporation of RGDC) individually, and ultimately their combined effect on MSC osteoblastic differentiation. It has been demonstrated in this study that there is an enhanced effect on MSC osteoblastic differentiation due to combination of the aforementioned means of stimulation.

The estimation of the degree of differentiation is based on different osteoblastic markers. In this study common markers were used: cell growth, alkaline phosphatase activity, and mineral deposition represented by the amount of calcium deposited by the cells. The levels of RGD modification were represented by the initial polyK incubation concentration after the acetone soaking of the PLLA foams (se section 6.2.2). Control scaffolds included plain foams soaked in an RGDC solution, represented as RGDC in the figures, and polyK-modified PLLA foams without RGDC, represented as polyK only. Cultures were carried out in a flow perfusion bioreactor at two different flow rates: 0.1 and 1.0 ml/min. Static cultures served as controls.

In the present study, MSCs underwent changes typical of the osteogenesis process reported in previous studies. An early stage was marked by a high proliferation rate. This phase was followed by a period where the proliferation was down-regulated and ALP activity was up-regulated, indicating early osteoblastic

differentiation. Once ALP activity reached a maximum (day 8), a mineralization stage followed with a characteristid down-regulation of ALP activity, continued decrease on the proliferation rate and the up-regulation of calcium deposition. Scaffold cellularity also presented a peak around day 8, indicating that at later time points cell death occurred possibly due to the achievement of the last stage of osteoblastic differentiation. The high levels of calcium and the decrease of ALP activity at day 16 support this hypothesis.

The effect of flow perfusion on the osteoblastic differentiation of MSCs has been previously reported in the literature. The exposure of MSCs to the shear forces exerted by the flow throughout the porous network of the scaffold induces higher levels of ALP activity and mineral deposition when compared to static cultures. The results obtained in the present study corroborate those findings. Not only were levels of ALP activity and calcium deposition encountered under flow perfusion significantly higher than those found under static conditions, but so was the scaffold cellularity. Furthermore, these makers were generally further up-regulated at a higher flow rate, agreeing with the results previously reported by Bancroft et al and other authors[62,70,73,74]. In addition to the improvement of MSC osteoblastic differentiation due to mechanical stimulation, a similar effect was induced by the presence of RGDC on the scaffold surface.

An amine-amine functionalized scaffold was previously developed in our laboratory through the controlled physical entrapment of poly-L-lysine (polyK) in the surface of PLLA foams. Further incorporation of RGD peptides was possible by forming a disulfide bond with SPDP linked to the amine group of the polyK. Thus,

the different amounts of entrapped polyK allow us to study the effect of different RGD surface concentrations on certain cellular responses, most specifically, the differentiation of MSCs towards an osteoblastic phenotype. An up-regulation of ALP activity, scaffold cellularity and mineral deposition on polyK-SPDP-RGDC modified scaffold when compared to the controls elucidates stronger cell-matrix interactions that result into greater differentiation. These results are in agreement with previous publications that report the effect of RGD on the osteoblastic differentiation of MSCs in a dose dependent manner [40,75,76]. In the present study, this behavior was observed at both static and flow perfusion cultures. Nonetheless, it is clear that, under flow perfusion, the extent of RGD modification has a definite effect on the differentiation.

Holtorf et have reported that the combination of shear forces due to flow perfusion combined with the presence of RGD peptides on the surface of titanium fiber meshes increases MSC osteogenesis when compared to their individual effects[70]. The results found in this study are in agreement with that finding, but they also show there is a critical level of RGD modification, and this level is dependent on the flow rate. A lower flow rate (0.1 ml/min) seemed to favor the middle modification level represented by a polyK incubation concentration of $1x10^{-4}$ mg/ml while the highest flow rate (1 ml/min) favored the lowest modification level (polyK incubation concentration of $1x10^{-7}$ mg/ml). Comisar et al found a similar behavior when culturing MC3T3 preosteoblastic cells on RGD nanopatterned hydrogels. They changed the spacing of RGD clusters and found that at lower levels of spacing, which translates in higher RGD surface density, there was decreased differentiation [75]. It is proposed that the integrin receptor primarily responsible for osteoblastic cell adhesion, $\alpha_v\beta_3$, also inhibits osteoblastic differentiation [75,77-79]. It is then possible that

this inhibitory effect is downplayed at lower RGD surface densities due to greater spacing of the RGD peptides. This would explain why there is a critical modification level, but the question on the shift of this critical level at different flow rates remains.

This may be explained by the enhanced cell-matrix interactions induced by the shear forces. When characterizing the seeding of RGD-modified scaffolds, we noticed that under static conditions few cells attached to the walls, and the rest formed clusters within the pores. At higher modification levels, some of the cells presented some stretching, indicating an improvement in cell matrix interactions. However, when seeded under oscillatory flow perfusion, the cells were clearly stretched along the edges of the pores, thus displaying a dramatic improvement on cell-matrix interactions [80]. The results of the present study suggest that the interactions found under static conditions of culture might be strong enough to show a difference in cell numbers at different modification levels but not strong enough to affect the other markers. Under flow perfusion, since these interactions are dramatically increased, the differences arouse and a behavior similar to that reported by Comisar et al. is observed [75]. It is possible that at higher flow rates, only strongly bound cells remain, and cell-matrix interactions are further strengthened, increasing the inhibitory effect of the $\alpha_v\beta_3$ receptor activation. The osteoblastic differentiation would then be down-regulated when compared to the lower flow rates. Consequently, the critical modification level would shift to a lower RGD surface concentration.

6.5. Conclusions

RGDC surface modification combined with flow perfusion conditions of culture improved MSC osteoblastic differentiation with respect to the influence of modification or flow perfusion individually. The presence of RGD peptides on the surface of PLLA foams up-regulated the ALP activity and calcium deposition, and this effect was more pronounced under conditions of flow perfusion. From our findings we conclude that there exists a critical RGD surface concentration that is different for every culture condition in a flow perfusion system. A balance must be reached so that this RGD surface concentration is high enough to improve cell-matrix interaction and avoid cell detachment due to the shear forces and, at the same time, low enough to avoid a strong inhibitory effect on the differentiation of mesenchymal stem cells towards an osteoblastic lineage.

6.6. References

1. Abousleiman, RI, Sikavitsas, VI. Bioreactors for tissues of the musculoskeletal system. Adv Exp Med Biol. 2006;585:243.
2. Alvarez-Barreto, JF, Sikavitsas, VI. Tissue Engineering Bioreactors. In: Boronzino JD, ed. Tissue Engineering and Artificial Organs. Vol 3. 3 ed. Boca Raton: Taylor & Francis Group; 2006:44-41.
3. Garvin, J, Qi, J, Maloney, M, Banes, AJ. Novel system for engineering bioartificial tendons and application of mechanical load. Tissue Eng. 2003;9:967-979.
4. Hillsley, MV, Frangos, JA. Bone tissue engineering: the role of interstitial fluid flow. Biotechnol Bioeng. 1994;43:573-581.
5. Hoerstrup, SP, Sodian, R, Sperling, JS, Vacanti, JP, Mayer, JE, Jr. New pulsatile bioreactor for *in vitro* formation of tissue engineered heart valves. Tissue Eng. 2000;6:75-79.
6. Meinel, L, Karageorgiou, V, Hofmann, S, et al. Engineering bone-like tissue *in vitro* using human bone marrow stem cells and silk scaffolds. J Biomed Mater Res A. 2004;71:25.
7. Bonassar, LJ, Vacanti, CA. Tissue engineering: the first decade and beyond. J Cell Biochem Suppl. 1998;30-31:297.
8. Bostrom, RD, Mikos, AG. Tissue Engineering of Bone. In: Atala A, Mooney DJ, eds. Synthetic biodegradable polymer scaffolds. Boston: Birkhäuser; 1997:215.

9. Holy, CE, Shoichet, MS, Davies, JE. Engineering three-dimensional bone tissue *in vitro* using biodegradable scaffolds: investigating initial cell-seeding density and culture period. J Biomed Mater Res. 2000;51:376.

10. Ma, PX, Zhang, R. Synthetic nano-scale fibrous extracellular matrix. J Biomed Mater Res. 1999;46:60.

11. Staltzman, MW. Cell Interactions with Polymers. In: Lanza R, Langer R, Vacanti J, eds. Principles of Tissue Engineering. 2 ed. San Diego: Academic Press; 2000:221.

12. Temenoff, JS, Lu, L, Mikos, AG. Bone Tissue Engineering Using Synthetic Biodegradable Polymer Scaffolds. In: Davies JE, ed. Bone Engineering. Toronto: University of Toronto; 2000:454.

13. Vacanti, JP, Langer, R, Upton, J, Marler, JJ. Transplantation of cells in matrices for tissue regeneration. Adv Drug Deliv Rev. 1998;33:165.

14. Yang, XB, Roach, HI, Clarke, NM, et al. Human osteoprogenitor growth and differentiation on synthetic biodegradable structures after surface modification. Bone. 2001;29:523.

15. Altman, GH, Diaz, F, Jakuba, C, et al. Silk-based biomaterials. Biomaterials. 2003;24:401.

16. Lutolf, MP, Hubbell, JA. Synthetic biomaterials as instructive extracellular microenvironments for morphogenesis in tissue engineering. Nat Biotechnol. 2005;23:47.

17. Mikos, AG, Bao, Y, Cima, LG, Ingber, DE, Vacanti, JP, Langer, R. Preparation of poly(glycolic acid) bonded fiber structures for cell attachment and transplantation. J Biomed Mater Res. 1993;27:189.

18. Nam, YS, Yoon, JJ, Park, TG. A novel fabrication method of macroporous biodegradable polymer scaffolds using gas foaming salt as a porogen additive. J Biomed Mater Res. 2000;53:1.

19. Ratner, BD, Bryant, SJ. Biomaterials: where we have been and where we are going. Annu Rev Biomed Eng. 2004;6:41.

20. Hollinger, JO, Battistone, GC. Biodegradable bone repair materials. Synthetic polymers and ceramics. Clin Orthop Relat Res. 1986:290.

21. Hubbell, JA. Bioactive biomaterials. Curr Opin Biotechnol. 1999;10:123.

22. Ishaug, SL, Crane, GM, Miller, MJ, Yasko, AW, Yaszemski, MJ, Mikos, AG. Bone formation by three-dimensional stromal osteoblast culture in biodegradable polymer scaffolds. J Biomed Mater Res. 1997;36:17.

23. Shin, H, Jo, S, Mikos, AG. Biomimetic materials for tissue engineering. Biomaterials. 2003;24:4353.

24. Liu, X, Ma, PX. Polymeric scaffolds for bone tissue engineering. Ann Biomed Eng. 2004;32:477.

25. Teraoka, F, Nakagawa, M, Hara, M. Surface modification of poly (L-lactide) by atmospheric pressure plasma treatment and cell response. Dent Mater J. 2006;25:560-565.

26. Cook, AD, Hrkach, JS, Gao, NN, et al. Characterization and development of RGD-peptide-modified poly(lactic acid-co-lysine) as an interactive, resorbable biomaterial. J Biomed Mater Res. 1997;35:513.

27. Elbert, DL, Hubbell, JA. Conjugate addition reactions combined with free-radical cross-linking for the design of materials for tissue engineering. Biomacromolecules. 2001;2:430.

28. Hsu, SH, Tsai, CL, Tang, CM. Evaluation of cellular affinity and compatibility to biodegradable polyesters and Type-II collagen-modified scaffolds using immortalized rat chondrocytes. Artif Organs. 2002;26:647.

29. Rowley, JA, Madlambayan, G, Mooney, DJ. Alginate hydrogels as synthetic extracellular matrix materials. Biomaterials. 1999;20:45.

30. Stile, RA, Healy, KE. Thermo-responsive peptide-modified hydrogels for tissue regeneration. Biomacromolecules. 2001;2:185.

31. Yuan, X, Mak, AF, Li, J. Formation of bone-like apatite on poly(L-lactic acid) fibers by a biomimetic process. J Biomed Mater Res. 2001;57:140.

32. Rezania, A, Healy, KE. The effect of peptide surface density on mineralization of a matrix deposited by osteogenic cells. J Biomed Mater Res. 2000;52:595.

33. Vunjak-Novakovic, G, Obradovic, B, Martin, I, Bursac, PM, Langer, R, Freed, LE. Dynamic cell seeding of polymer scaffolds for cartilage tissue engineering. Biotechnol Prog. 1998;14:193.

34. Cui, YL, Hou, X, Qi, AD, et al. Biomimetic surface modification of poly (L-lactic acid) with gelatin and its effects on articular chondrocytes *in vitro*. J Biomed Mater Res. 2003;66A:770.

35. Alvarez-Barreto, JF, Shreve, MC, DeAngelis, PL, Sikavitsas, VI. Preparation of a functionally flexible, three-dimensional, biomimetic scaffold for different tissue engineering applications. Tissue Eng. 2007;13:1205-1217.

36. Alsberg, E, Kong, HJ, Hirano, Y, Smith, MK, Albeiruti, A, Mooney, DJ. Regulating bone formation via controlled scaffold degradation. J Dent Res. 2003;82:903.

37. Elmengaard, B, Bechtold, JE, Soballe, K. *In vivo* effects of RGD-coated titanium implants inserted in two bone-gap models. J Biomed Mater Res A. 2005;75:249.

38. Kurihara, H, Nagamune, T. Cell adhesion ability of artificial extracellular matrix proteins containing a long repetitive Arg-Gly-Asp sequence. J Biosci Bioeng. 2005;100:82.

39. Sawyer, AA, Hennessy, KM, Bellis, SL. Regulation of mesenchymal stem cell attachment and spreading on hydroxyapatite by RGD peptides and adsorbed serum proteins. Biomaterials. 2005;26:1467.

40. Yang, F, Williams, CG, Wang, DA, Lee, H, Manson, PN, Elisseeff, J. The effect of incorporating RGD adhesive peptide in polyethylene glycol diacrylate hydrogel on osteogenesis of bone marrow stromal cells. Biomaterials. 2005;26:5991.

41. Lee, MH, Adams, CS, Boettiger, D, et al. Adhesion of MC3T3-E1 cells to RGD peptides of different flanking residues: Detachment strength and correlation with long-term cellular function. J Biomed Mater Res A. 2006.

42. Chan, BP, Reichert, WM, Truskey, GA. Effect of streptavidin RGD mutant on the adhesion of endothelial cells. Biotechnol Prog. 2004;20:566.

43. Chen, J, Altman, GH, Karageorgiou, V, et al. Human bone marrow stromal cell and ligament fibroblast responses on RGD-modified silk fibers. J Biomed Mater Res A. 2003;67:559.

44. Dard, M, Sewing, A, Meyer, J, Verrier, S, Roessler, S, Scharnweber, D. Tools for tissue engineering of mineralized oral structures. Clin Oral Investig. 2000;4:126.

45. Deng, C, Tian, H, Zhang, P, Sun, J, Chen, X, Jing, X. Synthesis and characterization of RGD peptide grafted poly(ethylene glycol)-b-poly(L-lactide)-b-poly(L-glutamic acid) triblock copolymer. Biomacromolecules. 2006;7:590.

46. Fussell, GW, Cooper, SL. Endothelial cell adhesion on RGD-containing methacrylate terpolymers. J Biomed Mater Res A. 2004;70:265.

47. Garcia, AJ, Ducheyne, P, Boettiger, D. Effect of surface reaction stage on fibronectin-mediated adhesion of osteoblast-like cells to bioactive glass. J Biomed Mater Res. 1998;40:48.

48. Gilbert, M, Shaw, WJ, Long, JR, et al. Chimeric peptides of statherin and osteopontin that bind hydroxyapatite and mediate cell adhesion. J Biol Chem. 2000;275:16213.

49. Ho, MH, Wang, DM, Hsieh, HJ, et al. Preparation and characterization of RGD-immobilized chitosan scaffolds. Biomaterials. 2005;26:3197.

50. Hsu, SH, Chang, SH, Yen, HJ, Whu, SW, Tsai, CL, Chen, DC. Evaluation of biodegradable polyesters modified by type II collagen and Arg-Gly-Asp as tissue engineering scaffolding materials for cartilage regeneration. Artif Organs. 2006;30:42.

51. Kang, CE, Gemeinhart, EJ, Gemeinhart, RA. Cellular alignment by grafted adhesion peptide surface density gradients. J Biomed Mater Res A. 2004;71:403.

52. Knerr, R, Weiser, B, Drotleff, S, Steinem, C, Gopferich, A. Measuring cell adhesion on RGD-modified, self-assembled PEG monolayers using the quartz crystal microbalance technique. Macromol Biosci. 2006;6:827.

53. Koo, LY, Irvine, DJ, Mayes, AM, Lauffenburger, DA, Griffith, LG. Co-regulation of cell adhesion by nanoscale RGD organization and mechanical stimulus. J Cell Sci. 2002;115:1423.

54. Moreau, JE, Chen, J, Horan, RL, Kaplan, DL, Altman, GH. Sequential growth factor application in bone marrow stromal cell ligament engineering. Tissue Eng. 2005;11:1887.

55. Park, KH, Na, K, Chung, HM. Enhancement of the adhesion of fibroblasts by peptide containing an Arg-Gly-Asp sequence with poly(ethylene glycol) into a thermo-reversible hydrogel as a synthetic extracellular matrix. Biotechnol Lett. 2005;27:227.

56. Rezania, A, Thomas, CH, Branger, AB, Waters, CM, Healy, KE. The detachment strength and morphology of bone cells contacting materials modified with a peptide sequence found within bone sialoprotein. J Biomed Mater Res. 1997;37:9.

57. Santiago, LY, Nowak, RW, Peter Rubin, J, Marra, KG. Peptide-surface modification of poly(caprolactone) with laminin-derived sequences for adipose-derived stem cell applications. Biomaterials. 2006;27:2962.

58. Shin, H, Temenoff, JS, Bowden, GC, et al. Osteogenic differentiation of rat bone marrow stromal cells cultured on Arg-Gly-Asp modified hydrogels without dexamethasone and beta-glycerol phosphate. Biomaterials. 2005;26:3645.

59. Smith, E, Yang, J, McGann, L, Sebald, W, Uludag, H. RGD-grafted thermoreversible polymers to facilitate attachment of BMP-2 responsive C2C12 cells. Biomaterials. 2005;26:7329.

60. Zhang, L, Hum, M, Wang, M, et al. Evaluation of modifying collagen matrix with RGD peptide through periodate oxidation. J Biomed Mater Res A. 2005;73:468.

61. Hsu, SH, Whu, SW, Hsieh, SC, Tsai, CL, Chen, DC, Tan, TS. Evaluation of chitosan-alginate-hyaluronate complexes modified by an RGD-containing protein as tissue-engineering scaffolds for cartilage regeneration. Artif Organs. 2004;28:693.

62. Bancroft, GN, Sikavitsas, VI, Mikos, AG. Design of a flow perfusion bioreactor system for bone tissue-engineering applications. Tissue Eng. 2003;9:549.

63. Burg, KJ, Holder, WDJ, Culberson, CR, et al. Comparative study of seeding methods for three-dimensional polymeric scaffolds. J Biomed Mater Res. 2000;52:576.

64. Cartmell, SH, Porter, BD, Garcia, AJ, Guldberg, RE. Effects of medium perfusion rate on cell-seeded three-dimensional bone constructs *in vitro*. Tissue Eng. 2003;9:1197.

65. Goldstein, AS, Juarez, TM, Helmke, CD, Gustin, MC, Mikos, AG. Effect of convection on osteoblastic cell growth and function in biodegradable polymer foam scaffolds. Biomaterials. 2001;22:1279.

66. Wendt, D, Marsano, A, Jakob, M, Heberer, M, Martin, I. Oscillating perfusion of cell suspensions through three-dimensional scaffolds enhances cell seeding efficiency and uniformity. Biotechnol Bioeng. 2003;84:205.

67. Alvarez-Barreto, JF, Linehan, SM, Shambaugh, RL, Sikavitsas, VI. Flow Perfusion Improves Seeding of Tissue Engineering Scaffolds with Different Architectures. Ann Biomed Eng. 2007.

68. Li, Y, Ma, T, Kniss, DA, Lasky, LC, Yang, ST. Effects of filtration seeding on cell density, spatial distribution, and proliferation in nonwoven fibrous matrices. Biotechnol Prog. 2001;17:935.

69. Zhao, F, Ma, T. Perfusion bioreactor system for human mesenchymal stem cell tissue engineering: dynamic cell seeding and construct development. Biotechnol Bioeng. 2005;91:482.

70. Holtorf, HL, Jansen, JA, Mikos, AG. Ectopic bone formation in rat marrow stromal cell/titanium fiber mesh scaffold constructs: effect of initial cell phenotype. Biomaterials. 2005;26:6208.

71. Mikos, AG, Lyman, MD, Freed, LE, Langer, R. Wetting of poly(L-lactic acid) and poly(DL-lactic-co-glycolic acid) foams for tissue culture. Biomaterials. 1994;15:55.

72. Datta, N, Holtorf, HL, Sikavitsas, VI, Jansen, JA, Mikos, AG. Effect of bone extracellular matrix synthesized *in vitro* on the osteoblastic differentiation of marrow stromal cells. Biomaterials. 2005;26:971.

73. Bancroft, GN, Sikavitsas, VI, van den Dolder, J, et al. Fluid flow increases mineralized matrix deposition in 3D perfusion culture of marrow stromal osteoblasts in a dose-dependent manner. Proc Natl Acad Sci U S A. 2002;99:12600.

74. Sikavitsas, VI, Bancroft, GN, Holtorf, HL, Jansen, JA, Mikos, AG. Mineralized matrix deposition by marrow stromal osteoblasts in 3D perfusion culture increases with increasing fluid shear forces. Proc Natl Acad Sci U S A. 2003;100:14683-14688.

75. Comisar, WA, Kazmers, NH, Mooney, DJ, Linderman, JJ. Engineering RGD nanopatterned hydrogels to control preosteoblast behavior: A combined computational and experimental approach. Biomaterials. 2007;28:4409-4417.

76. Hosseinkhani, H, Hosseinkhani, M, Tian, F, Kobayashi, H, Tabata, Y. Osteogenic differentiation of mesenchymal stem cells in self-assembled peptide-amphiphile nanofibers. Biomaterials. 2006;27:4079-4086.

77. Cheng, SL, Lai, CF, Blystone, SD, Avioli, LV. Bone mineralization and osteoblast differentiation are negatively modulated by integrin alpha(v)beta3. J Bone Miner Res. 2001;16:277-288.

78. Dunehoo, AL, Anderson, M, Majumdar, S, Kobayashi, N, Berkland, C, Siahaan, TJ. Cell adhesion molecules for targeted drug delivery. J Pharm Sci. 2006;95:1856-1872.

79. Lee, MH, Adams, CS, Boettiger, D, et al. Adhesion of MC3T3-E1 cells to RGD peptides of different flanking residues: detachment strength and correlation with long-term cellular function. J Biomed Mater Res A. 2007;81:150-160.

80. Alvarez-Barreto, JF, Sikavitsas, VI. Improved mesenchymal stem cell seeding on RGD-modified poly(L-lactic acid) scaffolds using flow perfusion. Macromol Biosci. 2007;7:579-588.

Chapter 7

Project Conclusions and Future Directions

In this chapter, conclusions directed towards the fulfillment of the specific aims established in Chapter 1 are stated. Ideas for future projects and complements of the ideas presented during the discussions to the results presented in Chapters 3 through 6 are also recommended.

7.1. Project Conclusions

Specific Aim 1: *To develop a dynamic scaffold seeding technique based on oscillatory flow perfusion and evaluate its effects on seeding efficiency, initial cellular distributions throughout the scaffold surface, and cell-matrix interactions.*

As mentioned in Chapter 2, a traditional and probably the most common seeding technique used in many long-term culture studies, including these involving flow perfusion, is the static seeding. In this technique, a cell suspension is added to the top of the scaffold in a drop-wise fashion, and the cells are allowed to attach for a certain period of time after which they are transferred into the desired culture environment. There major limitations with this seeding technique. Firstly, it yields low seeding efficiencies because the cell suspension goes through the scaffold thickness only once, and this is the only chance the cells have to attach to its surface. Secondly, due to transport limitations and capillary forces, the cellular distributions achieved by static seeding present poor homogeneity. Thus, it was important to design

a culture technique that allowed the penetration of the cells suspension throughout the entire scaffold porous network and give the cells more possibilities of attachment.

The oscillatory flow perfusion proposed in Chapter 3 meets these requirements. Due to the design of the flow perfusion system, the cell suspension is forced into the pores of the scaffold. Additionally, the stage of oscillatory flow allows the cells to go through the scaffold's thickness several times thereby giving them a greater chance to attach to the surface. Consequently, it was not only found that, by using this technique, homogeneous cell distributions and high seeding efficiencies were achieved as compared to static culture but also a stronger extent of cell attachment, as demonstrated by detachment experiments. In general, flow perfusion seeding is more convenient for many tissue engineering applications, especially if a long term culture is to be carried out in a similar system.

Specific Aim 2: *To create a biomimetic poly(L-lactic acid scaffold) with improved cell adhesion using RGD peptides that can additionally allow the evaluation of the effect of different modification levels on cell adhesion, proliferation and differentiation.*

To complete this aim, a poly(L-lactic acid) foam prepare by particulate leaching was used. Amine groups were incorporated on to the surface by physically entrapping poly-L-lysine. Due to the process of entrapment, the amount of polyK entrapped could be controlled by varying its concentration in the incubation solution. It is mentioned in Chapter 4 that this scaffold is functionally flexible because by having these amine groups on the surface, different moieties can be further

incorporated on the surface to elicit different cell functions. In this project, RGDC peptides were linked by creating a disulfide bond with a molecule of SPDP attached to the amine group on the surface. This scaffold supported increased cell adhesion when compared to unmodified scaffolds and other controls. Furthermore, it supported proliferation. The ability to control the extent of polyK entrapment also allowed for the preparation of biomimetic scaffolds with different degrees of RGD modification. This feature would later support the evaluation of different RGD surface modification levels on MSC attachment, proliferation and osteoblastic differentiation, as shown in Chapters 5 and 6.

Specific Aim 3: *To characterize the newly developed oscillatory flow perfusion seeding of mesenchymal stem cells on the modified scaffolds based on cell spatial distribution, seeding efficiency and strength of cell attachment at different modification levels and flow conditions.*

For the first time, the oscillatory flow perfusion seeding of rat MSC on RGD-modified PLLA foams was characterized, and the results of this characterization are shown in Chapter 5. Scaffold cellularity was improved by the incorporation of RGDC peptides in a dose-dependent manner. Cell spatial distribution and cell-matrix interactions were greater on dynamically seeded scaffolds than on those seeded statically. Cell detachment increased at higher unidirectional flow rates, and the extent of cell detachment was also dependent on the level of RGD modification. The use of oscillatory flow perfusion seeding of RGD-modified foams would allow the design of long term culture studies of MSCs seeded uniformly on three dimensional scaffolds, as shown in Chapter 6.

Specific Aim 4: *To evaluate the effect of the extent scaffold modification on the osteoblastic differentiation of mesenchymal stem cells under conditions of flow perfusion.*

It is shown in Chapter 6 that RGDC surface modification combined with flow perfusion conditions of culture improved MSC osteoblastic differentiation with respect to the influence of modification or flow perfusion individually. The presence of RGD peptides on the surface of PLLA foams up-regulated the ALP activity and calcium deposition, and this effect was more pronounced under conditions of flow perfusion. Moreover, there exists a critical RGD surface concentration that is different for every culture condition in a flow perfusion system. A balance must be reached so that this RGD surface concentration is high enough to improve cell-matrix interaction and avoid cell detachment due to the shear forces and, at the same time, low enough to avoid a strong inhibitory effect on the differentiation of mesenchymal stem cells towards an osteoblastic phenotype.

Through the fulfillment of these four specific aims, the main objective of the proposed research project has been achieved. An integral approach for bone tissue engineering has been proposed that uses the scaffolding, cellular and molecular components of traditional approaches. What makes this approach unique is the combination of mechanical and chemical stimulation of mesenchymal stem cells to direct them towards an osteoblastic path. This combinatorial approach resulted more successful than those based on chemical or mechanical stimulation alone.

7.2. Future Directions

Even though the main objective of this PhD research project have been reached, there are still ideas that can be used to look into the suggested hypotheses stated to explain some of the observed results. Regarding the preparation of the biomimetic scaffolds with different levels of RGD modification, it is recommended to quantify more accurately the amounts of RGD present on the surface. The fluorimetric technique explained in Chapter 4, based on the AmplexRed dye, only gives us rough estimates of these amounts and is only useful to corroborate that there are changes on the amount of polyK being entrapped. A more accurate technique that works directly on the RGDC peptides would be more desirable. Radioactive assays would provide this level of accuracy. Thus, radioactive RGDC peptides can be linked to the polyK modified scaffolds following a similar procedure to that explained in chapter 4. The quantification can be done by reading the RGDC solution after the reaction and each of the washes and subtracting that amount from the initial quantity of RGDC in solution. Another alternative is breaking down the RGD-modified scaffold manually, followed by sonication, and reading the resulting suspension. Actual RGDC amounts can be determined by the use of a standard curve. Once the amounts of RGD on the surface of the scaffold are established for every level of modification, the reported results can be compared with previous studies that report actual RGD surface density and its effect on specific cellular responses.

In Chapter 6, it was mentioned that the integrin receptor $\alpha_v\beta_3$ may have played an effect on MSC osteblastic differentiation; furthermore, it may explain the existence

of a critical RGD surface concentration and its shift at different flow rates. It is well known that fibronectin increases improves cell adhesion via activation of the $\alpha_5\beta_1$ and $\alpha_v\beta_3$ receptors. In addition to that, previous studies have reported that integrin $\alpha_5\beta_1$ activation up-regulates osteogenesis. Lee et al coated surfaces with fibronectin or RGD peptide sequences at similar densities, and found that the effect of fibronectin of mineral deposition and ALP activity was greater in the presence of fibronectin. This approach could be used in the flow perfusion studies. Once, a clear protocol has been established to estimate the surface concentration of certain bioactive molecules, PLLA foams can be modified with fibronectin or units of fibronectin responsible for cell adhesion at surface concentrations similar to those used in Chapter 4 for the RGDC peptides. Further blocking of the $\alpha_v\beta_3$ receptors on the MSC membrane can further help on determining whether the observed behavior was due to an inhibitory effect via this receptor.

With the preparation of the amine functionalized scaffold presented in Chapter 4, there are many modification patterns that can be created for studies carried out both *in vitro* and *in vivo* applications that can even go beyond bone regeneration. Further incorporation of different glycosaminoglycans can be used to study the effect of the different surface concentrations on the osteogenic or chondrocytic potential of MSCs, statically or under flow perfusion. Angiogenic factors such as vascular endothelial growth factor (VEGF) can also be incorporated using a peptide link that is digested by metallo proteinases (MMPs) so as to have its controlled release *in vivo*. Consequently, it would be possible to determine what amount of entrapped polyK would yield the highest degree of formation of new blood vessels once the construct is implanted in an

animal model. Modifications using different bioactive molecules, such as RGD and VEGF, are also possible using this amine functionalized PLLA foam.

Regarding oscillatory flow perfusion, it has been previously reported that cells cultured in flow chambers and subjected to changes in the direction of the flow presented higher motility and that this change in the direction of the flow up-regulated the secretion of certain bone ECM molecules. It would be interesting to carry out long term cultures on MSCs under flow perfusion with oscillatory flow at different sequences and periodicities and determine whether oscillatory flow further up-regulates ALP activity, mineral deposition and cell proliferation on three-dimensional environments.